Manufacturing and Cost Analysis for Aluminum and Copper Die Cast Induction Motors for GM's Powertrain and R&D Divisions

by

Gene Collin Mechler

B.S., Materials Science and Engineering (2009)

University of Arizona

Submitted to the Department of Materials Science and Engineering
in Partial Fulfillment of the Requirements for the Degree of
Master of Engineering in Materials Science and Engineering

at the

Massachusetts Institute of Technology

September 2010

Signature of Author . . . .
Department of Materials Science and Engineering
August 2, 2010

Certified by . . . .
Randolph Kirchain
Principle Research Scientist, Engineering Systems Division
Thesis Advisor

Certified by . . . .
Joel Clark
Professor of Materials Engineering
Thesis Reader

Accepted by . . . .
Christopher Schuh
Chair, Departmental Committee on Graduate Students

Manufacturing and Cost Analysis for Aluminum and Copper Die Cast Induction Motors for GM's
Powertrain and R&D Divisions

by

Gene Collin Mechler

Submitted to the Department of Materials Science and Engineering
on August 2, 2010 in Partial Fulfillment of the
Requirements for the Degree of Master of Engineering in
Material Science and Engineering

ABSTRACT

This study investigates the cost effects from changes in size of aluminum and copper die cast induction motors for traction purposes. This thesis uses two specific motors developed by General Motors, the BAS+ and the X26R Motor A, as the basis for the analysis. Induction motors for vehicle traction purposes have traditionally been manufactured using aluminum die casting as the conducting "squirrel cage" material, due to aluminum's light weight, low cost of processing, and relatively good electrical properties. Furthermore, copper offers an electrical conductivity of 160% that of aluminum, and as a result General Motors would like to investigate copper's feasibility as a replacement for aluminum. The use of a more electrically-conductive material would lead to an increase in motor efficiency.

However, die casting copper involves many significant challenges compared to the processing of aluminum, which ultimately result in a higher cost to manufacture the induction motor. Many of these challenges include higher processing temperatures, the need for more complex and higher-tonnage equipment, and more specialized and advanced tooling. Raw material cost is also significantly higher as well.

Using copper in place of aluminum would result in a motor efficiency higher than that of the original aluminum-based motor. Consequently, the motor can then be scaled down in size, thus decreasing the individual costs of many other steps in the manufacturing process and theoretically lowering motor cost as a whole. This study identifies the points of cost parity for various motor downsizing methods and compares them to what is known about motor efficiency as a function of motor size for these two motor architectures.

Acknowledgements

My time at MIT has proven far too short, an effect made possible by all the wonderful people with whom I have had the pleasure of working during my time here. The wealth of information and quality of people MIT produces has left me very thankful for having been given this invaluable opportunity. I will forever be in debt of Dr. Rich Roth, for his countless hours of mentorship and advisement, and for being the most influential person during my studies at MIT. I feel I have made a great friend in him and if he ever needs a companion to Detroit again, I hope he doesn't hesitate to call. Dr. Joel Clark was instrumental in allowing me to become involved in Materials Systems Laboratory, and for teaching me many of the core engineering principles that often become under-emphasized in standard engineering curriculum. Dr. Randy Kirchain and Dr. Frank Field III have forced me to look at complex problems in ways I never thought possible, as well as helped me approach engineering systems much more in-depth.

I must also vehemently thank the other members of MSL. The staff: Dr. Jeremy Gregory, Dr. Elsa Olivetti, Dr. Elisa Alonso, Dr. Trisha Montalbo, and visiting scientist Gundolph Kopp; as well as the graduate students: Siamrut Pantanavanich, Tracey Brommer, Katharine Chu, Nathan Fleming, Ece Gulsen, Thomas Rand-Nash, Hadi Zaklouta, Melissa Zgola, and Marco Leite. Our admin, Terra Cholfin, has been so helpful in "taking care of business" for all the little (and not so little) things I needed help with over the past year. I am truly grateful for the opportunity to work with all these exceptional people; I have made amazing friends in each of them. It is so refreshing to work with a group of people who genuinely enjoy each other's company, and I feel the first-rate work they do reflects this dynamic.

Of course, none of this would be possible without the work of GM's Fran Scancarello (Electric Powertrain and Cost Engineering) and John Agapiou (Research and Development). The knowledge they provided me throughout the course of this project was extraordinary, and I am so appreciative to having been given the opportunity to work with them both. It was because of them that I relished each opportunity to fly to Detroit and work at GM. Inez Ribeiro of MIT-Portugal Alliance provided me with much-needed insight into the die casting process, and helped me even further by laying the framework for my Die Casting model. Dr. James Kirtley of the Electrical Engineering and Computer Science department at MIT was instrumental in providing me with the in-depth efficiency analysis that I used to better understand the various motor architectures I investigated, as well as helping me to better understand induction motor design as a whole.

Finally, to my family and friends – here in Boston, back in Arizona, and everywhere I have travelled – thank you for everything. Seriously.

Gene Collin Mechler
Cambridge, Massachusetts
16 July, 2010
gcmechler@alum.mit.edu

Table of Contents

Table of Figures

7

1   Introduction

1.1   Background

The concept of an electric vehicle for the masses is not a new one. In fact, the personal electric vehicle can trace its roots back to the late 19th century, when Nikola Tesla was issued the very first U.S. patent for the AC-type electric motor in 1886 (1). However, due to the fierce competition from other methods of personal transport, namely steam and later on, gasoline, as well as a lack of ability to store electricity on-board the vehicles, the electric vehicle never saw widespread implementation.

This did, however, set the precedent for a continually evolving automobile industry. From the car's inception through today, the concept of lighter, faster, more fuel efficient vehicles is not a new one. Today, with over 254 million registered passenger vehicles in the United States alone (2, 3), the demand automobiles place on fossil fuels is enormous, and consequently the desire for more fuel-frugal vehicles has become even more pressing in recent years. Coupled with the far-reaching, government-issued Corporate Average Fuel Economy (CAFE)[1] mandate originally implemented in 1975 – which has now become the single-largest fuel-related regulation in U.S. history -- many pundits claim a personal-transportation revolution is underway (4).

One significant advantage electric vehicles have over the incumbent gasoline- and diesel-fueled vehicles is the concept of consuming zero petroleum-based fuel. Of course, EV's still require energy to operate, but are nevertheless more efficient than gasoline vehicles, and therefore less costly to operate – both in energy and in dollars. The emissions and environmental impact is removed directly from the tailpipe (although some environmental impacts still remain over the lifecycle of the vehicle), which enables the use of other, more environmentally beneficial technologies. Furthermore, electricity production has the capability of being produced via carbon-free methods, further reducing the environmental impact. However, the actual widespread implementation of electric vehicles into the US market has not been possible until recently. The enabling of such a technology is multifaceted, with battery technology remaining an area with significant challenges. Unfortunately, many consumers claim that electric vehicles still have not achieved many of the characteristics that consumers have come to expect in a vehicle, notably range and power, and have been unsuccessful at achieving costs similar to their gasoline-powered counterparts (5). To increase the range and power density, gains in conversion efficiency[2] are necessary.

Just as with battery technology, motor technology research is in a continual state of flux, always with the goal of maximizing these performance metrics that have so far been largely unattainable. In recent years there has been a push on the part of electric motor manufacturers to design more efficient motors. From a technological standpoint, motor design has come quite far as compared to where it was just a few decades ago (6, 7). There are two primary approaches to advancing motor efficiency. The

---

[1] The CAFE bill was essentially designed to require all auto manufacturers of the US market to meet an average fuel economy, in hopes that the collective fuel efficiency of US-sold vehicles would increase dramatically.

[2] Conversion efficiency in electric vehicles is the analog to fuel efficiency in traditional vehicles, typically measured in miles per kWh of electricity.

first is the invention of new, more efficient motor architectures. For example, one of the first patents on a new architecture, the axial flux motor, dates back to only 1998. The second approach involves advancements in pre-existing motor technologies, for example increasing efficiency through materials selection or geometry optimization. While the basis for many of the currently-existing motor technologies trace their roots back many decades – even centuries – the ability to scale these designs up in an efficient and effective manner (e.g., to power a vehicle) would not have been possible without this continual evolution.

1.2   Performance and Efficiency

In the automobile industry, there exist many metrics by which the manufacturer and consumer measure performance. As alluded to above, the most important are considered to be range, power, and cost. Commonly, there is a tradeoff between range and power, in that more powerful vehicles require increased energy demands. This relationship holds especially true in battery production. Furthermore, increasing range and power can often result in a higher-cost vehicle. However, the engineering challenge is to develop a design yielding increased power and range, while simultaneously decreasing overall cost. In the automobile, range and power are linked by the commonality known very broadly as *efficiency*. In the internal combustion engine world (i.e., for gasoline- or diesel-powered vehicles), efficiency often refers to *thermodynamic* efficiency, based off the amount of work (gains) and heat (losses) and engine can produce. The same holds true for the electric motor, though in this case the work comes from the presence of magnetic fields in the motor while the losses still come in the form of heat. In electric vehicle terminology, "range" is known as *energy density,* and "power" is commonly viewed as *power density*, or the power the car produces over its weight.

The engineers' ever-present goal for motor design is to maximize efficiency gains while simultaneously minimizing the resultant losses subject to any constraints on the mechanical performance of the device. Consequently, efficiency becomes the driving metric in electric motor design. While individual motor designs may have differing output torques, peak RPMs, maximum current or voltage, etc., the one normalizing performance metric by which all electric motors can be measured is via efficiency. The standard definition of electric motor efficiency can be expressed by Eq. 1:

$$\eta = \frac{P_{out}}{P_{in}} \tag{1}$$

Where P_{out} is the amount of power the motor produces, in watts (W), and P_{in} is the amount of power the motor consumes (also known as the input power), in watts (W). Typically, power is used to calculate efficiency (as in Eq. 1) but energy (or energy-time) can also be used. This means that "energy efficiency" and "power efficiency" are identical terms. While consumers desire range, power, and cost, it is sufficient to investigate only cost and efficiency instead, due to the overlapping impact efficiency has with both range and power.

While this method for calculating the thermodynamic efficiency of an electric motor is an effective metric to compare performance, it does not explicitly deal with motor losses. Typically, losses are reported in units of power, but are a function of the input current and the resistance of the medium through which the current is flowing. A more detailed discussion of motor design and optimization is in Section 2.

While there are other forms of losses in the induction motor (which will be covered later), it is clear that minimizing resistive losses is crucial to boosting motor efficiency. Resistive losses typically account for the vast majority of the losses in an electric motor (7, 8).

(a)   (b)
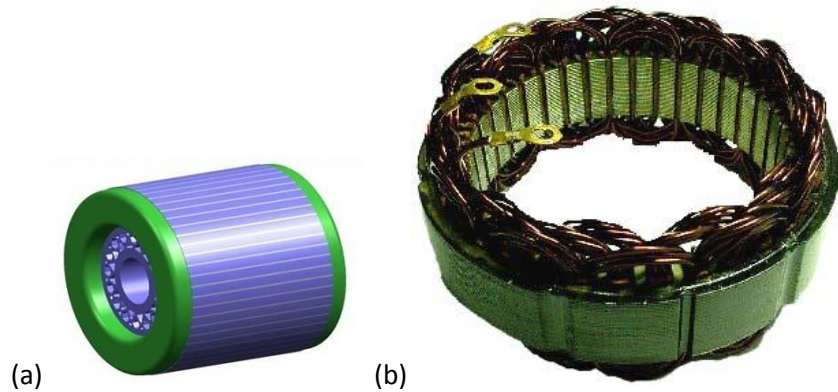
Figure 1: (a) Typical induction rotor; green color represents conducting material. Photo courtesy GM R&D (9). (b) Typical induction stator. Photo courtesy Weber State University (10).

There are ultimately two main components to an induction motor: the rotor and the stator (Figure 1). The conductive material in the stator is nearly always copper, but the conductive material in the rotor varies depending on motor application, size, and the production volume (i.e., cost). It makes sense that improving electrical conduction in these elements would result in increased motor performance. As alluded to before, this study focuses on induction motors for electric vehicle traction purposes. As such, one of the recurring functional requirements for induction traction motors is high performance at low cost. Consequently, induction traction motors have been utilizing aluminum in the rotor to conduct electricity due to its relatively low manufacturing costs and good electrical properties (Figure 2). Since the resistive losses are a direct function of the resistance of the motor, materials selection plays a key role. Unfortunately, this price advantage comes at a significant efficiency loss, given that aluminum is not nearly as electrically conductive as copper. Copper, which is over 60% more conductive than aluminum, is much more difficult (i.e., costly) to process, given its significantly higher melting point (1080°C vs. 660°C), density, and price-per-unit (the latter two by a factor of nearly 3.5). However, utilizing copper in the rotor comes with an additional benefit: given the significant increase in motor efficiency (as compared to using aluminum as the rotor's conducting material), many other aspects of the motor may be downsized. Efficiency, being used as a proxy for both range and power, allows for downsizing that may lead to decreases in overall manufacturing costs. Both material costs and

manufacturing times will be decreased in many of the induction motor's wide array of manufacturing steps. This means the cost of these steps would be reduced as a result. Again, other related performance considerations that affect power, such as torque, were also not investigated in this study.

Figure 2: Finished induction rotor core with aluminum as the conducting material. Photo courtesy Bühler Group (11).

This study involves investigating the manufacturing and cost trade-offs for using various materials as the rotor's conducting material, namely aluminum versus copper. Will efficiency gains due to copper be enough to offset its massive increase in processing cost? In particular, will the cost savings in downsizing the new, copper-based motor create a case in which cost parity is reached to that of the original aluminum-based motor, and will this also result in a motor with adequate efficiency, or even output torque and horsepower?

1.3   Goals of the Work

The goals of this project are two-fold. The first involves understanding the cost-efficiency tradeoff for two different motor cases currently under development by GM. By increasing the efficiency, the motor can be downsized, thus decreasing the overall motor cost. However, this cost decrease may not be enough to offset the initial cost increases associated with using copper. The second and more broadly-reaching goal involves the development of the modeling framework needed to perform the aforementioned analysis. This framework makes use of Process Based Cost Modeling to estimate the costs associated with the induction motor process on a fundamental level and therefore allows for the versatility to investigate varying types of motor architectures. These models also have the functionality necessary to encompass the entire current induction motor manufacturing process while also incorporating the versatility and appropriate flexibility to involve other steps not typically included in the process.

2 Induction Motor Architecture

2.1 Basic Construction

The induction motor is a type of AC electric motor. Typical advantages induction motors have include low cost to manufacture and greater life due to their brushless construction. Induction motors are often used in industrial settings, given that they can be easily scaled up to a large size.

There are two primary components to any electric motor: the stator and the rotor (also called the *armature*) (Figure 3). The stator is a stationary ferrous ring with many slots for copper windings, and receives the input current and voltage. The main component in the rotor is colloquially referred to as the "squirrel cage." The squirrel cage is a series of conducting metal bars running parallel to the axis of rotation that are connected at their end by a shorting ring. The simplest (and least efficient) induction motors commonly available are often referred to as "squirrel cage motors" due to the simple rotor construction (12).
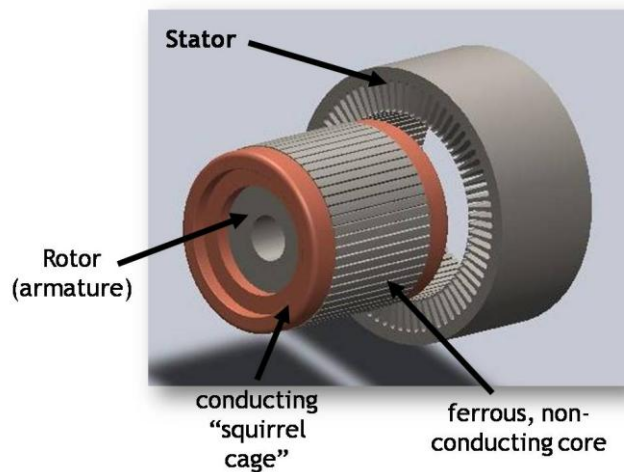
Figure 3: Simplified model of stator and rotor core

2.2 Principles and Governing Equations

Since the input current is both alternating and poly-phase, a rotating electromagnetic field is created. Through Maxwell's correction to Ampere's Law[3], this field then induces a current through the conductive squirrel cage, which in turn produces its own magnetic field around the armature. Often referred to as Lenz's Law, the rotating magnetic field of the stator interacts with that of the rotor, producing a force at the surface of the rotor. This force is known as the Lorentz Force (Eq. 2), and results in a torque (given that the force is acting at a distance from the axis of rotation).

---

[3] Maxwell's correction to Ampere's Law states that while a changing magnetic field will create an electric field, a changing electric field will create a magnetic field.

$$F = q(E + v \times B) \tag{2}$$

Where q is the electric charge of a particle in space, E is the electric field, and $v \times B$ is the cross product of the instantaneous velocity of the particle and the magnetic field, measured in teslas.

Many advanced induction motor architectures make use of a minimally-conducting ferrous core to surround the squirrel cage and aid in electromagnetic induction. Both of the motors to be considered in this study incorporate this design element.

However, the advantages typically associated with induction motors come with a caveat. Given that the output torque is wholly dependent on the induced magnetic field on the rotor, the *inducing* magnetic field from the stator must be able to *pass by* the rotor conductors in order for a current to be induced in the first place. This effectively means that the stator's magnetic field must be traveling at a rate greater than that of the rotor, or else a current will not be induced at the squirrel cage. This slight imbalance between the stator's magnetic field and the rotating armature itself is called a *slip*. Without this slip, an induction motor will not function. For this reason, induction motors are often referred to as *asynchronous*.

Unfortunately, the presence of this slip comes with a slight efficiency cost. By contrast, another common AC brushless motor type is the Permanent Magnet motor, in which the rotor has many high-powered magnets in place of a conducting squirrel cage. As a result, the stator's rotating magnetic field interacts with the stationary magnetic field of the rotor's permanent magnets, producing a torque. Clearly, with a Permanent Magnet motor there is no slip and therefore are considered to be more efficient that their induction-based counterparts. Permanent Magnet motors are commonly referred to as *synchronous*. The downside of permanent magnet motors is typically cost as the permanent magnet materials can be quite expensive.

The amount of slip in an induction motor is crucial to overall motor performance, and can be easily calculated by Eq. 3 and is expressed in units of percent.

$$s = \frac{(n_s - n_r)}{n_s} \tag{3}$$

Where s is the slip, and n_s and n_r are the stator magnetic field speed and rotor speed (in RPM), respectively.

Most advanced induction motors also feature a "skew," in which the stator slots and squirrel cage bars are shifted slightly from end-to-end (Figure 4). Skew is implemented to aid in dealing with harmonic imbalances. While an induction motor will function without the presence of skew, efficiency is greatly improved due to the reduction of these issues with harmonics (13, 14).
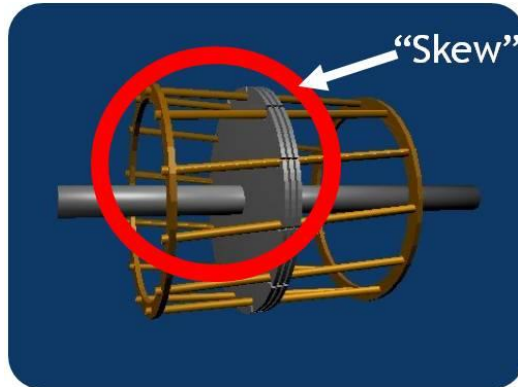
2.3   Other important components

Despite the fact that the stator and rotor are by far the most important components to the induction motor, there are also a number of other components, without which the induction motor would not function. In addition to the ferrous cores of both the rotor and the stator, precise placement of the copper windings through the stator slots is extremely important. Likewise, integration of the squirrel cage to the rotor core is also essential and is the subject of much research. While this particular project investigates the cost and manufacturing effects of die casting, a smaller and higher-level investigation into two other processing methods has also been performed. Completing the assembly of the rotor includes the installation of the hub and shaft, as well as bearings to allow the rotor to spin with minimal friction.

Other important components include the tonewheel, which is necessary for the power electronics to know the absolute position of the rotor relative to the stator in order for the motor to operate at optimum efficiency. Finally, the housing and power electronics are necessary to integrate the entire package. While the housing is included in the manufacturing of the two motor cases investigated in this project, future designs might allow the housing to be eliminated altogether by integrating the motor directly into the vehicle's transmission itself, thereby simultaneously reducing weight and manufacturing cost.
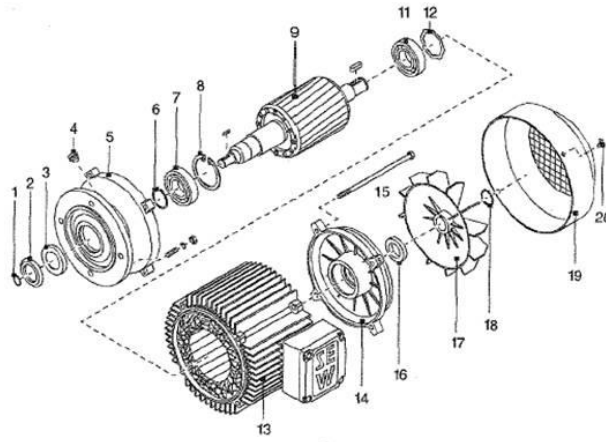
Figure 5: Exploded view of a typical induction motor. Photo courtesy Buhler (11).

2.4   Construction of Stator and Rotor Cores

One of the characteristics of induction motors that allows for higher efficiency is the way in which the stator and rotor are constructed. Rather than simply being constructed from billet iron, very thin steel cross-sectional laminations are blanked and subsequently stacked to compose the rotor and stator stacks. Electric motors using this manufacturing method can have anywhere from a few tens to a thousand laminations making up the stator and rotor stacks (13).

(a)   (b)
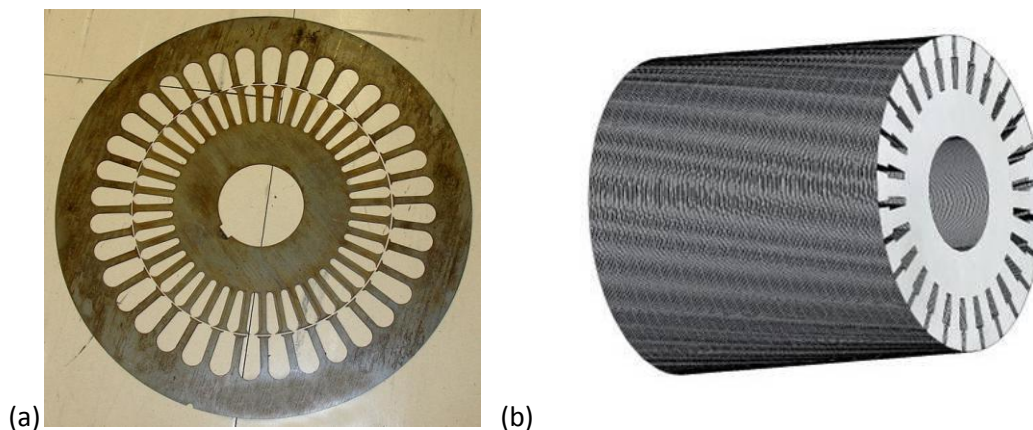
Figure 6: (a) Example of a stator and rotor lamination. Note the rotor lamination fits into the stator. Photo courtesy R. Bourgeois (16). (b) Rotor stack comprising laminations. Photo courtesy GM R&D (9).

The iron core cannot interfere with the induced current in the squirrel cage and is instead utilized for its magnetic properties. Therefore, keeping it as minimally-conductive as possible is absolutely essential.

16

As a result, the steel used to make the laminations is not typical mild steel, but is instead an electrical-grade steel with a non-conductive coating. In most electrical steel grades, this coating is an inorganic polymer. Organic compounds are often added to the inorganic coating, depending on the application. For the case of the two motors investigated in this project, the steel used is 35JNE250, indicating the gauge thickness is 0.35mm and utilizes an N-Core steel. This particular steel has an additional A-type coating, meaning an organic resin has been added to the inorganic base layer. According to JFE Steel Corporation (17), organic compounds bonded to an inorganic coating helps make the material easier to blank, while simultaneously increasing chemical, corrosion, and interlamination resistance. This is particularly useful for larger, home- and industrial-sized motors. Due to the specialized nature of the steel, effectively no scrap credit can be retained (13).

One of the more significant roadblocks to maximizing efficiency is the gauge thickness of the laminations. In order to minimize electrical conductivity and thereby minimize core loss through maximizing magnetic flux density, the laminations must be as thin as possible. Unfortunately, steel price (particularly the specialized type used in these motors) is inversely proportional to the thickness for very small thicknesses. As a result, while 0.35mm laminations are considered to be quite thin, JFE Steel Corporation is capable of producing as low as 0.1mm gauge thickness for very specialized applications (17). In addition to the added cost per kilogram of the raw material, the motor manufacturing cost also increases significantly due to the need for more laminations for a given motor size, as well as increased reject rates due to the increasingly fragile nature of the thinner motor laminations.

2.5   Types of Stators

2.5.1   Bar Wound "Hairpin"

There are three main types of stators. The first is the Bar Wound stator, and is the type of stator that will be considered in the two motor cases investigated in this project. Bar Wound stators have a conventional stator stack with slots, typically with two-to-four "hairpins" per slot. The hairpins are thick (~3mm) and are typically high-purity copper coated with an insulating polymer resin. Bar Wound stators are generally the most efficient of the three stator types, but also are the most expensive to manufacture, given the high labor costs associated with inserting, bending, and welding the hairpins. As of yet there is no straightforward means of automating the wire insertion and bending steps (13).
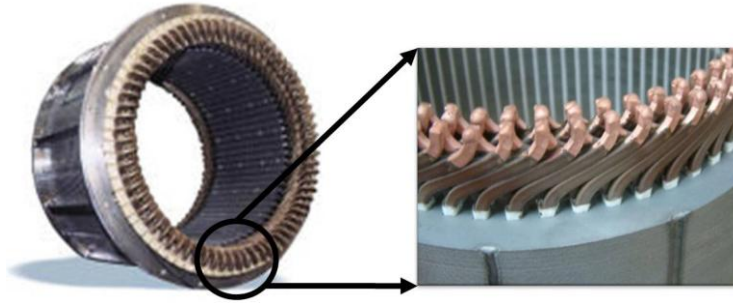
Figure 7: Example of a bar-wound stator. Picture on the right shows the hairpins. Photo on left courtesy General Electric (18)**; photo on right courtesy GM Powertrain** (19)**.**

2.5.2 Wire Wound "Conventional"

The Wire Wound stator is similar in construction to the Bar Wound, in that it utilizes a stacked-lamination core with slots, through which the windings are inserted. However, the windings are typically bunched-together sets of thin-gauge wires. The Wire Wound stator is typically less efficient than the Bar Wound stator due to the thinner-gauge windings. However, it is also less costly to manufacture, given that the windings are more easily manipulated.
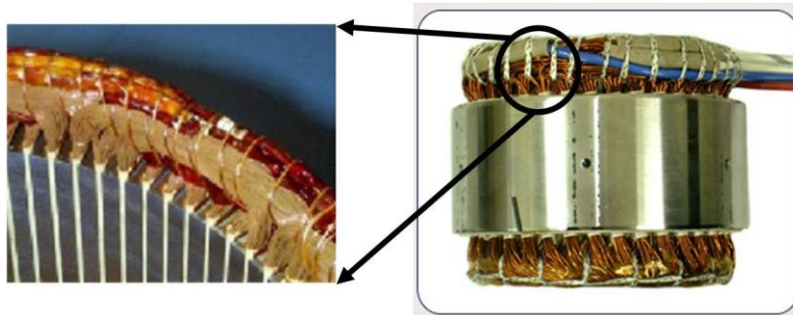
Figure 8: Example of a wire-wound stator. Photo on left courtesy GM Powertrain (19)**; photo on right courtesy Cletronics** (20)**.**

2.5.3 Concentrated Wound "Segmented"

The Concentrated Wound stator does not utilize the same construction as the previous two stator types, and is typically the cheapest to manufacture (21). Rather than blanking cross-sectional laminations, the stator is made up of many "nodes," where each node is made up of many small T-shaped laminations. These laminations are stacked, a plastic bobbin is installed to the stack, and the copper windings are wrapped around the bobbin. Each finished node is then installed around a center retaining ring. The Concentrated Wound stator is typically the least efficient of the three stator types (13, 22).

While the Bar Wound stator is the stator of focus for this investigation, optional steps have been added to the cost model to allow the end user (GM) to look into Concentrated Wound stators if so desired.
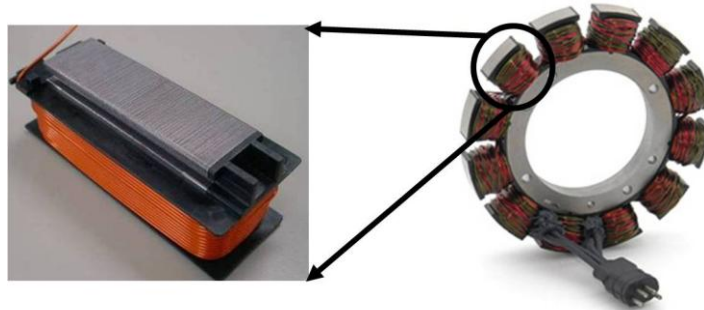
Figure 9: Example of a concentrated wound motor. Photo on left courtesy GM Powertrain (19); photo on right courtesy Honda (23).

2.6   Die Casting the Squirrel Cage

Die Casting is a process involving injecting molten metal at a high pressure (1,500 – 25,000 psi) into a mold or cavity (called a "die") in order to manufacture a part quickly and repeatedly. Typically, die casting is done with low melting temperature metals, given their typically lower cost of processing. Occasionally, higher melting temperature metals such as ferrous alloys are also used in die casting, but this is rare given the higher processing costs. Die casting is commonly used in high production volume applications to manufacture small- or medium-sized parts. An analogous process for plastics is injection molding.

Just as with any casting process, die casting requires a gating system. In fact, the gating system for die casting is often more complex than for other metal casting methods due to the high-pressure of the injected molten metal. Such a high pressure causes a significant amount of turbulence in the molten metal which can hamper filling of the mold cavity. As a result, a significant amount of engineering goes into the development of the gating system to promote as laminar a flow as possible. The die is usually significantly more complex than a pour-casting mold.

During the die casting process, the die is first coated in a mold release, to allow the finished part to quickly separate from the mold. In some die casting processes, the die is then heated to aid in wetting between the mold surface and the molten metal. The molten metal is then injected into the die, and the metal is allowed to solidify. The shot, which consists of the gating system + the final part, is ejected from the die using a strategic placement of pins which snap out of the surface of the die. Finally, the gating system is removed, the part is deburred, and the part then continues on for final-level finishing (often involving further machining steps and/or polishing).

The benefits of die casting include the quickest cycle time of all metal casting methods, which is vital for economical production of small metal parts. Additionally, very high dimensional accuracy and high surface quality can be achieved, often completely eliminating the need for subsequent machining operations. However, the die cast metal parts suffer from poor mechanical properties. The high amount of turbulence in the injected metal, coupled with the quick solidifying time cause a much higher amount of porosity in the finished part, thus decreasing the mechanical properties of the part. Furthermore, high production volume and low part weight are necessary to make the process economical (11).

2.6.1   Copper vs. Aluminum: Processing Tradeoffs

Using copper in the rotor as the conducting material (where aluminum has previously been used) has great potential to increase overall motor efficiency given copper's 60% higher electrical conductivity (7). Unfortunately, there are a number of difficulties presented when processing copper in place of aluminum. Table 1 shows the main processing tradeoffs when die casting copper vs. aluminum.

Cost Drivers	Aluminum Rotor	Copper Rotor
Material Cost	Density = 2.7 g/cm³, Price = $2.13 /kg	Density = 8.7 g/cm³, Price = $7.40 /kg
Energy	Melting temperature 660ªC No Preheated Dies	Melting Temperature 1080ºC Preheated Dies
Tool Life	200k shots with H13	4000 – 10k shots with H13 40k – 100k shots with Nickel-based alloys
Tool Cost	~ $ 45,000	~ $ 100,000
Auxiliary Equipment	Standard die casting	Temperature control is required and it is also necessary to preheat the dies
Furnaces	Gas or electric resistance	Induction

Table 1: Processing tradeoffs between copper and aluminum

As mentioned before, not only does copper have a high raw material price, but the higher melting temperature and density necessitate the use of more specialized tooling, higher-tonnage presses, and preheated dies (24).

2.6.2 Optimizing Die Casting

The gating system is of utmost importance when die casting. There are two ways to orient the gating system: centrally and at the side (11). Central gating systems have the gates positioned on-end of the end ring, as seen in Figure 10(a). Advantages to this configuration include homogenous filling of the end ring coupled with a limited risk of flash. However, disadvantages are significant and include increased wear at the gate area, uneven temperature distribution, a more complex die, and some inherent randomness as to how the gating system would break off at the end ring.

For the side gating system, the gates are oriented at the side of one of the end rings, as seen in Figure 10(b). Side gating systems have the advantages of inducing less wear on the gating area, having a more uniform temperature distribution, and can obtain a higher max pressure and utilize more of a "standard" die configuration. Disadvantages include the potential for poor filling behavior due to the gate location, as well as a greater risk of flash.

This project does not investigate the processing differences between the two gating configurations, and assumes the use of a more simplified side gating system. However, the model developed for die casting has the capability of dealing with the either type with the manipulation of a few key inputs.

(a)   (b)
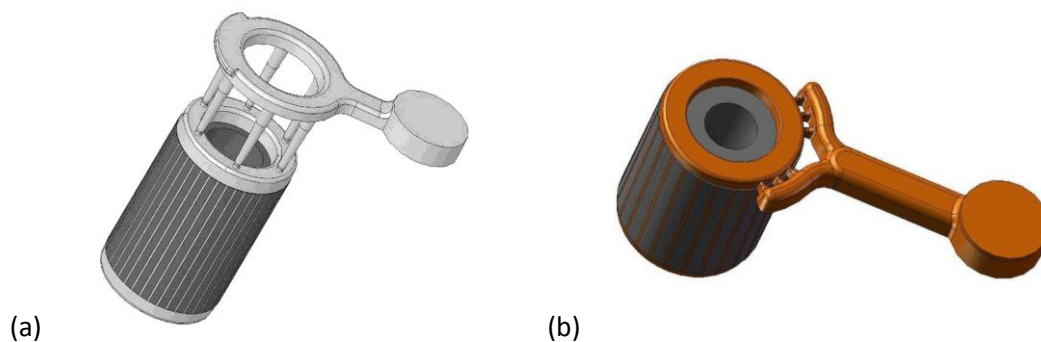
Figure 10: (a) Central gating system. (b) Side gating system. Both photos courtesy Buhler (11).

3   Problem Statement

Using copper in place of aluminum in the die casting process allows for a greater motor efficiency, which in turn allows for a decrease in motor size. However, copper is more expensive both to process and as a raw material. For the die casting step, the use of copper over aluminum demands increases in equipment, tooling, and cycle time, not to mention a material cost of three times that of aluminum. The improved efficiency also results in less expenditure on materials, equipment, tooling, and labor in many other motor manufacturing steps. Consequently, the purpose of this project is to investigate how savings from motor shrinkage compare to the expenses accrued from using copper.

When downsizing the motor, costs can be saved in the amount of raw material used, specifically the amount of steel needed to manufacture the stator and rotor cores, as well as copper for the pins and squirrel cage. Additionally, many steps associated with the production of these components are also affected. For example, less production time is required for the manufacturing of the stator and rotor laminations. Additionally, the cycle time for steps such as inserting and welding the pins into the stator also decrease. Furthermore, for a given die cast metal, reductions in motor size result in reductions in processing and material costs.

This project aims to understand the savings and costs involved in varying the size of the two motor architectures in response to the potential efficiency gains achieved by using copper. Specifically, is it possible to compare the expenses and savings in order to achieve a case where cost parity occurs? These motor architectures are both used for vehicle traction and would be in both hybrid and pure-electric vehicles. Despite these similarities, these motors are very different in both dimensions and output ratings. In a subsequent analysis, it would then be useful to know if this cost parity case yields a motor with sufficient performance numbers to that of the original, aluminum-based motor. Ideally, an understanding of the motor size-cost-efficiency relationship for comparing the small versus large motors would also aid in a better working knowledge of the project as a whole.

The final piece of the project involves a cursory investigation into alternative forms of induction motor manufacturing, and laying the framework for further, more detailed analysis. For example, specific methods investigated are Friction Stir Welding and Inertia "Spin" Welding (which are covered in more detail in Section 4.4.1), and are used as alternatives to die casting in the rotor manufacturing processes.

4 General Method

4.1 Overview

Process based cost modeling was chosen as the method to analyze the costs of the different motor designs using different conductive materials. Historically, cost modeling has functioned as a method to calculate cost for a given business based off a set of fundamental inputs using simple equations. Process Based Cost Modeling (PCBM) expands on this use, and focuses on the collection of manufacturing processes used to fabricate a given product. As a result, fundamental inputs include material properties, part descriptions, economic characteristics, and operating conditions. A detailed definition is covered below:

> PCBM is an analytical tool to calculate the cost of a manufacturing process by breaking it down into elemental process steps (25). Each steps' relevant costs rely on the governing engineering principles and equations therein, rather than on historical accounting data or rules of thumb. Consequently,

production costs can be investigated as a function of process variables that are sensitive to a change in the manufacturing process.

PCBM is intended to provide a map of a process description to an operating cost for a given manufacturing process. Its purpose is to appropriately inform the user so that s/he may make decisions concerning technology alternatives *before* operations are in place (26).

The first step in this analysis dealt with the development of a set of process based cost models to address the manufacturing processes used to produce induction motors, complete with all necessary steps for the two motor cases. The production of an induction motor involves numerous individual production processes each of which needs to be understood in sufficient detail to provide insight into the competitive economic position of each approach.

To aid with analysis, a better understanding is needed into the performance characteristics of general induction motor design (which was covered in more detail in Section 2), notably how the three performance metrics (Range, Power, and Cost) are affected by a change in a given induction motor architecture. While this particular study investigates these effects on the costs associated with motor manufacturing, it is also helpful (and arguably necessary) to also begin with an understanding into the size effects for both efficiency and power, in order to have a point of comparison.

4.2 Structure and Function of the Models

4.2.1 Performance Metrics

As mentioned earlier, there are three ways consumers measure the overall "effectiveness" of an electric vehicle: Range, Power, and Cost. From a motor design standpoint, range can be addressed by looking at motor efficiency. As discussed in Section 2.2, motor efficiency is defined as the power produced by the motor divided by the power taken in by the system. Since power is simply work-over-time, efficiency can be seen as either "power efficiency" or "energy efficiency;" both methods yield the same outcome. As a result, efficiency is unitless (typically expressed as a percent), and is a suitable way to express the effectiveness with which an electric motor converts energy (or power) into work (or work-per-time).

Another way of expressing motor performance involves comparing torque and horsepower of each respective motor. From a motor design standpoint, the output horsepower/torque of any given motor can be seen largely as a binary metric: either it is sufficient for the vehicle platform, or it is not (13, 14). As has been mentioned before, range can be understood by investigating efficiency, since the efficiency directly impacts the energy available for vehicle propulsion. That said, the ultimate driver behind this study is to understand the costs associated with each motor design while ensuring that the designs meet the required performance targets.

Induction motors are considered to be a cheap, albeit moderately inefficient solution for traction motors. As a result, only two metrics are investigated in this study: cost and efficiency. Consequently, a

tool is needed to better understand these costs for each motor design, which is manifested in the form of a series of linked process based cost models. Each design is also evaluated on the basis of efficiency, and furthermore efficiency is used to provide a way to discuss motors that have similar levels of performance. In that way, motors that have copper in place of aluminum in their conducting squirrel cages can be resized for comparable performance giving a more clear picture of the relative economics of the use of copper and aluminum. The efficiency metric also allows for a way of comparing motors, regardless of individual dimensions and specifications.

4.2.2   Manufacturing Process Overview

In Sections 2.1 and 2.3, the components of the induction motor are outlined and the general structure of the manufacturing process is briefly touched on. Many steps are involved in the induction motor manufacturing process. First, the stator and rotor cores need to be manufactured. The incoming steel coil is slit to the proper width and subsequently blanked, at which point the loose laminations continue on to an annealing step (27). From here, the stator laminations are stacked and joined using TIG welding, though laser welding may be used instead. The rotor laminations, on the other hand, are stacked into a die casting press and molten aluminum (or copper) is injected into the rotor core to make the squirrel cage. The rotor cores then are deburred and a keyway is broached. If Al 6101 is used, the rotor cores are also heat treated for increased strength (13).

As for the stator, the stacked and welded cores are ready to be assembled into finished stators. The stator slots are insulated and paper-like sleeves are installed, at which point copper "hairpin" windings are installed into the slots. The pins are then crowded, bent, and organized in order to be trimmed and subsequently welded to one another in the pattern the specific motor architecture dictates. To protect the stator from possible electrical shortage, the windings are covered in epoxy and tested. The laced stator core enters a cursory machining step to lathe both the ID and OD, and the housing is installed onto the finished stator (28).

For the rotor, a hub is installed and staked into its ID, at which point the rotor is balanced and further deburred. Bearings are then installed onto the ends of the rotor, and the entire armature is tested and a rust-resistant coating is applied. The finished rotor is complete and ready for installation into the stator (28).

4.2.3   Dividing the Process into Four Total Models

To aid in the modeling process and to provide an easier platform to view the cost results more clearly, the total manufacturing process was divided into four primary steps and cost models were created for each. Two of these models dealt with the steps of the process typically done by the automaker, while the other two models covered the steps typically done by suppliers.

The induction motor process can be seen as two separate lines (one for the stator and one for the rotor), beginning at the same point, diverging into separate models, and finally converging to a common final model. For this project, models previously developed at General Motors were employed for the process activities typically done directly by the automakers. Given the direct experience GM had with these processes, their existing cost models were deemed to have more than the accuracy needed to address the cost issues arising from the use of copper versus aluminum in the rotors. However, due to their limited direct experience with the remaining manufacturing processes and the high degree of uncertainty regarding these processes, new process based cost models needed to be constructed to the address the costs arising from these activities. In addition, a "summary model" that pulls together all four of the individual process based cost models was also developed to allow for ease of analysis and to ensure that all data flowed correctly between the various steps (despite not containing any manufacturing steps itself). Given that all four models have many of the same inputs (for example, Exogenous Variables, part description, etc.), they could all be linked together in the Summary Model. A final advantage to this organizational method is that nearly all of the necessary data tables and charts would be displayed on one model. The relationships among the various cost models and the summary model are shown in Figure 11.
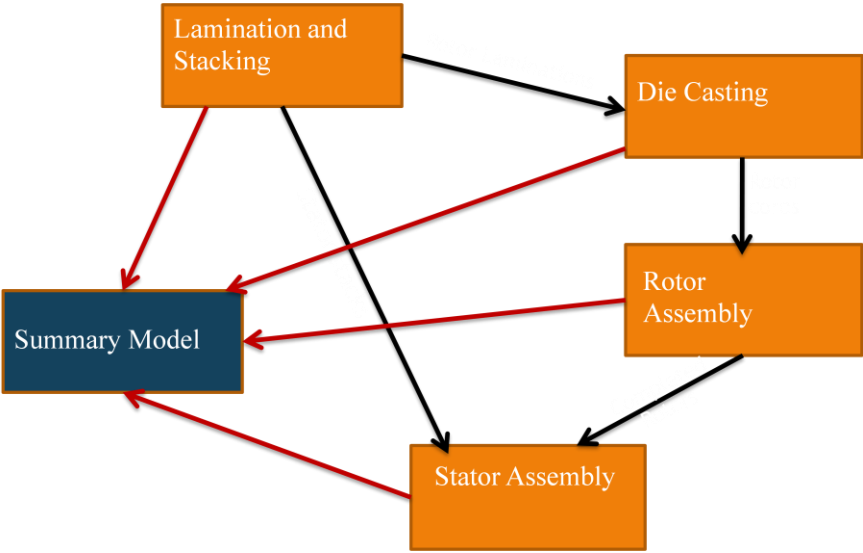
Figure 11: Broad process breakdown illustrating how each of the models interact.

As is evident from Figure 11, the overall analysis begins with the Lamination and Stacking model. From there outputs describing the loose rotor laminations are used as the inputs to the Die Casting process model, which provides outputs about the completed rotor cores to the Rotor Assembly process model. For the stator line, information about the completed stator stacks are the output from the Lamination and Stacking model, which, in the model architecture, function as the inputs to the Stator Assembly

process model. Finally, the completed rotors and the finished stators are then combined and final assembly is performed (where all associated costs are accounted for in the Stator Assembly model).

4.3   Model Breakdown: Lamination and Stacking

The Lamination and Stacking model address the initial steps in the entire manufacturing process, and would typically take place at a supplier's manufacturing location. A detailed model of this step including all individual sub-process steps was built. Many optional steps that address activities not typically done today, but show promise in the future were included in the model to provide the ability to address different technological considerations at a later date. Since the current analysis did not require the use of these optional steps, they were simply "turned off." Additionally, the models were built in a way to allow the addition of new features if so needed for investigating different motor architectures in the future.
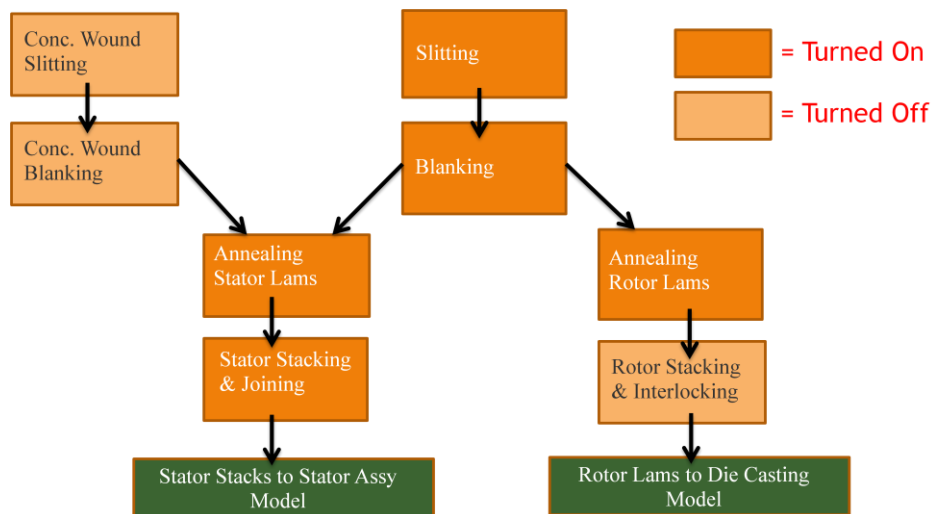
Figure 12: Process breakdown for the Lamination and Stacking model.

Figure 12 illustrates the specific steps which are accounted for in the Lamination and Stacking model. The initial two steps are not unlike any other straightforward blanking step, involving first a slitting and second the blanking step itself. As alluded to before, in most motor cases the laminations are blanked as a unit, with the stator lamination blanked at the same time as the accompanying rotor lamination, using a progressive die operation (Figure 13). However in some instances, such as when the air gap between the rotor OD and the stator ID is too small, the stator and rotor must be blanked separately. In addition, the rotor stack is defined as slightly longer than the stator stack (typically by ~5 mm (13)), meaning more rotor laminations would need to be produced than stator lams. One way to accurately deal with this discrepancy is to manufacture the additional amount of rotors separately from the rest of

the laminations. However, this results in a large amount of scrap and extra tooling for the rotor alone. Another method is to blank the total number of rotor laminations needed (which would also blank the same number of stator laminations), and simply throw the unneeded stator laminations to scrap. Unfortunately, it is not clear which approach would be taken in the real world manufacturing applications. Instead the model simply used the average number of laminations needed when calculating costs[4]. While this introduces some inaccuracy, it is considered to be very small given the very high volume of laminations needed to make the annual volume of motors likely to be produced.

Figure 13: Example of a progressive die for a 2-pole motor. Note how the entire lamination is not blanked all at once; instead, each feature is blanked using multiple presses. This ensures accuracy of the finished part. Photo courtesy Zhenyu Mould Co., Ltd (29).

After blanking, both the stator and rotor laminations are placed in loose stacks, bound with a wire, and go to an annealing step. For simplicity's sake, it was easier to model the stator lamination and rotor lamination annealing as being separate steps, though in reality the laminations go together to the annealing oven. From a cost standpoint this assumption leads to little to no inaccuracy since at high production volumes, the annealing ovens would be expected to be fully utilized and thus the costs would not depend on the configuration of the laminations within the ovens.

From here, the stator laminations get pressed together and a small bead of weld is applied to hold the stack together. For this particular process, TIG is welding typically used. Assuming the squirrel cage is die cast, the rotor laminations need not go through the optional independent "stacking and interlocking" process, but rather continue directly to the die casting process where they are stacked and pressed together directly in the mold. These activities are covered in the Die Casting model. As is noted in Figure 12, this model has the capability of dealing with steps that can be turned either on or off,

---

[4] This is accomplished by adding the number of laminations per stator and rotor, respectively, and dividing by two.

depending on what type of motor architecture is of interest. Figure 15 indicates which of these steps are turned on and off for the standard die cast induction motor architecture.

Generally speaking, annealing is a thermal process used to remove stresses present in a material. The material is held at a temperature well below the creep temperature of the material for extended periods of time (typically on the order of a few hours) resulting in improved electromagnetic properties (as well as changes in the mechanical properties of the material). For motor applications, annealing is typically performed in a continuous process, though sometimes batch processes are specified. For this application, particularly at high annual production volumes, batch processing is typically slightly more expensive than continuous processing due to the increased production time and less efficient use of heat. However, at lower production volumes, batch annealing may be cost effective (30). Specific annealing procedures are considered to be proprietary information, and therefore the inputs to this process are user-defined. In the model, the user has the capability of utilizing either batch or continuous processing based off of the inputs s/he selects.

Interlocking is a method of joining a stack of laminations together, involving the interlocking of male-female indentations on each rotor lamination under the application of a very high force. Figure 14 shows an example of an interlocked stator stack. For the standard die cast induction motor, this step is bypassed because it is unnecessary – the stacking is accounted for in the die casting steps, and the interlocking is effectively the die cast squirrel cage, holding the laminations together tightly.
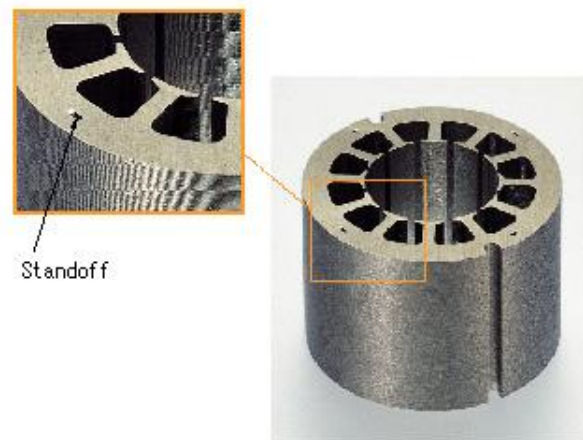
Figure 14: An example of an interlocked stator stack. Here, the interlocking point is referred to as a "standoff." Photo courtesy JFE Steel Corporation (17)**.**

The Lamination and Stacking model also allows for the implementation of other optional steps as well. If, for example, die casting was not to be performed (such as with other methods of manufacturing the squirrel cage, or with a permanent magnet motor) then the Rotor Stacking and Interlocking step would be turned on. It is worth noting that some motor geometries do not call for an annealing step. If this

happens, then the rotors would be stacked and interlocked at the blanking step, thus having no need for the standalone rotor stacking and interlocking step. If this causes an increase in cycle time for the blanking step, the model user should change the associated input accordingly (though for most motor architectures, the interlocking can be done within the cycle time of the blanking press (13)). Neither of the two cases investigated in this thesis make use of this feature, but are provided for analysis of different technological approaches and designs in the future.

The other optional steps integrated into the Lamination and Stacking model are those to manufacture the blanks necessary for a concentrated wound stator. Given the significantly different processing required to manufacture a concentrated wound motor, it was easiest to simply add steps that would account for this change in manufacturing method. Additionally, the slitting/blanking processes used for concentrated wound motors are addressed separately from those analogous processes in the conventional motors (i.e., bar-wound and wire-wound stators) since the process requirements are very different (22). Finally, given that the majority of the analysis of concentrated wound stators was to be independent from the rotor manufacturing process, only one of the blanking types can be turned "on" at a time[5].

4.4   Model Breakdown: Die Casting and Rotor Core Manufacturing Model

The Die Casting model handled the final steps in manufacturing the rotor core (i.e., the parts sourced to other companies to manufacture), but not the rest of the rotor assembly after the finished cores are manufactured. This means that the final steps in rotor manufacturing are dealt with by the Induction Rotor Assembly model, which is dealt with in Section 4.5. As mentioned above, the inputs to the steps covered in this model are the outputs of the Lamination model that concern only the rotor, meaning that no stator components are involved with this part of the process. In the standard production process, the loose rotor laminations are stacked in the die casting press. From here, the die is preheated and injected with molten die cast metal. Because the rotor lamination stacking and heating can be done completely within the cycle time of the die casting, there is no need to model them as a separate step. The rotor cores then continue on to a deburring step, and then to a keyway broaching step, which is necessary in order to install the hub through the axis of the rotor (which is covered in the following model).

An optional heat treating step is also considered. For copper, this step is not necessary, and is only necessary for one type aluminum: Al 6101. Typically, high-purity aluminum is used in induction motors, but occasionally Al 6101 must be used to achieve required efficiency enabled by its slightly higher electrical conductivity. However, Al 6101 does not have adequate strength to cope with the high spinning loads placed on the rotor during motor operation, and therefore must be heat treated.

---

[5] This means that the conventional slitting/blanking steps are to be turned "off" when the concentrated wound stator slitting/blanking steps are "on," and *vice versa*.

The final step accounted for in this model deals with application of a protective coating. This step is primarily intended for magnesium die casting, and given magnesium's relatively low electrical conductivity, this process is currently not considered in any of the analyses in this thesis. From here, the completed rotor cores continue to a series of assembly operations which are modeled in the Induction Rotor Assembly model.
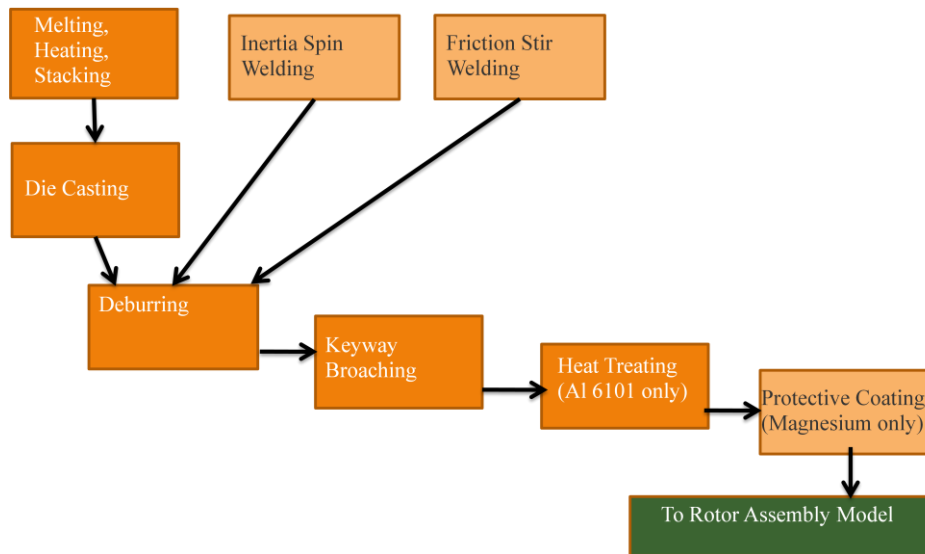
Figure 15: Process breakdown for the Die Casting model

4.4.1   Alternatives to Die Casting for Squirrel Cage Manufacturing

There are two ways in which the squirrel cage can be introduced to the rotor core that do not involve die casting. Both methods involve inserting pre-extruded copper (or aluminum) bars into the rotor core and placing premade end rings on the ends of the stack. However, the method of joining the bars to the end rings varies with the two methods.

Friction Stir Welding is a solid-state process to join two (often dissimilar) metals together that utilizes the principles of plastic deformation and creep in metals. A spinning spindle holding a blunt probe is inserted below the surface of the metal and given that the metal is not molten, creates a significant amount of heat due to friction (Figure 16). This heat is sufficient to induce localized creep around the tip and, through the application of a significant amount of lateral force, is able to move the probe through the solid metal, causing the wake metal to flow together, thus creating a homogeneous weldment in the metal. Friction Stir Welding is an excellent method of joining two materials if maintaining microstructure is important (i.e., minimal heat affected zone is created) and subsequent heat treatment or annealing is not possible. As a result, FSW is often done with aluminum (31).
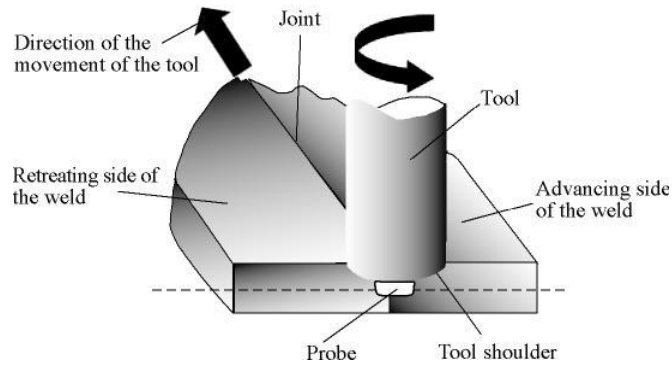
Figure 16: Friction Stir Welding tool setup. Photo courtesy Somasekharan et al (31).

Inertia "Spin" Welding is another method that provides an alternative to die casting. The principles behind Spin Welding are quite similar to those in FSW, but the tooling and methods of achieving creep are significantly different. In Spin Welding, the rotor stack with inserted rotor bars is held stationary while the end ring is held in a spinning fixture and forced on the end of the rotor core with a high force until the copper (or aluminum) of the bars and end rings heats up enough to induce creep and subsequent homogenization of the two materials (see Figure 17) (13).

(a)   (b)
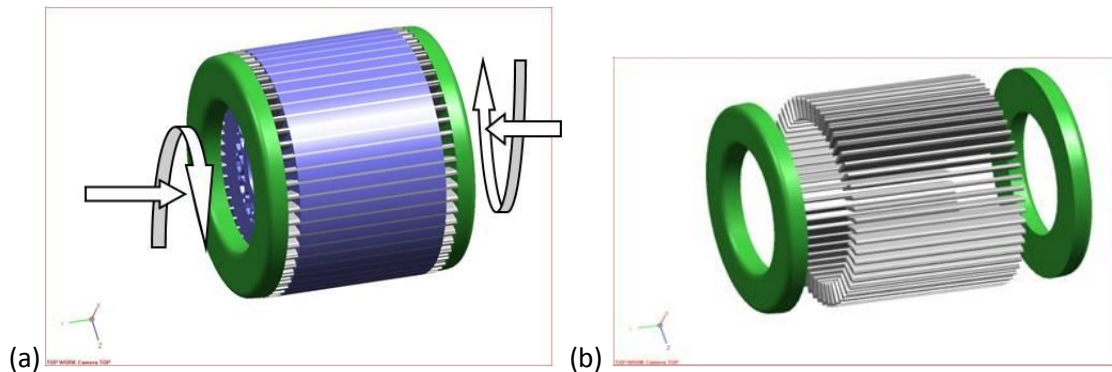
Figure 17: Spin Welding. (a) How forces are applied to the rotating end rings. (b) The construction of the squirrel cage. Photos courtesy GM (9).

One of the significant downsides to using the aforementioned two steps is given current technology restraints, zero skew can be dialed into the rotor geometry. This will decrease the efficiency of the motor, as well as its ability to counter harmonic issues throughout the rev range (14).

4.5   Model Breakdown: Induction Rotor Assembly Model (28)
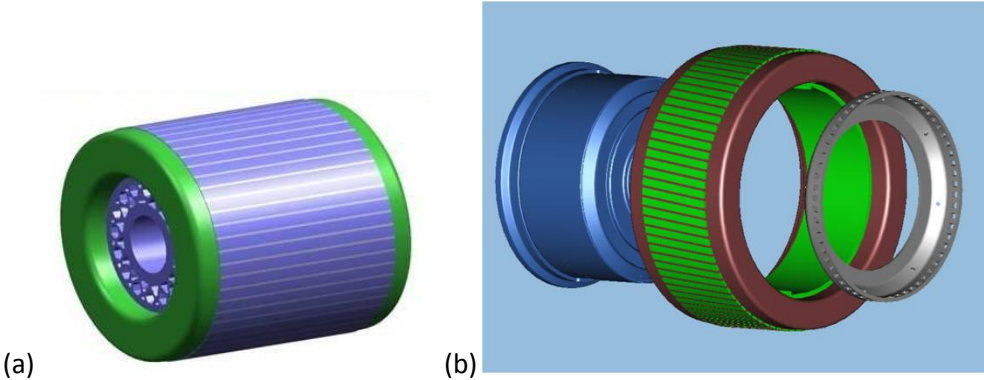
Figure 18: (a) Example of a rotor core. (b) Assembly of the hub (blue) to a rotor (red/green). It is staked in using the grey ring. Note that the rotor in (a) is for a different motor than (b). Photos courtesy GM (9).

The rotor assembly process begins at the point in the manufacturing process where rotor cores (Figure 18(a)) have already been made and the squirrel cage has been die cast. These steps are analyzed using a pre-existing Induction Rotor Assembly model (28). The rotor assembly process starts with an inspection of the rotor after which the tonewheel is installed. The rotor is then balanced, the bearings are assembled, the rotor is tested, and a rust preventative is added to the surface of the rotor. The finished rotors are now complete and ready for final installation. The inputs the model uses to calculate costs are largely user-defined, and many aspects such as material costs (e.g., hub cost, bearing cost) must be manually changed for different motor dimensions.
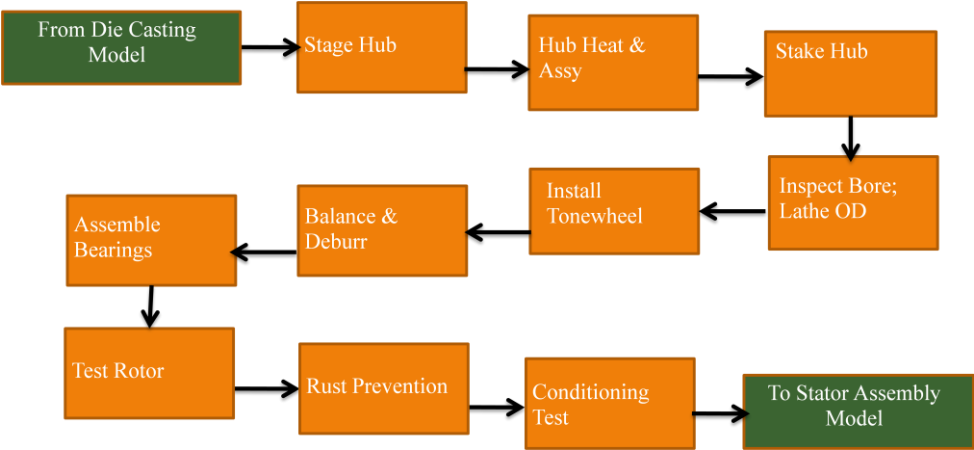
Figure 19: Process breakdown for Induction Rotor Assembly model

4.6   Model Breakdown: Bar-Wound Stator Assembly Model (28)

To obtain a complete motor, stators must also be assembled and the complete rotors then need to be added to those stators. These activities are modeled in the Bar-Wound Stator Assembly model. Given that the stator stacks are merely cores at this point, the vast majority of the process steps focus on the final manufacturing of the stators.
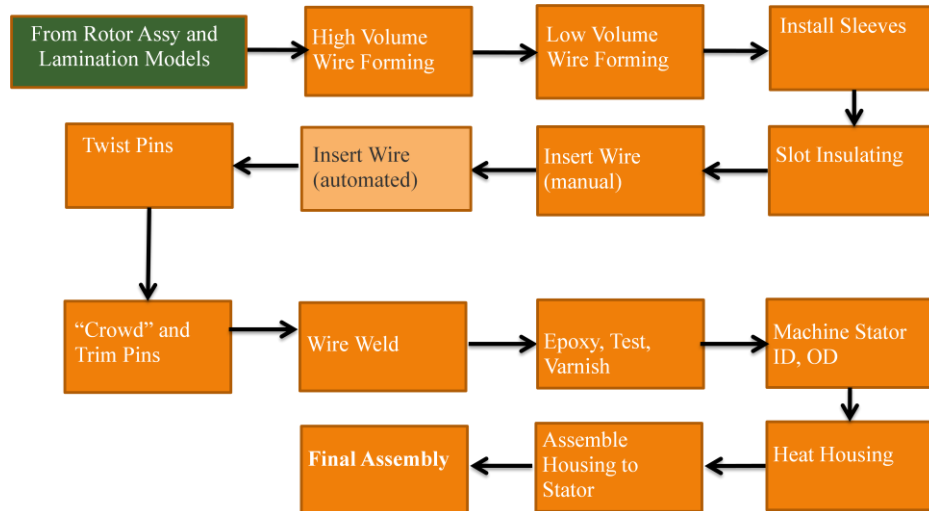
Figure 20: Process breakdown for Bar-Wound Stator Assembly model

The first steps of stator assembly involve the forming and insertion of the hairpins into the stator slots. There are two types of hairpins used, and are slightly different in construction (hence the need for two different forming steps; one for high volume, one for low). The high-volume pins (or "wires" as they are referred to in the model) make up the vast majority of the pins inserted into the stator core, while the low-volume pins are slightly different and are much fewer in number. Given that each pin's direction and orientation relative to the next is of critical importance with regard to current flow, motor design calls for a low number of pins to be slightly different in construction to those typically used.

After the wire stock is formed, thin paper sleeves and insulation are installed into the slots in the rotor to protect the copper windings from shorting. At this point, the formed pins are manually inserted into the insulated slots. The wire insertion step is currently performed as a manual operation (i.e., labor-intensive) and as of the time of writing this no automated solution has been found. The pins are then twisted, oriented, and trimmed to equal length for the following step: wire welding. Figure 7 shows this particular construction. From here, the wires are coated in epoxy to aid in insulation and corrosion protection. The stator is then tested to ensure continuity. The stator ID and OD are then machined to ensure proper fitment of the rest of the components.

Currently housings are typically necessary to hold all motor components together, and the entire assembly is installed to the vehicle transmission. However, for future iterations of traction motors, it may be possible to remove the motor housing by allowing the transmission to play this role, thus decreasing overall system weight and hopefully reducing cost. The cost model considers both possibilities.

Once the housing is installed and assembled to the stator, the rotor and ancillary components are installed in the Final Assembly step.

5 Analytical Methodology: Downsizing

5.1 Overview

Given the increase in efficiency that can be had when using copper over aluminum as a squirrel cage material, the motor can be decreased in size to bring the efficiency back to that of the original aluminum motor. This particular sensitivity analysis only analyzes the cost effects when downsizing a given motor, meaning that power- and efficiency-oriented optimization is not explicitly investigated. That said, the Efficiency Analysis was utilized to provide benchmark points of interest on which to center the cost-size investigation (8) The resulting effects on power and efficiency from downsizing a given motor architecture to XX% are not investigated and would be of interest for subsequent analysis. However, the analysis does attempt to investigate cost effects surrounding aluminum- and copper-based motors with equal efficiency, and compare these results to those for points of cost parity.

All of the downsizing performed in this analysis for a given motor architecture is based on the original dimensions of that motor, and downsizing to 60% of the original size is the minimum for this analytical consideration. This means that the motors' fundamental dimensions are scaled down, from 100% to 60% of the original size. Realistically, a motor smaller than 60% of the original will not have the performance requirements necessary for its vehicle platform and therefore is unnecessary to consider. Additionally, as the motor is downsized, the uncertainty of any given variable increases and therefore bears less and less functional resemblance to the original motor architecture. Finally, preliminary analyses showed that the motor cost scales straightforwardly until a given point (~60%), when the cost of additional components scale down enough to warrant their own decrease in cost (e.g., rotor bearings, tonewheel, housing design). For small decreases in motor size, it can be assumed that the same initial motor geometry will be used. However, for significant decreases in motor size, it becomes entirely possible that a completely different geometry could be a better solution altogether. In sum, the likelihood that a copper-based motor 60% of its original size will be sufficiently replaceable for the original aluminum-based motor is almost zero, and therefore conducting analyses for smaller than 60% is purely academic.

5.2 Downsizing by Length vs. Diameter: General Trends

There are two main ways by which the motor can be downsized based off of the assumptions outlined in the previous section. The first (and most straightforward) involves decreasing the length of the motor while keeping the diameter constant. Likewise, the other downsizing method is to decrease the diameter of the motor while keeping the length constant.

If motor geometry was the only component affecting total motor cost, it is immediately noticeable that the amount of material used in the motor will vary depending on which downsizing method is used, given that the volume of the motor varies linearly with length and quadratically with radius:

$$V = \pi r^2 l \tag{4}$$

As seen in Table 2, downsizing via length affects the practical aspects (performance and cost) similarly, but for different mechanisms. As the length of the motor is reduced (with constant diameter), core loss is also reduced, given that the amount of core loss inherent in a motor is directly proportional to the length of the motor. Additionally, the output torque of the motor is decreased due primarily to a decreased current capability[6] in the smaller motor. The smaller rotor induces a weaker total magnetic field, resulting in a lower output torque. Given that both output torque and core loss decrease with motor length, the resulting motor efficiency is also reduced. On the other hand, when downsizing via diameter (keeping length constant), the core loss stays roughly constant, given that the length has also remained constant. Output torque, on the other hand, decreases due simply to a smaller moment from the surface of the armature to the axis of rotation. As a result, efficiency does not scale as straightforwardly as when decreasing by length (14). The precise decreases in efficiency with motor size are not investigated in this portion of this project and should be of interest to the motor designer.

By Length (Constant Diameter)	By Diameter (Constant Length)
Core Loss is proportionally reduced	Core Loss remains constant
Output Torque decreases	Output Torque decreases
Efficiency decreases straightforwardly	Efficiency does not decrease straightforwardly

Table 2: Differences between decreasing via length vs. via diameter.

When downsizing via the two different methods, the squirrel cage itself is differently-affected. When downsizing by length, the amount of copper in the die cast end rings remains constant, while the squirrel cage itself is shortened (but maintains the same number of bars). When downsizing by diameter, the overall length of the squirrel cage remains constant, but the number of bars needed

---

[6] Generally, for a given input voltage, raising input current will also raise the output torque of the motor. Likewise, for a given current, raising voltage will tend to increase the maximum power the motor can produce (14).

decreases, as does the amount of copper for the end rings. This means that the material reduction for a given percent reduction is greater for downsizing by diameter than it is when downsizing by length.

In addition to the amount of material reduction in each downsizing method, the processing costs associated with the die casting process will also change, depending primarily on the type of material used, but also on the relative amounts of material. Given that this size relationship affects more steps in the manufacturing process than simply die casting, this project aims to address these steps, explain in what way these steps are affected, and illustrate by how much. The steps affected are in Table 3:

Steps Affected by Each Downsizing Method	
By Length:	**By Diameter:**
• Slitting • Blanking • Die Casting • High Volume Wire Forming • Low Volume Wire Forming • Stator Housing	• Slitting • Blanking • Die Casting • High Volume Wire Forming • Low Volume Wire Forming • Stator Housing • Wire Welding • Slot Insulation • Wire Insertion • Hub Heating & Installation

Table 3: Steps affected by different ways to downsize motors: by length and by diameter. Not only does by-diameter downsizing affect more steps than by length, it also differently affects the same steps as by-length.

5.2.1 Downsizing by Length: Steps Affected

For the slitting and blanking steps, less total material is needed to be cut and blanked due to the decreased stack heights. Less time is spent slitting and blanking (thus lowering processing costs), as well as less actual material is being consumed, and a lower cost for equipment. Die Casting is downsized for the aforementioned reasons, and affects both processing and material costs, in that less material used decreases the cycle time of the process by reducing the time required to cool the part. For the amount of downsizing investigated in this study, the amount of downsizing the hub experiences due to shorter motor length is minimal, if at all (13). Severe decreases in motor length may allow for reductions in hub and bearing size, but not for the small reductions investigated in this study[7]. Both High and Low Volume Wire Forming costs are decreased due to the need for less material per-pin. However, the total number of pins and the time to form them remains constant (i.e., processing cost remains unchanged). Stator housing scales with the outside stator surface area; installation time is unaffected but the material needed for the stamped metal housing is decreased.

---

[7] As an example, a reduction of 25% by length in one motor case results in only a 17.5 mm reduction in motor length.

5.2.2 Downsizing by Diameter: Steps Affected

The slitting and blanking steps are affected differently to the By Length scenario, in that the processing costs are not affected, given that the actual number of laminations to be produced remains unchanged. Instead, the total amount of steel consumed is decreased due to the reduction in motor diameter. For die casting, a smaller diameter results in less material usage, lower processing costs (due to decreased cooling time), and, for significant reductions in diameter, potentially allows for decreases in tooling and equipment cost. High and Low Volume Wire Forming costs are decreased due to fewer pins being needed, which decreases both material and processing costs. Again, the amount of material needed for the stator housing decreases more steeply than By Length, but installation time and other aspects associated with processing cost remain constant. Wire Welding, Slot Insulation, and Wire Insertion processing costs decrease due to the need for less time per stator (i.e., there are fewer pins to insert, insulate, and weld). A very slight decrease in slot insulation material is expected for the same reasons. Finally, the rotor hub material cost is decreased due to decreasing rotor I.D. Heating time also decreases marginally (quicker heat transfer) but installation time is remains unchanged.

5.3 Efficiency Analysis (8): Understanding How Downsizing Affects Efficiency

It is desirable to be capable of understanding the size-efficiency relationship for induction motors, so that benchmark points can be identified and subsequently analyzed. While the goals of this project are to investigate points of cost parity for various motor cases, it is important to be able to compare these points to those for efficiency parity in order to accurately inform decisions on the manufacturing process. While analytical models do exist to be able to perform this type of efficiency analysis, it was beyond the scope of the motor cost-size work performed in this study.

One such model was developed by Dr. James Kirtley of the Electrical Engineering and Computer Science department at MIT and looked into the effects of using copper in place of aluminum in the squirrel cage of induction motors for vehicle traction purposes. Dr. Kirtley's analysis, to be henceforth referred to as the *Efficiency Analysis*, also investigated the efficiency, power, and torque effects when downsizing the motor by length, although an analysis of downsizing by diameter was not pursued (8).

The Efficiency Analysis is Matlab-based and uses a set of inputs specific to a given motor case based on characteristics such as stator and rotor ID and OD, the size and shape of the rotor slots and copper/aluminum therein, and the operating current, voltage, phase, and number of poles. Once a baseline is achieved (i.e., the aluminum motor), the model is then modified according to the new materials used and/or motor dimensions.

6 Motor Architecture #1: BAS+

Now that the two methods of downsizing can be understood, it is important to apply this methodology to two different motor cases, both motors developed by GM. The two motors are intended for vehicle traction purposes and have not yet reached production. The goal of the following analysis is to inform decisions to accurately determine the correct course of action for these two motors.
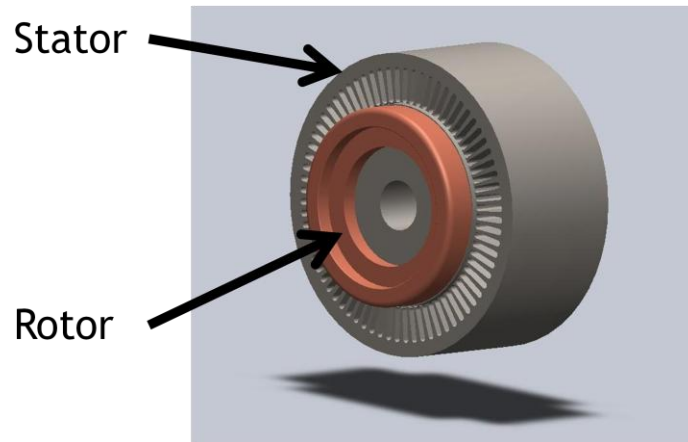
Figure 21: Very simplified model of the BAS+ architecture. Only stator and rotor cores are shown. The inside edge of the stator slots delineates the inside diameter of the stator (and therefore outside diameter of the rotor).

6.1 Motor Description

The BAS+ is a small induction motor designed by General Motors with a low horsepower (13 hp) rating and is not explicitly intended for traction purposes in electric vehicles. Instead, it was designed to act in conjunction with an engine to boost the power (and torque) output of a vehicle during off-the-line acceleration. One application the BAS+ has seen most regularly has been in ICE-powered vehicles[8] that have the ability to turn the motor off while idling (e.g., at stoplights). The electric motor is then required to start the vehicle accelerating while the ICE turns back on, at which point the vehicle continues driving largely under the power of the engine (13).

Another potential application for the BAS+ has been in hybrid vehicles. Recent concepts have involved a smaller, inline-4, turbocharged engine with a battery pack and BAS+ motor. At low-RPM acceleration, the small-displacement engine will increase fuel economy, while the turbocharger will enhance high-rpm power. The electric motor would then be used to further increase low-rpm power without the reduction in power that would ordinarily be seen by using a larger-displacement engine (32, 33).

---

[8] ICE (Internal Combustion Engine) is the conventional style of engine found in a motor vehicle, requiring the burning of a fuel (often gasoline or diesel) in order to produce work.

Table 4 shows the standard motor dimensions for the standard aluminum motor. The standard aluminum BAS+ was previously analyzed to determine its efficiency as a way of providing a consistent baseline for the cost analysis performed in this report. According to the Efficiency Analysis, the standard aluminum motor has an efficiency of 66%, producing 13 hp (9.7 kW) and 57 ft-lbs (77 N-m) of torque, with a power factor of 79.5%. When substituting copper directly for aluminum in the squirrel cage manufacturing (and keeping all other parameters constant), the efficiency and power factor increase to 77% and 81%, respectively. The output horsepower stays constant at 9.7 kW, and output torque increases slightly to 79 N-m (58 ft-lbs). Additionally, the motor weight increases due to the higher density of copper[9]. According to the Efficiency Analysis, this use of copper causes an increase in motor efficiency of approximately 15% (8).

Table 4 also shows how size varies for all of the cases investigated for the BAS+. The first two cases are identical in size, but the second uses copper in place of aluminum in the squirrel cage manufacturing. The third case, to be discussed in Section 6.2, analyzes the point of equal efficiency to the standard aluminum baseline case. The fourth and fifth cases look at motor downsizing by diameter, with the fourth case achieving equal cost to the "optimized" (3rd) case, and the fifth achieving cost parity to the standard aluminum baseline. The fourth and fifth cases will be discussed in Section 6.3.

	Standard Aluminum	Copper, Equal Size	"Optimized;" 90% Length Copper	96% Diameter Copper	88.5% Diameter Copper
Total Length (mm)	106.1	106.1	99.1	106.1	106.1
Stator OD (mm)	144	144	144	138.5	127.7
Rotor OD (mm)	96.2	96.2	96.2	92.3	85.1
Rotor ID (mm)	23.8	23.8	23.8	23.1	21.3

Table 4: Important dimensions of for the BAS+, and how it scales for each motor case. The third case is relevant to downsizing by length, while the last two cases are relevant for downsizing by diameter.

6.2   Baseline Results: Standard Aluminum vs. 90% Length Copper Motors

The Efficiency Analysis indicates that due to the 15% increase in efficiency when switching from aluminum to copper in the squirrel cage manufacturing, the resulting copper motor can be downsized by 10% in length in order to reach the same efficiency as the original standard aluminum case. Figure 22(a) shows the cost breakdown for the standard aluminum motor, broken down by each model's contribution to total motor cost. It should be noted that aluminum die casting contributes very little cost to the process. Figure 22(b) represents the cost breakdown for the 90% length copper motor,

---

[9] Copper has a density of 8.96 g/cc versus aluminum's density of 2.70 g/cc.

referred to as the "Optimized Motor." As is expected, copper die casting greatly increases overall motor cost. However, the cost contributions from all other process steps have decreased. For the purposes of the following figures, the results from the Lamination and Stacking model is divided into the costs for the stator and rotor laminations, respectively. This is done because the manufacturing methods needed for the stator and the rotor are slightly different.   From Figure 22(b) it is apparent that the cost of the optimized motor is still significantly higher than for the standard aluminum, despite the size reduction enabled by the efficiency gains.

From a manufacturing standpoint, the BAS+ is a rare exception in that the stator and rotor laminations are blanked separately (13). This manufacturing method is necessary when the air gap specified in the motor is too small to blank the stator and the rotor as a unit. As a result, the slitting and blanking costs are significantly higher than they might be in cases when these components can be blanked simultaneously from a single sheet of metal.
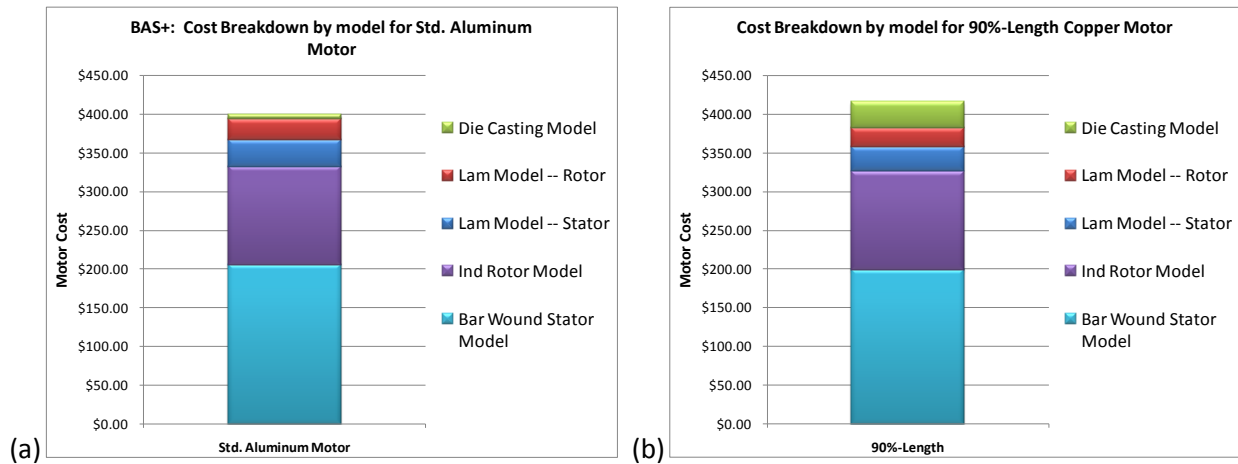
Figure 22: (a) BAS+ Cost Breakdown by model for the standard aluminum baseline. (b) Cost Breakdown by model for the 90%-length copper motor. BAS+.

Figure 23(a) shows the cost breakdown for the standard aluminum motor. Even without the use of copper die casting, incoming raw material is the single largest portion of the motor cost. Figure 3(b) shows the cost breakdown for the Optimized Motor. Note that the material usage increases only roughly one percent when switching between the two motor cases. As will be seen later, the ~$20 increase in material usage when die casting copper over aluminum is offset by the reductions in other steps' material use (e.g., the number of steel laminations produced), resulting in a net increase of ~$12, or 1%. However, the use of copper does cause changes in other areas as well. Figure 24(a) and (b) shows the cost breakdown for the Processing Costs for the standard aluminum and Optimized motors, respectively. If one combines the direct and overhead labor, this accounts for the largest cost, with equipment making up a noticeable portion as well. One area that increases significantly when switching

to a copper motor design is the tooling, which despite decreases in some of the other manufacturing steps, experiences a significant increase due solely to the use of copper in die casting.
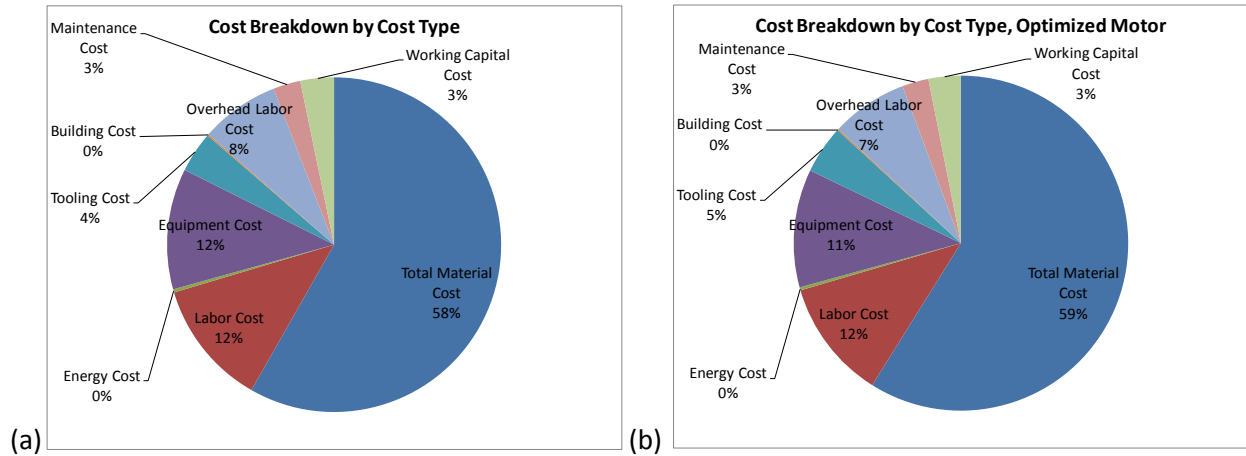
Figure 23: (a) Cost Breakdown for the BAS+ standard aluminum motor. (b) Cost Breakdown for the BAS+ Optimized Motor (90% length copper motor)
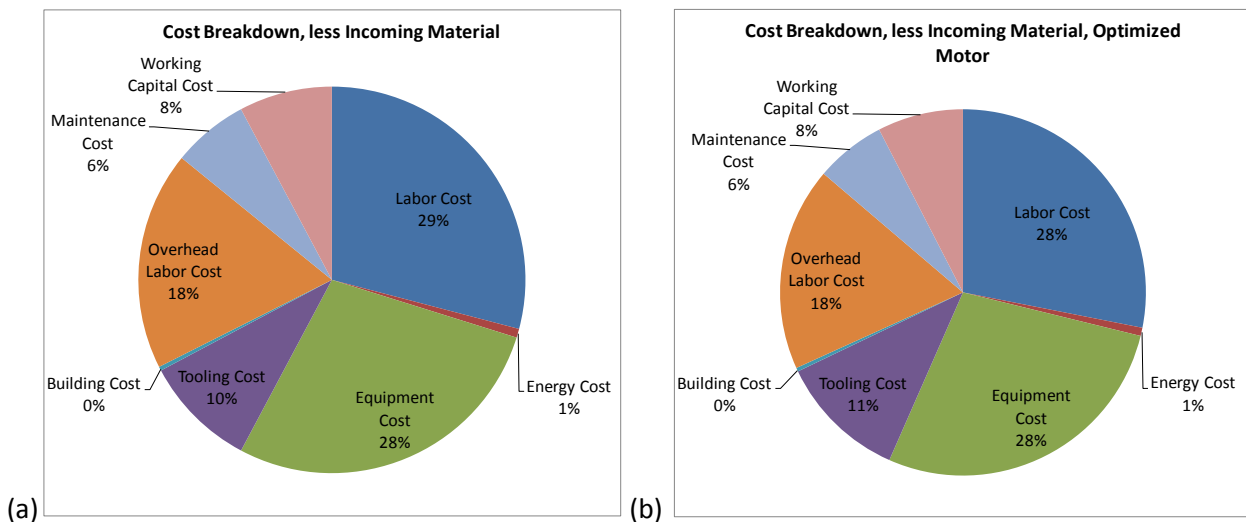
Figure 24: (a) Cost Breakdown for the Processing Cost of the BAS+ standard aluminum motor (i.e., without incoming material). (b) Cost Breakdown for the Processing Cost of the BAS+ Optimized Motor.

As mentioned earlier in Section 5.2, downsizing by length yields different results than downsizing by diameter. Material usage is different, and the processing costs scale differently as well. Figure 25 shows the BAS+ manufacturing cost's sensitivity to downsizing via length. At 90% length (i.e., at the point of equal efficiency), the motor cost is still significantly higher than the standard aluminum baseline. Furthermore, it is not until the motor can be downsized to ~74% of the baseline length that the point of

cost parity is reached. Unfortunately, this size motor will result in performance characteristics well below those of the original standard aluminum motor.
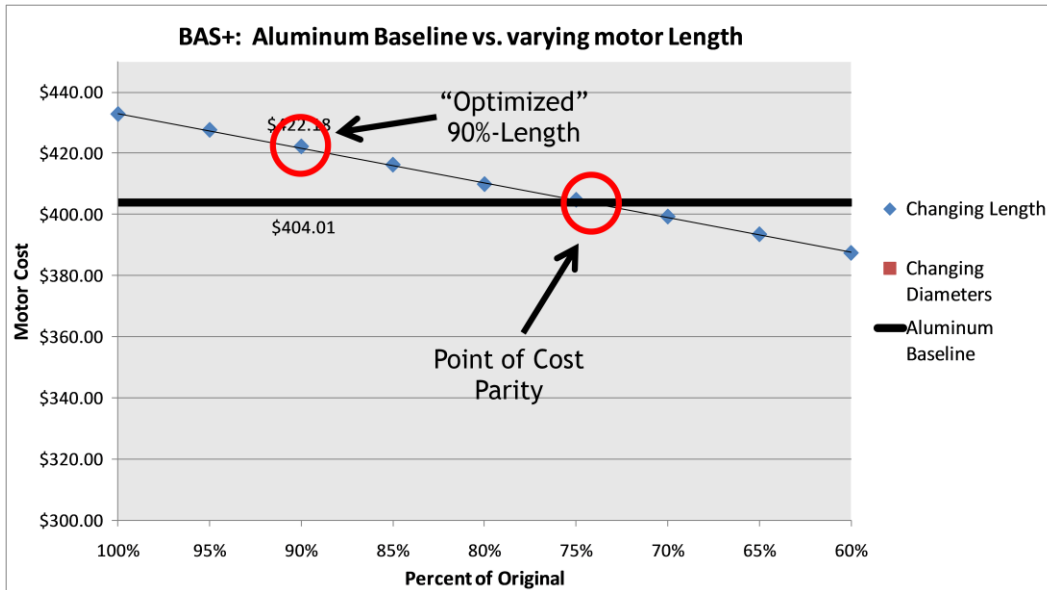
Figure 25: Motor cost sensitivity to reduction in length, BAS+.

Figure 26 through Figure 29 show the cost results from each of the process based cost models including a breakdown of the cost by individual process step for the standard aluminum motor and Optimized Motor. As expected, the only area in which there was an insignificant cost increase was die casting which was due to the direct effects of the switch from aluminum to copper on the materials costs, tooling costs and cycle times. In the all other processes costs decreased. For Figure 26, the most significant reductions in cost came from the slitting and blanking steps. As was just mentioned, the largest increase in Figure 27 was due to die casting copper in place of aluminum. In Figure 28, all of the steps remained roughly constant, given that none of the steps are significantly affected by downsizing by length. Figure 29 indicates the most reductions occur in the initial steps (i.e., lower steps on the bar graph). A more thorough investigation of this breakdown is later, in Section 6.3.
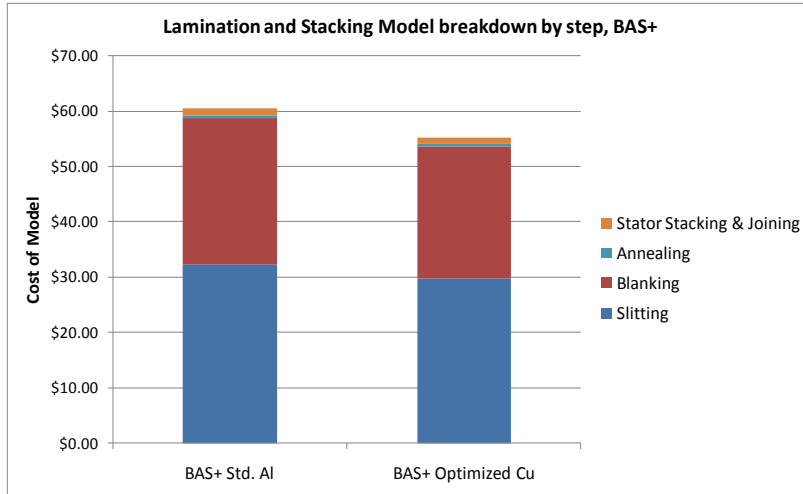
Figure 26: Lamination and Stacking model breakdown by step for standard aluminum and 90% length motors. BAS+.
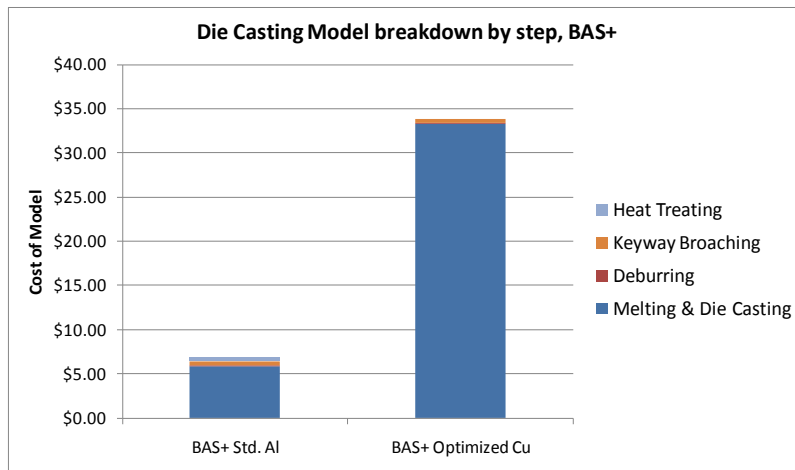
Figure 27: Die Casting model breakdown by step for standard aluminum and 90% length motors. BAS+.
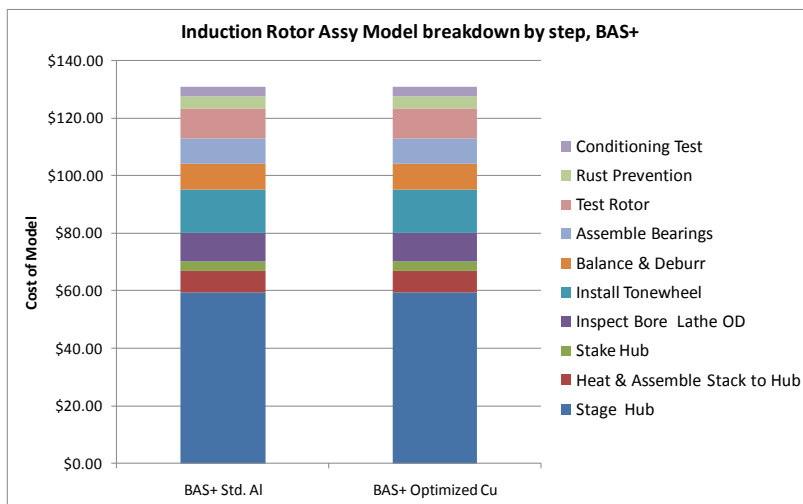
Figure 28: Induction Rotor Assy model breakdown by step for standard aluminum and 90% length motors. BAS+.

43
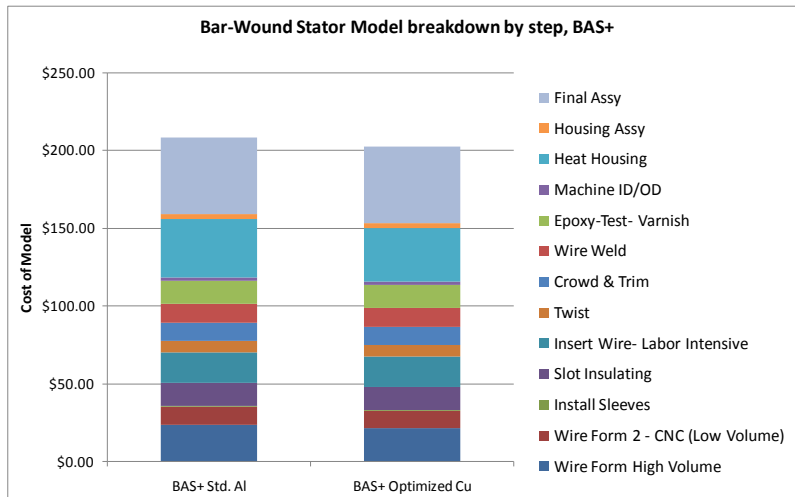
Figure 29: Bar-Wound Stator model breakdown by step for standard aluminum and 90% length motors. BAS+.

While the total cost of the motors changes with each case, it is worth noting that not every step changes equally, if at all. Consequently, it is useful to look at each case and compare the relevant steps (i.e., those that change with the respective downsizing method) to the original standard aluminum baseline. As mentioned in Section 5.2, the steps affected by downsizing are different and the amount with which they change differs depending on motor size. Figure 30 depicts the difference in cost between the standard aluminum and 90% length motors for the BAS+, showing every step affected by downsizing. Note that the collective negative deltas are not enough to offset the significant jump in die casting cost. Additionally, as mentioned earlier, not only does the increase in cost affect the incoming raw material, but also the associated processing costs as well. The cost breakdown for the die casting step itself is included in Section 7.4.

The five other major process steps are where losses are recouped. Given that the motor is decreased via length, the number of laminations needed decreases, giving way to a decrease in both raw material consumption and processing cost. The cost reductions in the Form Wire process steps are largely raw material-based, in that the total amount of copper used per pin is less. However, the total number of pins remains the same and thus the cycle time and other process-based parameters remain constant. Finally, the cost for producing the stator housing is essentially a reduction in the amount of material needed to make the housing. Processing costs are seen as unaffected for this amount of downsizing; it is entirely possible that for significantly smaller motors the processing time to manufacture and install each housing to the stator would decrease as well.
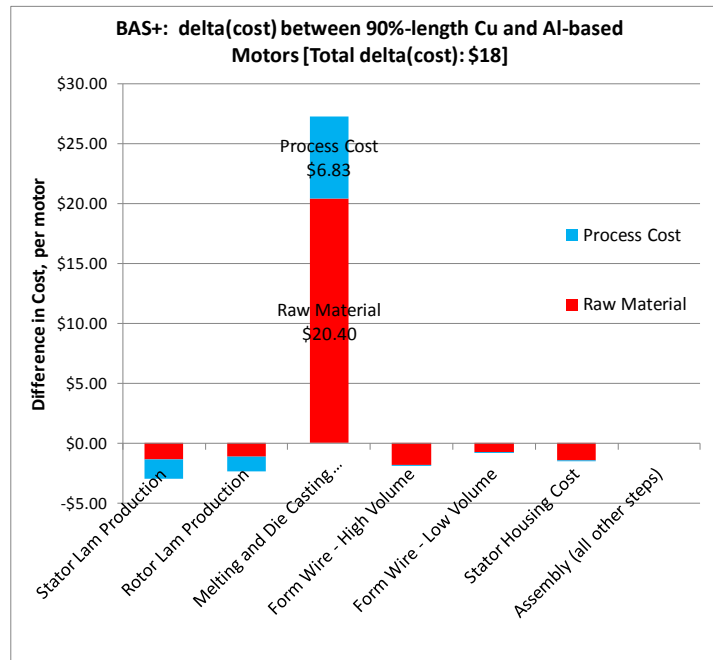
Figure 30: Difference in cost between standard aluminum baseline and optimized (90% length) copper motor, showing all steps affected by downsizing.

Given that incoming material makes up a very large percentage of the total motor cost (over 58% for the BAS+ Std. Aluminum motor), one can expect to see a very high sensitivity of cost to raw and scrap[10] material prices. Figure 33 represents three cases: a "best case," a "worst case," and a baseline. The best case scenario involves a situation in which both the incoming steel (35JNE250) and the copper/aluminum are 25% *cheaper* (per kg) than the baseline. Likewise, the worst case scenario is defined by the incoming material prices being 25% *greater* than the baseline. The three green circles represent the points of intersection between the standard aluminum baselines and their respective best- and worst cases.   Note that as mentioned before, to achieve cost parity, the baseline motor must be downsized to ~75% of its original length. However for the "best case" (-25%) material cost scenario, the motor only needs to be downsized to ~80% of its original length, whereas for the "worst case" (+25%) material cost scenario, the motor must be downsized to ~70% of its original length in order to achieve cost parity.

While steel prices are historically the most stable of the three main materials used in motor manufacturing (the others being aluminum and copper), the specialized nature of 35JNE250 steel may cause the market to be more volatile. Additionally, a change of 25% in copper or aluminum price is certainly not impossible, as shown by Figure 31 and Figure 32. While ten years ago copper prices had been at record lows, the past five years have seen rapid growth in copper prices to near-record highs. Furthermore, the past two years alone have seen extremely high volatility in copper prices, meaning

---

[10] Of note, given the highly specialized nature of the incoming steel (35JNE250), effectively no scrap credit can be retained. The raw copper and aluminum, however, can retain scrap credit.

that ultimately, the exact sensitivity of motor price to downsizing will be largely dependent on the current state of the metal market.

Figure 31: Copper pricing (in $/tonne), photo courtesy Reuters (34)**.**
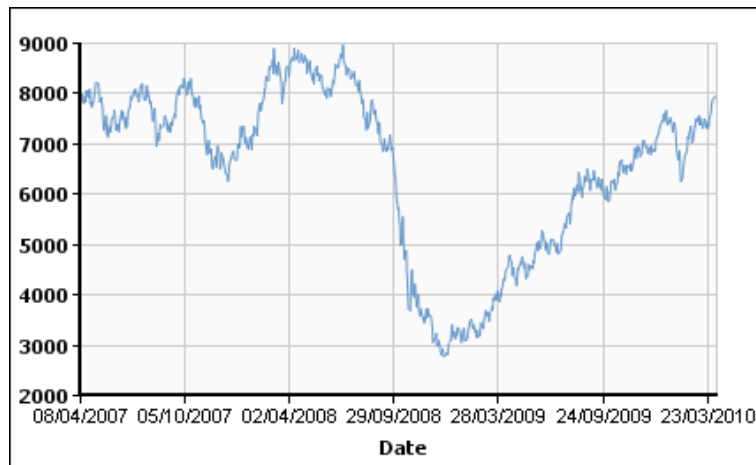
Figure 32: Copper pricing (in $/tonne) for the past 2.5 years. Photo courtesy US Geological Survey and AG Metal Miner (35)**.**

The respective trends for the by-length downsizing also have a tendency to "shallow-out" as primary raw material price decreases. The slope of the worst case materials cost scenario (the top trendline) is $1.26 per percent downsized, whereas the best case scenario has a slope of $1.00 per percent downsized. This is a decrease in slope of approximately 21%. As materials prices decrease, the influence of downsizing is reduced since variation in materials costs are a major driving force behind how much downsizing is needed to achieve cost parity.
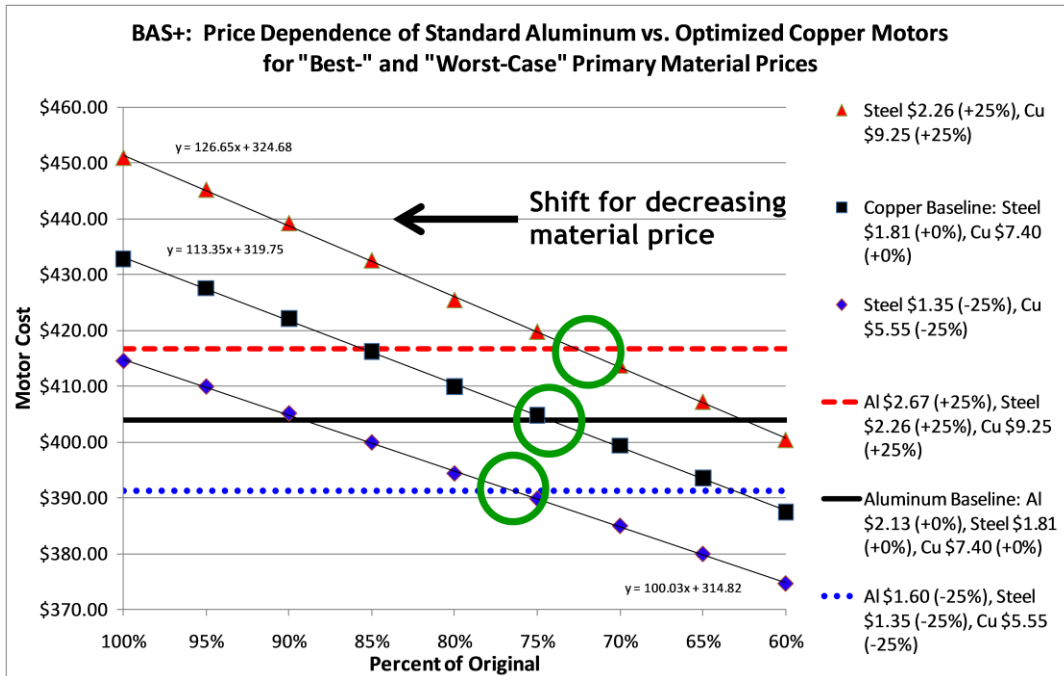
Figure 33: Material pricing effect on motor cost when downsizing via length.

6.3   Downsizing by Diameter

Given that the Efficiency Analysis showed that the BAS+ motor can be downsized by 10% by length when using copper and still achieve efficiency parity, the next steps in the analysis investigate the costs associated with a reduction in diameter rather than length. Unfortunately "Efficiency Analysis" modeling was not done for the case of downsizing "by diameter". However, one can still calculate the diameter size reduction needed to achieve cost parity with the "length optimized" (90% of baseline length) copper design. In this case, reducing the diameter to 96% of the baseline size results in the same cost as the 90% length copper motor. That said, nothing is known about the resulting efficiency decrease in this case.

Finally, the analysis explores the point at which "by diameter" downsizing achieves cost parity with the standard aluminum motor. As previously discussed, downsizing by length while maintaining equal motor efficiency (Figure 25) does not allow for cost parity with the baseline aluminum design. Furthermore, the amount of downsizing required, 75% assuming base materials price conditions, is infeasible from a motor performance standpoint. However, as shown in Figure 35, downsizing by diameter causes the motor cost to drop much more quickly. While it is not known if these motors will perform according to requirements, a copper motor with a diameter that is 88.5% of the baseline will have the same cost as that baseline design. It may be possible to achieve required performance targets at this size. A more detailed efficiency/performance analysis is needed to determine if this is the case.

47

	Standard Aluminum	Copper, Equal Size	"Optimized;" 90% Length Copper	96% Diameter Copper	88.5% Diameter Copper
Amount of Die Cast Metal (kg)	0.681	2.260	2.198	2.106	1.728
Amount of Steel (kg)	8.116	8.116	7.297	7.502	6.378
Efficiency	66%	78%	66%	Unknown	Unknown
Total Cost	$404.01	$432.73	$422.18	$422.22	$404.06

Table 5: Basic intermediate calculations and motor cost for each case, BAS+.

Table 5 outlines various important calculations for the respective motor cases, notably motor core weight, efficiency, and total motor cost. Figure 34 shows how raw steel and copper usage scale for the two downsizing methods. Note that copper is used in both the squirrel cage and the windings of the motor. Consequently, the total amount of copper used does not decrease nearly as much when downsizing via length as it does when downsizing by diameter. However, given that fewer laminations are needed when downsizing via length, the total amount of steel needed decreases at a much higher rate. Just as with the copper usage, scaling by diameter results in a much greater cost drop.
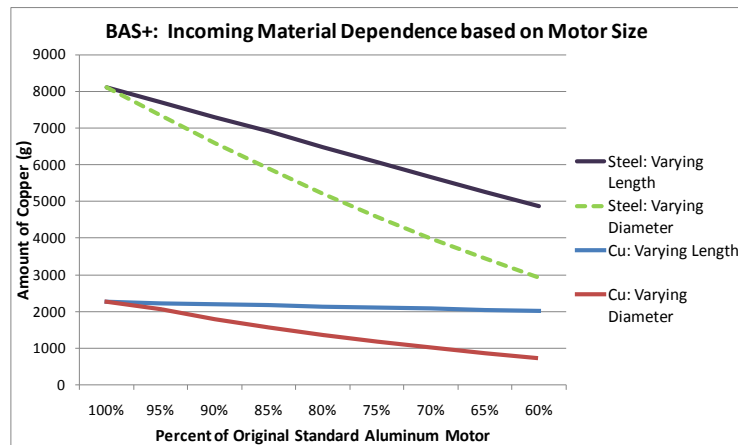
Figure 34: Incoming material vs. amount motor is downsized, BAS+.

It is also worth noting that for the BAS+, a reduction of 25% by length would result in a decrease in motor length of 17.5 mm, whereas a reduction of 11.5% by diameter would result in a decrease of overall motor OD of 16.3 mm.
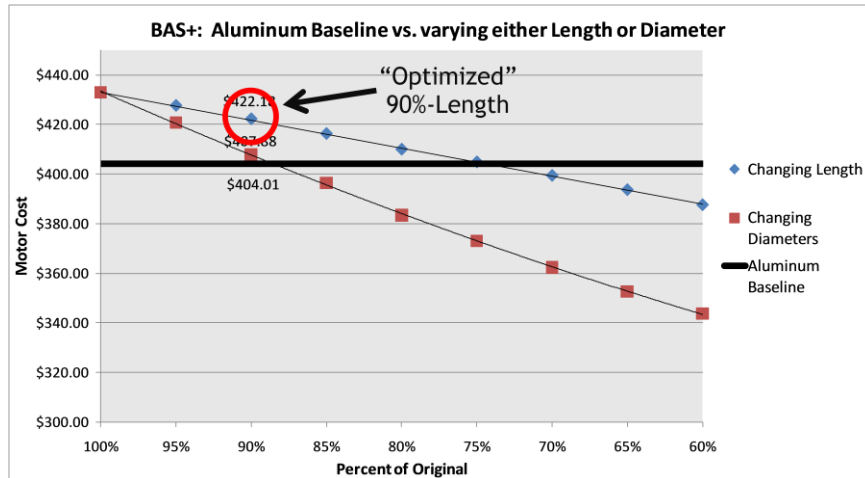
Figure 35: Motor cost sensitivity to motor size, BAS+.

6.3.1 Diameter Reduction: 96% diameter vs. 90% length

As mentioned above, downsizing by diameter affects the manufacturing process differently than downsizing by length. And, since 90% length yields a point of efficiency parity, it is worth investigating the by-diameter downsizing point that achieves the same cost to the aforementioned 90% length copper motor. Nothing can be said about the efficiency of the 96% diameter copper motor. Given the very minimal downsizing amount (only 4%), the 96% diameter copper motor may prove to be more efficient than the optimized copper motor (and therefore standard aluminum motor as well). On the other hand, efficiency does not scale as directly when downsizing via diameter as it does for length, and this could have a negative effect on the final motor efficiency. Regardless, this would be worth subsequent investigation.

Figure 36 is a slight variation on Figure 30, in that it represents the by-diameter downsized motor that corresponds to the same cost as for the optimized motor. Downsizing by diameter affects more total steps, including those affected in by-length downsizing. However, these crossover steps are affected in different ways.

49
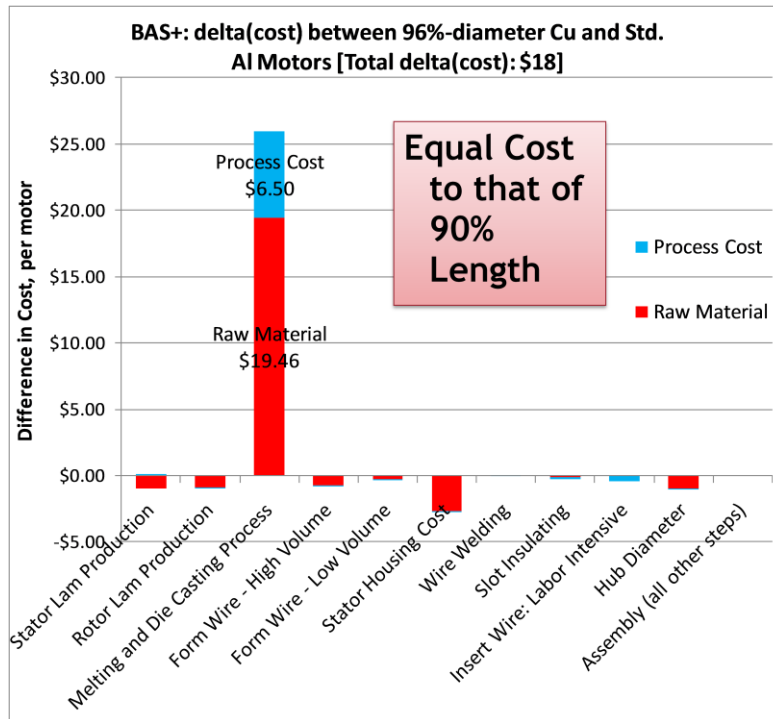
Figure 36: Difference in cost between the standard aluminum baseline and 96% diameter copper motor. This motor cost is equal to the optimized copper motor. However, more steps are affected when downsizing by diameter.

Note that despite the total motor cost for each downsizing method being equal (90% length vs. 96% diameter), the total die casting cost difference for 96% diameter is actually less than for the optimized motor. This is due to less copper being used in the squirrel cage for the 96% diameter copper motor. Additionally, while the total cost for the lamination production steps is decreased (just as with the 90% length copper motor), there is virtually no change in processing cost, in that the same number of laminations must still be manufactured. Again, for significantly smaller motor architectures, the processing cost may indeed decrease as well, but for the small downsizing amount (4% by diameter), processing changes are small. This implies that the total production time is equal to that of the standard aluminum baseline. Other notable decreases in cost are for the stator housing, given that the amount of material used for the housing decreases more significantly with motor diameter than with motor length.

The rest of the affected steps are more clearly represented in Figure 41, which shows the difference in cost between the optimized 90% length case and the 96% diameter case for each process step.

6.3.2   Diameter Reduction: Cost Parity

The final point of interest investigated for the BAS+ motor is the amount of downsizing by diameter needed to achieve cost parity with the standard aluminum motor and the distribution of the cost changes across individual process steps. Again, since downsizing by diameter has a greater effect on

motor cost (and size) than by length, the point of cost parity requires a lower percent of size reduction. As was already seen in Figure 35, the copper motor has a cost equal to the baseline aluminum motor if its diameter is only 88.5% of that of the baseline design.

As was expected, the cost to die cast significantly increased when using copper. However, downsizing of the motor diameter provided sufficient cost reductions in other areas of the manufacturing process to offset this cost. Note that all things being equal, a reduction in motor size causes a decrease in die casting cost, due to (a) less copper being used in the die casting process, and (b) a reduction in the cycle time and other processing variables.

Figure 37 through Figure 40 show the cost breakdown for each major process broken down by the individual process steps. Note that there is a cost increase for the die casting processes while the other three major processes all exhibit decreases in output cost. Only the steps that are relevant to this particular manufacturing process are included in the cost. The sum of these four major processes is the total motor cost. Additionally, incoming material is accounted for in the step where the material is first utilized (e.g., incoming steel is first used in the Slitting step). The order of the steps in the manufacturing process is from the bottom-to-top direction in each bar graph.

Figure 37 illustrates the additional decrease in motor cost over the optimized copper motor when downsizing to the point of cost parity (88.5% diameter). As has been mentioned, downsizing by diameter essentially does not decrease the processing costs of the blanking process. However, it does have a greater effect on material usage, hence the significant reduction in the slitting step. Figure 38 helps to show how reliant the die casting process is on the amount and type of material used, in that the 88.5% diameter case showed a reduction when compared to the optimized (90% length) case. Both were, however, significantly higher than the standard aluminum motor.

As was mentioned in Section 6.2, downsizing by length does not affect the Induction Rotor Assy model, whereas downsizing by diameter does (Figure 39), with a significant reduction in cost coming from the amount of hub needed. Finally, Figure 20 indicates that there are a number of steps that are affected by both downsizing and length. A more detailed look at these steps' sensitivity is in Figure 30 and Figure 41.
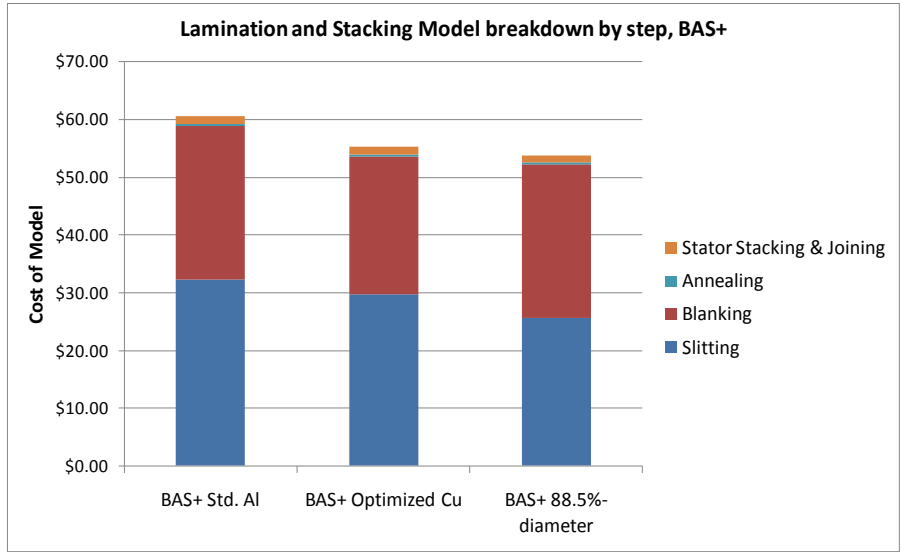
Figure 37: Lamination and Stacking model breakdown by step, BAS+.
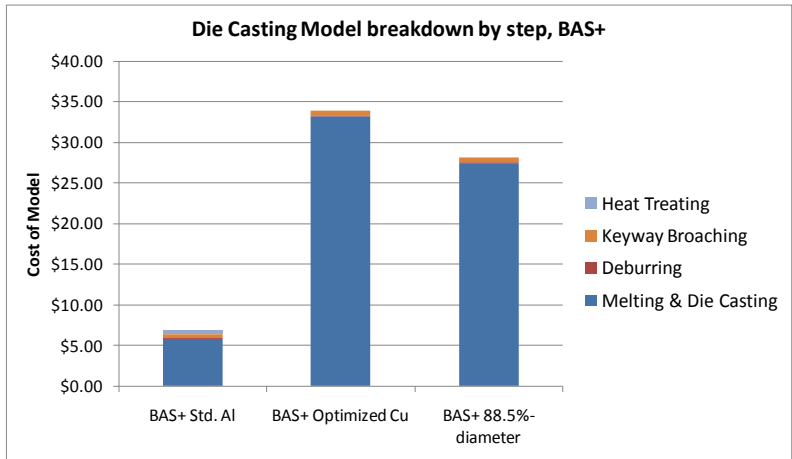
Figure 38: Die Casting model breakdown by step, BAS+.

Induction Rotor Assy Model breakdown by step, BAS+
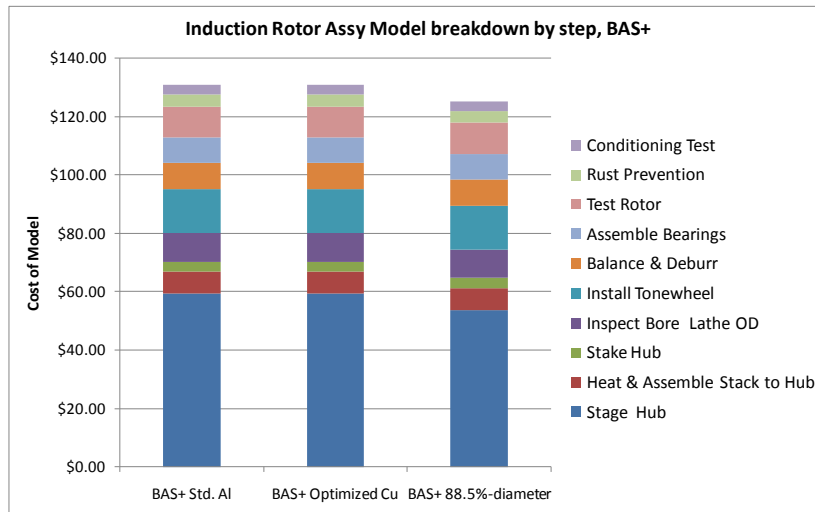
Figure 39: Induction Rotor Assy model breakdown by step, BAS+.

Bar-Wound Stator Model breakdown by step, BAS+
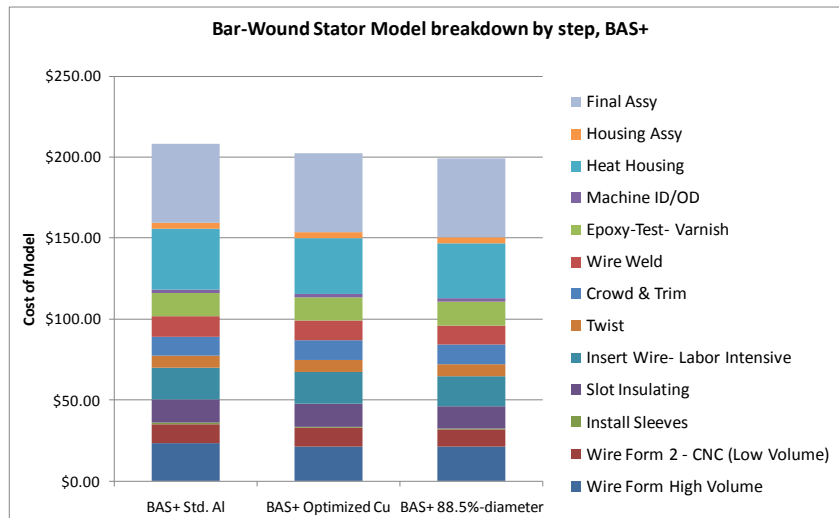
Figure 40: Bar-Wound Stator (and Motor) Assy model breakdown by step, BAS+.

Figure 41 shows the difference in costs for each affected step between the standard aluminum motor and the 88.5% diameter copper motor. This shows that all of the costs incurred when die casting copper are made negligible by the collective cost reductions that can be achieved for the other affected steps. As mentioned before, the mechanisms allowing cost equality to occur are two-fold. First, given the significantly smaller motor architecture of the 88.5% diameter copper motor, the total die casting cost difference is less than for the previous two figures. Second, the cost reductions for the rest of the steps are significant enough to offset the high die casting cost.
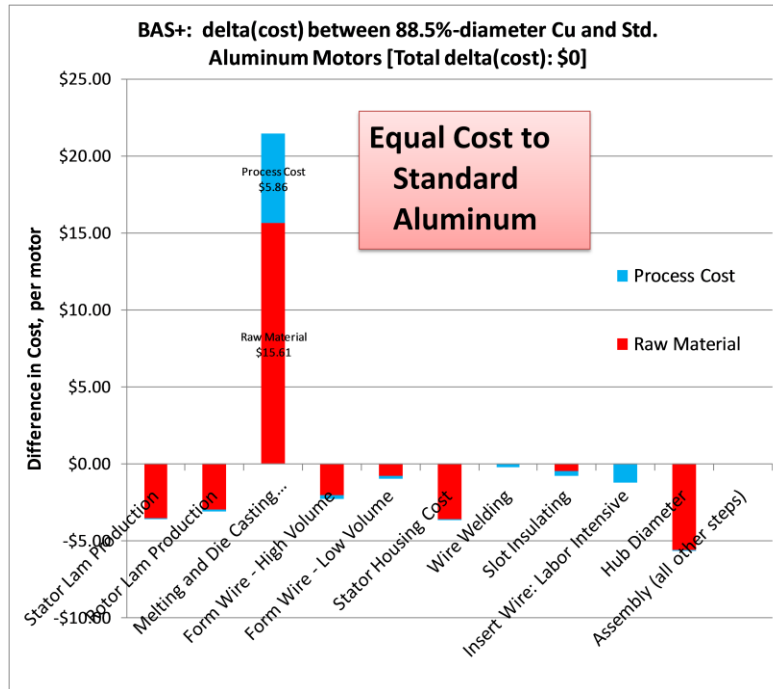
Figure 41: Difference in cost between the standard aluminum baseline and 88.5% diameter copper motor. The cost of each of these motors is equal to one another.

As shown in the case in the figure above, the vast majority of the cost difference in lamination production is due to the reduced raw material usage. However, for the Form Wire process steps there is a decrease in both the processing and material costs, given that there are fewer pins needed per stator. Fewer pins correspond to less material needed, and a shorter cycle time per stator. Accordingly, the time to insert the wires and weld them together is also slightly decreased, resulting in a lower processing Cost. Finally, given that the rotor hub is both large and requires very accurate installation, a smaller diameter motor gives way to a significant reduction in hub cost[11].

No assumptions can be made on the resulting efficiency from the 88.5% diameter copper motor.

---

[11] A note about stator housing and hub costs: the exact scaling of the costs of these components with motor size is unknown. Consequently, assumptions were made on the material use, involving downsizing proportionally. As a result, the exact sensitivity of these two components in particular could be slightly different but for the purposes of this analysis their role in motor cost is far overshadowed by other, more relevant steps.

6.3.3 Comparison of Diameter and Length Size Reductions
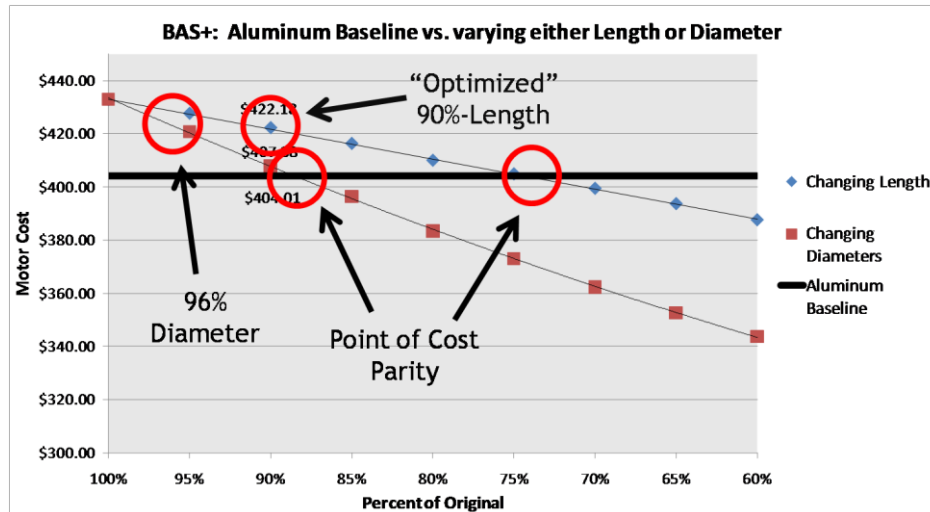
Figure 42: Motor cost vs. amount of downsizing with the four points of interest highlighted.

In order to better understand the different cost impacts involved with length and diameter reductions, a comparison of both conditions is provided simultaneously. In particular, four design points of interest were explored and their costs compared (Figure 42). Two designs involving downsizing by each method (length and diameter) where explored. One set of cases looks at the downsizing needed to achieve cost parity with the baseline aluminum design. The other set of cases looks at the designs that achieve equal efficiency with the baseline aluminum design. Since no efficiency analysis modeling was conducted for the downsizing by diameter case, the 96% diameter case was used since this is the design that has an equal cost to the optimized 90% length case. The four design cases are summarized below:

- Cost parity by length (74% length copper motor)
- 90% length copper motor
- 96% diameter copper motor
- Cost parity by diameter (88.5% diameter copper motor)

The first point of interest above is also the most idealized and most difficult to attain. Given that it is significantly smaller than the original standard aluminum motor (as well as the optimized copper motor), it can be expected that a 75% length copper motor would provide performance well below the desired range, and is essentially not worth investigating any further. Furthermore, the 90% length copper motor attains equal efficiency to the aluminum baseline, but suffers from a significantly higher manufacturing cost. Even if raw material price was at record lows, efficiency parity would still not equal cost parity for the BAS+ architecture.

In downsizing by diameter, nothing is known about the resulting efficiency of either of the two points of interest. 96% diameter copper motor results in a cost equal to the 90% length copper motor (and

therefore higher than the aluminum baseline), but it was a useful point to help understand how the manufacturing process is affected differently for a given downsizing method. Finally, 88.5% diameter copper motor results in a motor cost equal to that of the aluminum baseline, but in addition to the unknown efficiency, an 11.5% decrease in motor diameter results in a still-high decrease in overall motor size, indicating at the very least that output torque would suffer significantly[12]. Between the two copper motor cases, a decrease of 16.6% in die casting cost occurs, due to the greater sensitivity to by-diameter downsizing.

7   Motor Architecture #2: X26R Motor A

Despite the significant differences in dimensions and specifications between the BAS+ and X26R Motor A, many of the principle trends and sensitivity analysis is quite similar between the two. As is expected, the X26R Motor A's greater size necessitates more material usage, but a relative savings is retained in the fact that the stator and rotor laminations can be blanked as a unit (unlike the BAS+, which are blanked separately)(13). Thus, the amount of material usage, while still more than for the BAS+, is not proportionally greater based on size.
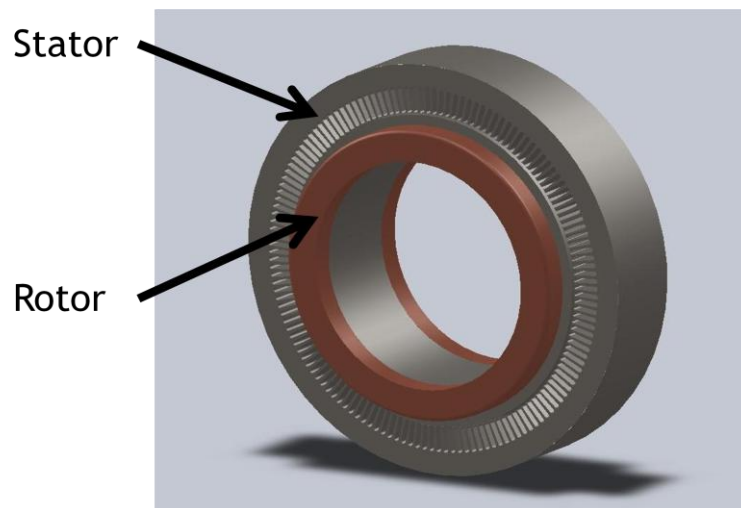
Figure 43: A very simplified CAD model of the X26R Motor A. Only rotor and stator cores are shown. The inside diameter of the stator (and therefore outside diameter of the rotor) is delineated by the inner edge of the slots.

---

[12] For the BAS+, downsizing to 75% length decreases the motor length by 17.5 mm, while downsizing to 88.5% diameter decreases motor diameter by 16.3 mm. Such a significant decrease in diameter would negatively affect output torque, given the smaller moment arm.

7.1   Motor Description

Unlike the BAS+, the X26R-series of motors was developed explicitly for battery electric vehicle traction purposes. There are two motors using similar dimensions that are referred to by the X26R label: Motor A and Motor B. Motor A is the induction motor; Motor B, a permanent magnet. Currently, the X26R Motor A has not reached production and GM has been in the process of sourcing suppliers for the first stages in the induction motor manufacturing process. The X26R Motor A is designed to produce 141 hp (105 kW) and 148 ft-lbs (200 N-m) of torque (13).

Table 6 shows the principle dimensions for the X26R Motor A. Given that the Efficiency Analysis is only relevant to BAS+, it is difficult to make any inferences on the efficiency-size dependence of the motor. As a result, there is no case entitled "Optimized Motor," and should be the focus of further work on the X26R Motor A. Instead, a much generalized assumption has been made and the BAS+'s optimized motor case has been used as a benchmark for the investigation of the X26R Motor A. As a result, the by-length downsize case investigated is identical to the BAS+: 90%. Given the somewhat unorthodox dimensions of the X26R motors, little can be assumed as to their exact efficiency without the presence of a detailed efficiency analysis similar to that for the BAS+.

Table 6 shows the principle dimensions for the X26R Motor A for each of the cases investigated in this analysis. The first two cases are identical to one another, with the only difference being the use of copper rather than aluminum. As was just mentioned, the "by length" downsizing case is for a 90% length copper motor. Note that this only causes a decrease of 6.9 mm from the total length of the motor. Likewise, the "by diameter" downsizing case is the point of cost parity between the copper and standard aluminum baseline motors. Due to the motor being much larger in diameter than in length, downsizing by diameter has an increased effect on motor size than for length. The 88.5% diameter copper motor causes a decrease of 29.9 mm – significantly more than the corresponding by-length downsizing amount.

	Standard Aluminum	Copper, Equal Size	"Optimized;" 90% Length Copper	88.5% Diameter Copper
Total Length (mm)	96	96	89.1	96
Stator OD (mm)	263.7	364.7	263.7	233.8
Rotor OD (mm)	200.1	200.1	200.1	177.1
Rotor ID (mm)	146.6	146.6	146.6	129.3

Table 6: Basic dimensions for the X26R Motor A, and how they scale with each case. The third case is for downsizing by length, while the fourth case is for downsizing by diameter.

7.2 Baseline Results: Standard Aluminum vs. 90% Length Copper Motors

Most of the sensitivity analysis for the X26R Motor A is quite similar to that for the BAS+. Figure 44(a) and (b) represent the cost breakdown, by model, for the X26R Motor A for the standard aluminum baseline and the 90% length copper motor. Note that while the total motor cost is higher than that for the BAS+, the general trends are similar, especially with the baselines. As noted earlier in Section 4.2.2, the X26R Motor A blanks the stator and rotor laminations as a unit (as opposed to separately, like the BAS+). This has the effect of reducing slitting and blanking costs significantly. As a result, the total cost of the X26R Motor A is not much more expensive to manufacture than the BAS+, despite its significantly larger dimensions (55% larger stator OD).

(a)   (b)
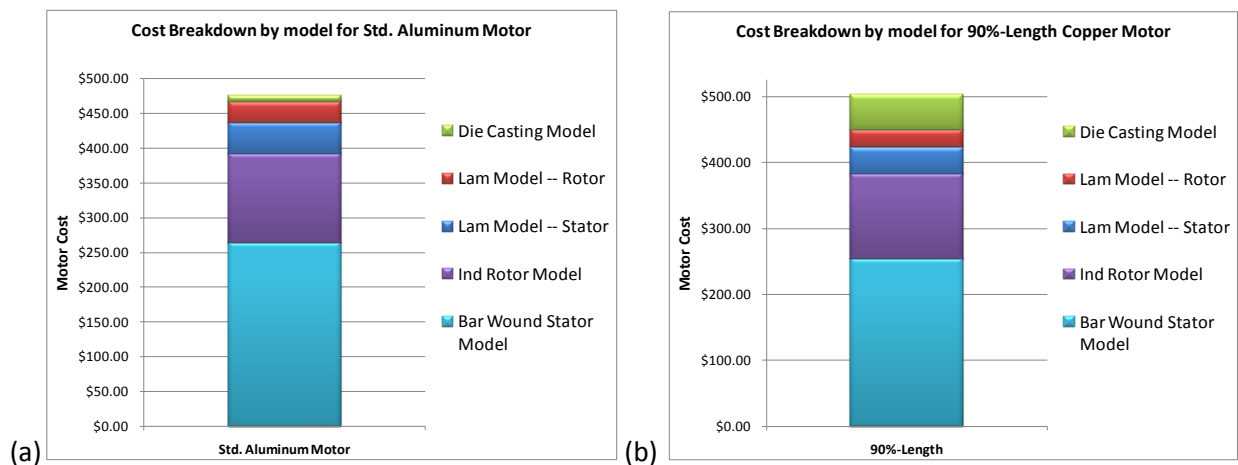
Figure 44: (a) Cost breakdown by model for the X26R Motor A standard aluminum baseline. (b) Cost breakdown by model for the 90% length copper motor.

Figure 45(a) and (b) shows the cost breakdown by cost type for the standard aluminum baseline motor and 90% length copper motor. Note that when compared to the BAS+ (Figure 23), the total material usage accounts for slightly more of the total motor cost, due to the larger motor architecture. Additionally, direct labor cost also increases due to more weight being placed on labor-intensive steps (for example, more pins to insert to the stator result in higher cycle times and therefore higher labor costs). Similarly to the BAS+, there is only a slight increase in material usage when comparing the aluminum to 90% length copper motors. While the use of copper does increase material usage, there are many other materials used in the manufacturing process that collectively contribute a much larger percentage of total material cost than the copper die casting. As a result, the use of copper only increases material percentage by a mere 1%. Tooling also experiences an increase in cost percentage due to the more sophisticated tooling required for copper die casting. Figure 46(a) and (b) illustrate the cost breakdown of the Processing Costs (i.e., no incoming material is accounted for) for the standard

aluminum baseline motor and 90% length copper motor. Overall, changes between the standard aluminum and 90% length copper motors are minimal due to the small change in motor dimensions.
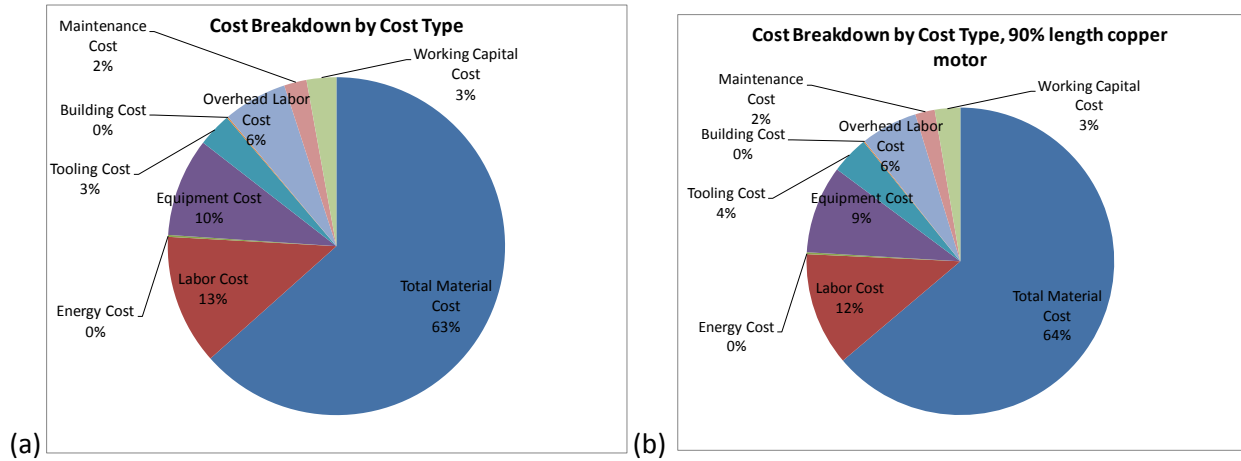
Figure 45: (a) Cost breakdown by cost type for the standard aluminum. (b) Cost breakdown by cost type for the 90% length copper motor. X26R Motor A.
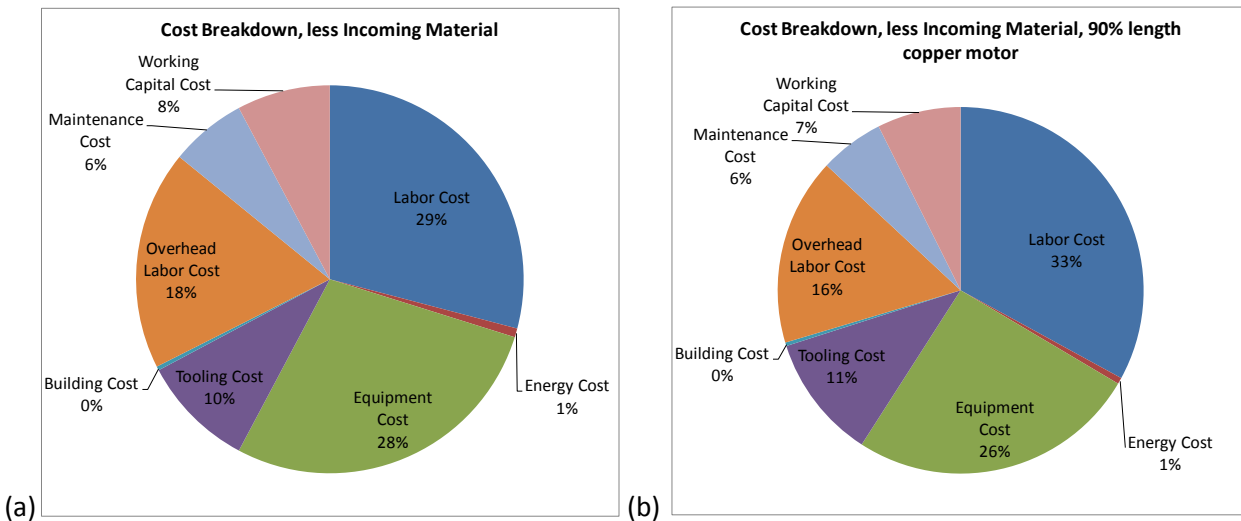
Figure 46: (a) Cost breakdown for Processing Costs (i.e., costs without including material costs) For the Standard aluminum. (b) Cost breakdown for Processing Costs for the 90% length motor. X26R Motor A.

Figure 47 shows the X26R Motor A's sensitivity to downsizing by length. Just as with the BAS+, the 90% length copper motor does not result in cost parity with the standard aluminum baseline. Additionally, the point of cost parity between the standard aluminum and copper motors occurs at ~74% length. However, the geometry for the X26R Motor A is significantly different from the BAS+, in that downsizing by X% decreases the diameter quicker than the length. As a result, it is truly unknown what this effect will do to motor efficiency.
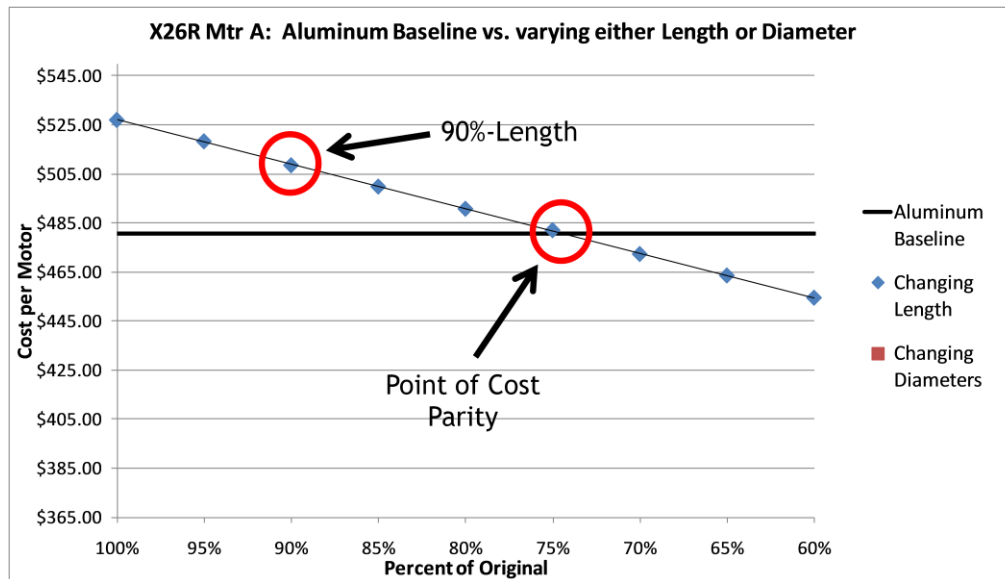
Figure 47: Motor cost sensitivity to downsizing by length

Figure 48 through Figure 51 show each models' steps and their respective contribution to total model cost for the standard aluminum motor and Optimized Motor. As was expected, the only model to experience an increase in cost was the Die Casting model, in which the switch from aluminum to copper was made. In the other three models, however, costs decreased. In Figure 48, the vast majority of the costs accrued are in the slitting step, which is slightly misleading in that all of the incoming steel used for the laminations is accounted for in this step. Blanking costs are significantly lower due to the more economical method of blanking stator and rotor laminations (i.e., as a unit). While annealing theoretically decreases, its small cost and low production time means that any changes due to motor geometry are minimal.   Figure 49 illustrates the significant increase due to die casting copper over aluminum. Note also that the heat treating step is not needed when using copper. Just as with the BAS+, the Rotor Assembly model steps are largely unaffected due to the lack of sensitivity to downsizing by length (Figure 50). For the Bar Wound Stator Assembly model, the majority of the cost savings are in the initial steps (i.e., at the bottom of the graph) – exactly the same as for the BAS+ (Figure 51). A more thorough investigation of this breakdown is later, in Section 7.3.
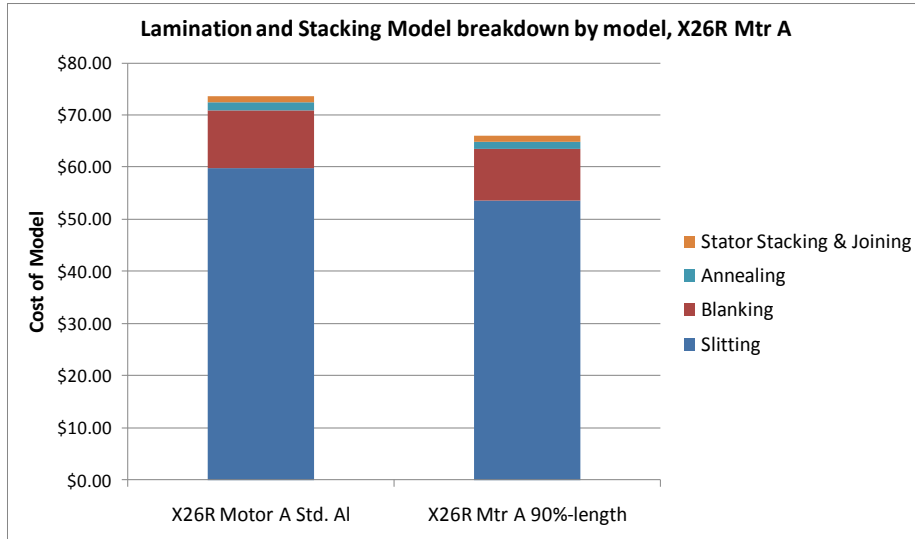
Figure 48: Lamination and Stacking model breakdown by step, X26R Motor A.
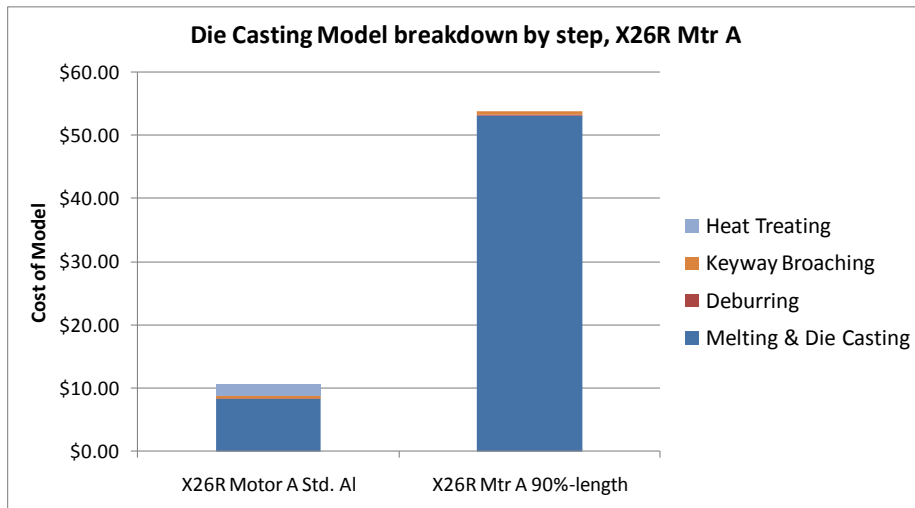
Figure 49: Die Casting model breakdown by step, X26R Motor A.

Induction Rotor Assy Model breakdown by step, X26R Mtr A

Legend (top to bottom):
- Conditioning Test
- Rust Prevention
- Test Rotor
- Assemble Bearings
- Balance & Deburr
- Install Tonewheel
- Inspect Bore Lathe OD
- Stake Hub
- Heat & Assemble Stack to Hub
- Stage Hub

Y-axis: Cost of Model ($0.00 to $140.00)
X-axis categories: X26R Motor A Std. Al, X26R Mtr A 90%-length
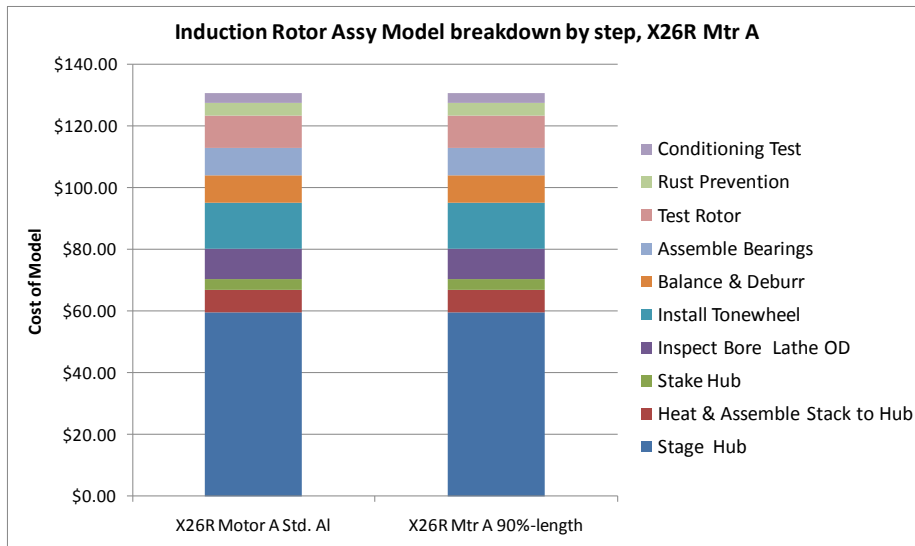
Figure 50: Induction Rotor Assy model breakdown by step, X26R Motor A.

Bar-Wound Stator Model breakdown by step, X26R Motor A

Legend (top to bottom):
- Final Assy
- Housing Assy
- Heat Housing
- Machine ID/OD
- Epoxy-Test- Varnish
- Wire Weld
- Crowd & Trim
- Twist
- Insert Wire- Labor Intensive
- Slot Insulating
- Install Sleeves
- Wire Form 2 - CNC (Low Volume)
- Wire Form High Volume

Y-axis: Cost of Model ($0.00 to $300.00)
X-axis categories: X26R Motor A Std. Al, X26R Mtr A 90%-length
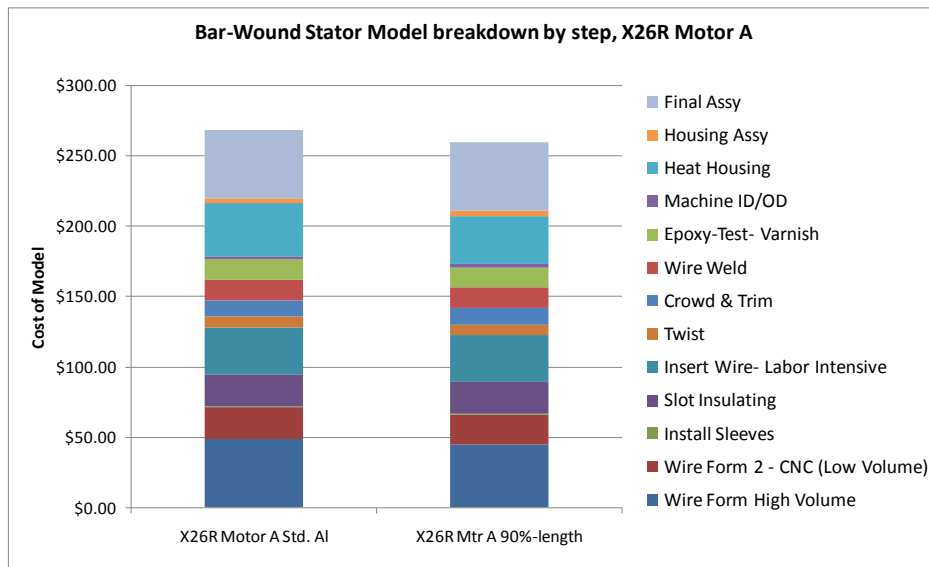
Figure 51: Bar-Wound Stator Assy model breakdown by step, X26R Motor A.

Since not all of the steps in the manufacturing process are affected equally (if at all) by motor downsizing, it is worthwhile to compare the two copper motor cases to the standard aluminum baseline. Figure 52 shows the difference in cost (denoted by, "delta(cost)") between the 90% length copper motor and standard aluminum motor

The same steps are affected with the X26R Motor A as with the BAS+ for each downsizing method. Again, note that the use of copper die casting to manufacture the squirrel cage causes both a jump in material cost as well as processing costs. However, when downsizing by length (Figure 52), the X26R Motor A experiences a lower processing cost difference for die casting than the BAS+. Again, this is due

to the lower sensitivity to motor length than the BAS+[13]. As a result, the majority of the cost difference is in material usage. The other steps scale similarly to the BAS+ cases.
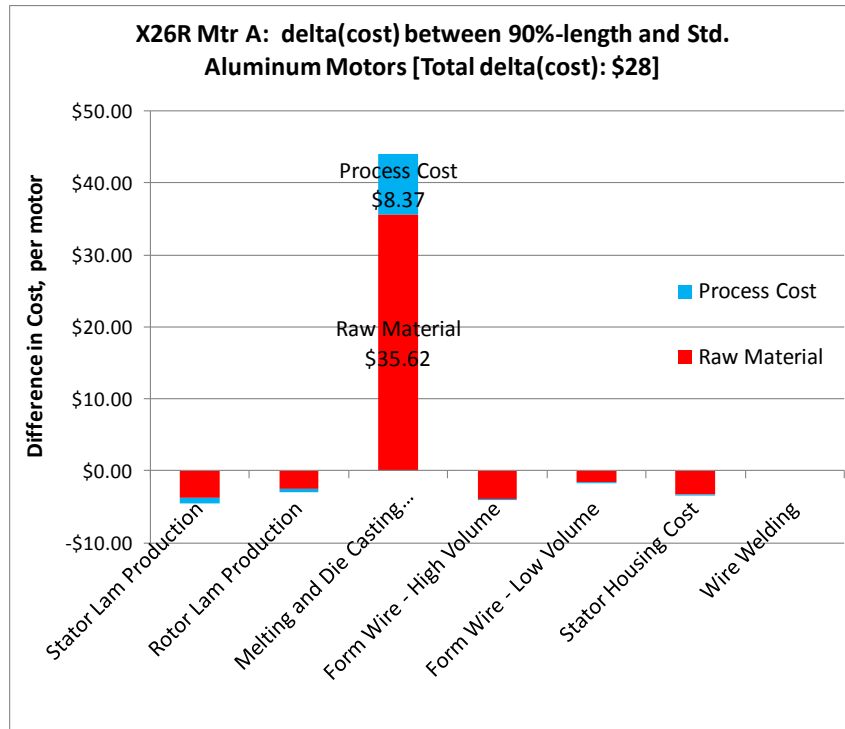
Figure 52: Difference in cost between standard aluminum baseline and 90% length copper motor for all affected steps. X26R Motor A.

Just as with the BAS+, the X26R Motor A overall cost is highly sensitive to the price of incoming raw material. Figure 53 shows a similar case setup to that for the BAS+, in which the incoming steel and copper/aluminum prices (per kg) are increased and decreased by 25%, and then compared to the baseline. Given that incoming material accounts for 58% of the total motor cost in the BAS+ and 63% of the total motor cost for the X26R Motor A, there is a slightly greater sensitivity to primary raw material pricing for the X26R Motor A. Just as with the BAS+, no scrap credit can be retained for the steel (also 35JNE250), however some can be for the aluminum and copper die casting.

The trendlines for downsizing the X26R Motor A for each raw material price case are also nearly twice as steep as for the BAS+, reinforcing the high sensitivity to incoming material. The worst case slope is $2.08 per percent downsized, whereas the best case slope is $1.56 per percent downsized, resulting in a total drop of 25%. Furthermore, if the X26R Motor A laminations were blanked similarly to the BAS+ (i.e., separately), this dependence would be even more severe. This further illustrates the notion that as material prices increase, the relative materials effect on total motor price also increases.

---

[13] 90% length is only a reduction of 7.1 mm for the BAS+, and 5.9 mm for the X26R Motor A.
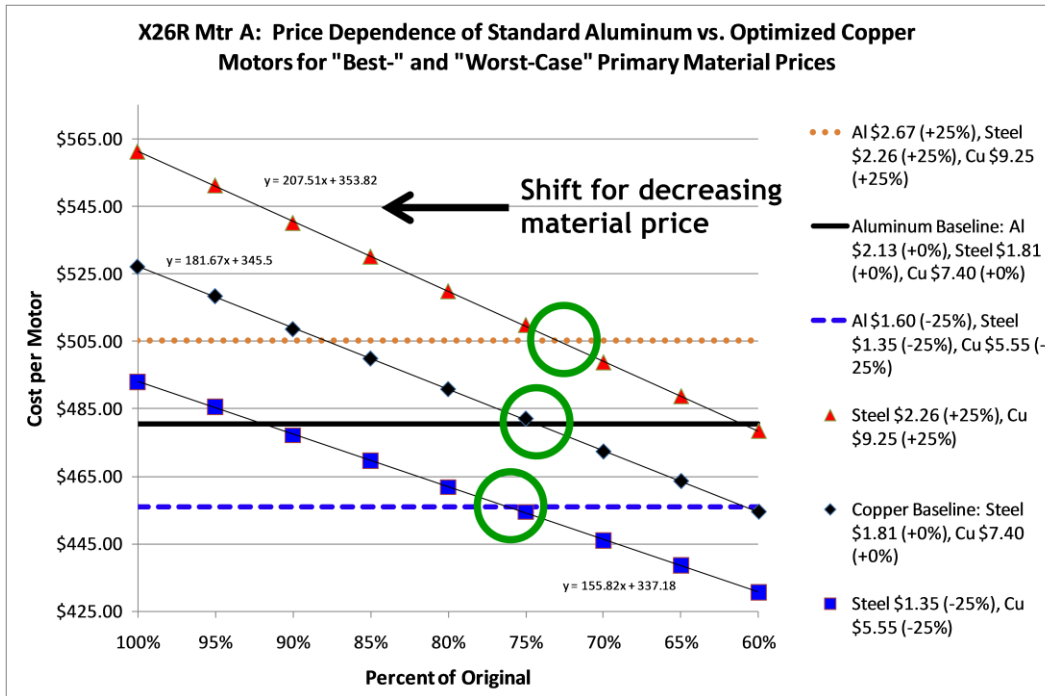
Figure 53: Material pricing effect on motor price when downsizing by length. X26R Motor A.

7.3 Downsizing by Diameter

	Standard Aluminum	Copper, Equal Size	"Optimized;" 90% Length Copper	88.5% Diameter Copper
Amount of Die Cast Metal (kg)	1.190	3.949	3.839	2.972
Amount of Steel (kg)	16.185	16.185	14.541	12.782
Efficiency	Unknown	Unknown	Unknown	Unknown
Total Cost	$480.59	$527.12	$508.62	$480.85

Table 7: Intermediate calculations and motor cost for X26R Motor A for each downsizing case.

Table 7 outlines important calculations for each of the important motor cases for the X26R Motor A, including the weight of the die cast metal, amount of steel in the motor core, and total motor cost. The downsizing of the X26R Motor A is fundamentally identical to that of the BAS+, as are the assumptions made therein. As a result, the incoming steel and copper scale quite similarly for the X26R Motor A as with the BAS+, in that the amount of material has a greater sensitivity to by-diameter downsizing vs. by-

64

length, and the amount of steel used decreases more quickly with motor size than copper does (Figure 54).

X26R Mtr A: Incoming Material dependance based on Motor Size
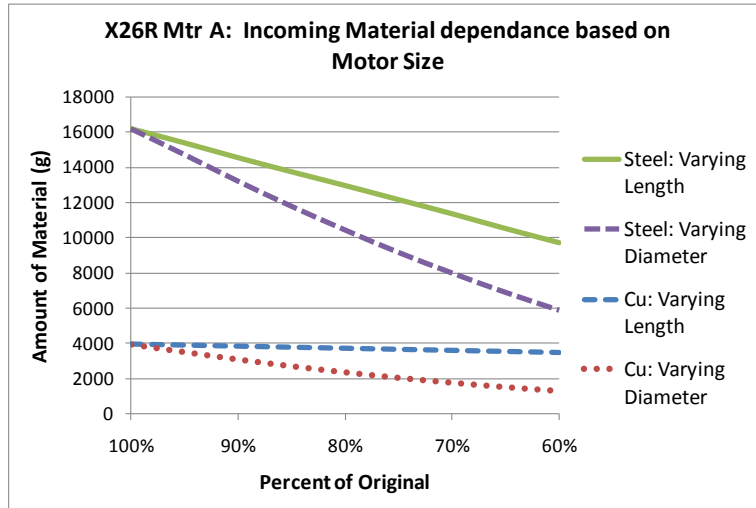
Figure 54: Amount of material in X26R Motor A as a function of motor size.

Scaling the X26R Motor A by length and by diameter does not result in equal cost affects (Figure 55). The standard aluminum baseline has a motor cost of $480.59. And, just as with the BAS+, downsizing for the X26R Motor A requires a ~25% reduction in length or an 11.5% reduction in diameter in order for cost uniformity to be reached. Despite not knowing the efficiency-size relationship of the motor for either downsizing method, it would not be surprising that a motor with dimensions of 75% would exhibit inadequate performance. However, given the pancake-like configuration of the motor (whereas the BAS+ is longer and narrower in diameter), a reduction in motor length of 25% results in a decrease of only 14.75 mm, whereas a decrease of 11.5% in the diameter results in a decrease of motor OD by 29.9 mm. And, given that efficiency does not scale as directly with diameter as it does with length, it is entirely possible that the 88.5% diameter copper motor exhibits worse performance than the 75% length copper motor. It is interesting that the cost parity numbers for the X26R Motor A are similar to the BAS+ despite significantly different motor geometries; much of this effect can be attributed to the relatively higher blanking cost of the BAS+ as compared to the X26R Motor A.
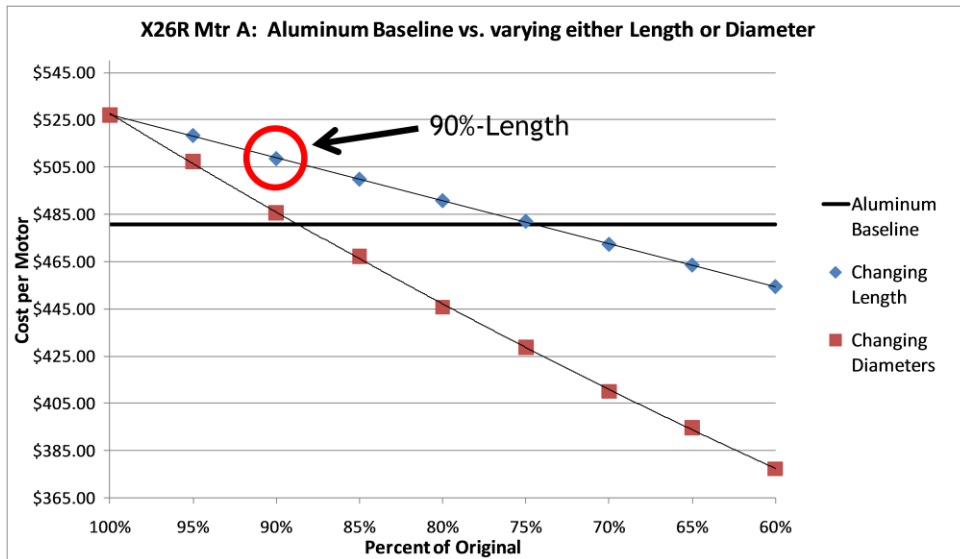
Figure 55: Motor cost as a function of size for downsizing by diameter and by length. X26R Motor A.

7.3.1   Diameter Reduction: Cost Parity

There are three main cases of interest for the X26R Motor A. The first is the standard aluminum baseline, while the second is the arbitrary 90% length copper motor. The third is the point of cost parity for downsizing by diameter, at 88.5%. The individual motor cases are similar to those for the BAS+, and are discussed in more detail in Section 6.1.

Just as with the BAS+, the jump in motor cost comes from the use of copper in the die casting step. Consequently, each other model experiences a decrease in their respective manufacturing costs. Since the X26R Motor A is so much wider in diameter than it is in length, the majority of the copper for die casting is in the end rings. As a result, a much more significant reduction in die casting copper occurs when downsizing by diameter (as opposed to length). Additionally, the significantly larger motor and required torque output as compared to the BAS+ necessitates an increase in the size and capability of many components (for example, bearings). While the exact increase in many of these ancillary components is unknown (and therefore assumptions were made on appropriate cost), the sensitivity trends would remain the same.

Figure 56 through Figure 59 show the cost breakdown by step for each model. Given that the laminations for the X26R are manufactured as a unit, the resulting blanking costs are significantly reduced (as compared to if they were blanked separately). Consequently, the majority of the cost in the Lamination & Stamping model comes from the slitting step, in which the incoming raw steel is accounted for[14]. However, because of the greater incoming material dependence of the X26R Motor A,

---

[14] Just as with the BAS+, the incoming material is accounted for in the first step in which the material is used. For example, the incoming raw steel is accounted for in the slitting step, given that it is first used in this step.

a greater reduction in model cost occurs for the two copper motor cases than for the same cases of the BAS+.

As is expected, the vast majority of the cost increase occurs in the melting and die casting steps within the Die Casting model itself. Between the 90% length and 88.5% diameter copper motors, there is a decrease of nearly 20% in motor cost, as compared to the BAS+'s reduction of only 16.6%. Again, this is due to the majority of the squirrel cage metal being in the end rings and not in the copper bars themselves.

Again, the order of the steps in the manufacturing process occurs from the bottom-up in the bar graph. Figure 56 shows the significant decrease in manufacturing cost for the steps involved in the Lamination and Stacking model. Here, the majority of the decrease in cost for the 88.5% diameter copper motor comes from a reduction of steel used for the laminations. The total number of laminations, however, remains t the same. For the die casting processes, note the reduction in die casting cost when comparing the two copper motors, given the high sensitivity to downsizing by diameter (Figure 57). Figure 58 illustrates the slight sensitivity the Rotor Assembly steps have to downsizing by diameter, but not to downsizing by length. Finally, just as with the BAS+, the majority of the savings in manufacturing cost for the steps in the Bar Wound Stator model occur in the initial steps, most notably the Form Wire and Wire Insertion steps (Figure 59).
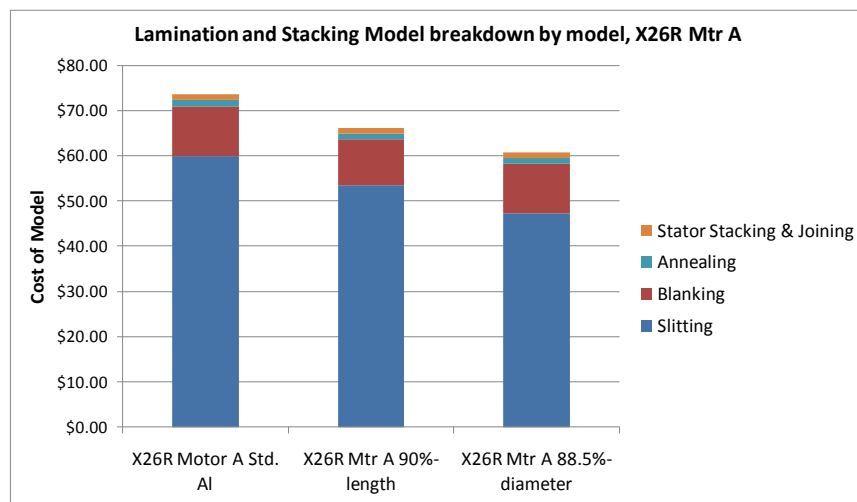
Figure 56: Lamination and Stacking model breakdown by step, X26R Motor A.
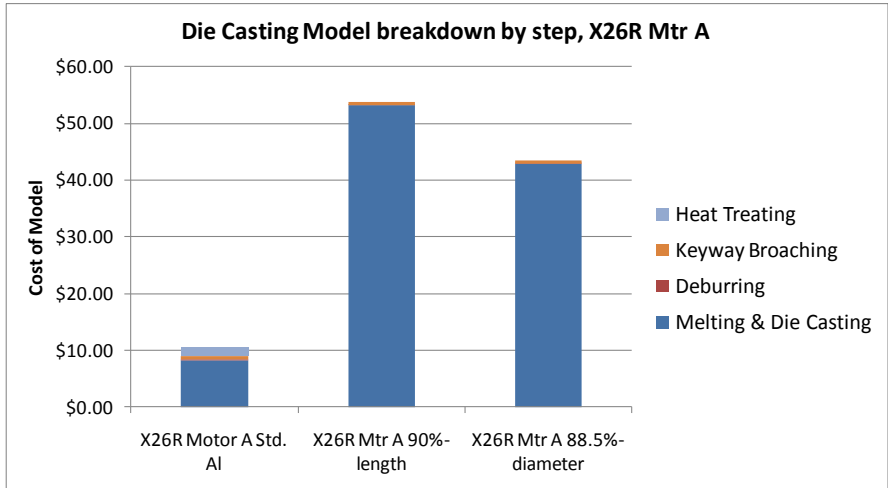
Figure 57: Die Casting model breakdown by step, X26R Motor A.
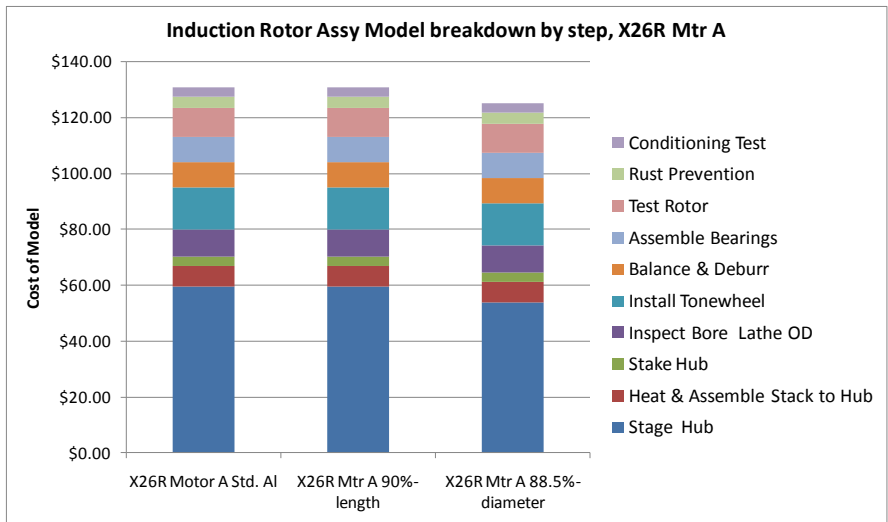
Figure 58: Induction Rotor Assy model breakdown by step, X26R Motor A.

68
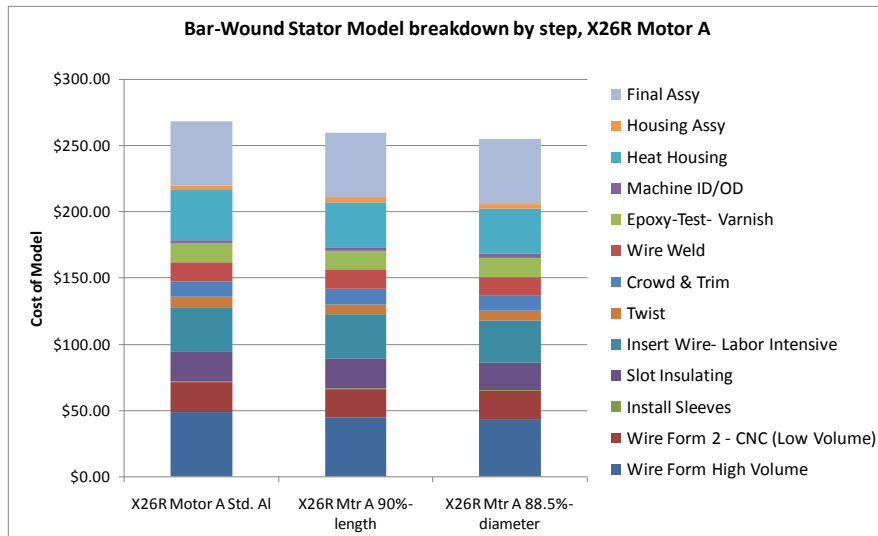
Figure 59: Bar-Wound Stator (& Motor) Assy model breakdown by step, X26R Motor A.

Figure 60 shows the comparison between the standard aluminum baseline and downsizing by diameter for the 88.5% diameter copper motor. Here, the cost to die cast equals the collective credits provided by the other affected steps. Just as with the BAS+, material usage is where the majority of costs are recouped. Particularly with the lamination production steps, very little processing cost is recouped, indicating that the total production time is similar to the standard aluminum baseline. As has been mentioned before, there is also a significant reduction in die casting cost as compared to the 90% length copper motor. The rest of the steps are quite similar to the BAS+, including the high labor dependence of the wire insertion, slot insulation, and wire welding. Finally, the hub of the X26R Motor A is also substantially larger than for the BAS+ (given the much larger rotor ID), and therefore the sensitivity to downsizing by diameter can be expected to be equally sufficient. Unfortunately, just as with the BAS+, the precise cost-size relationship for both the stator housing and rotor hub is unknown. The resulting discrepancies expected from this uncertainty are minimal.
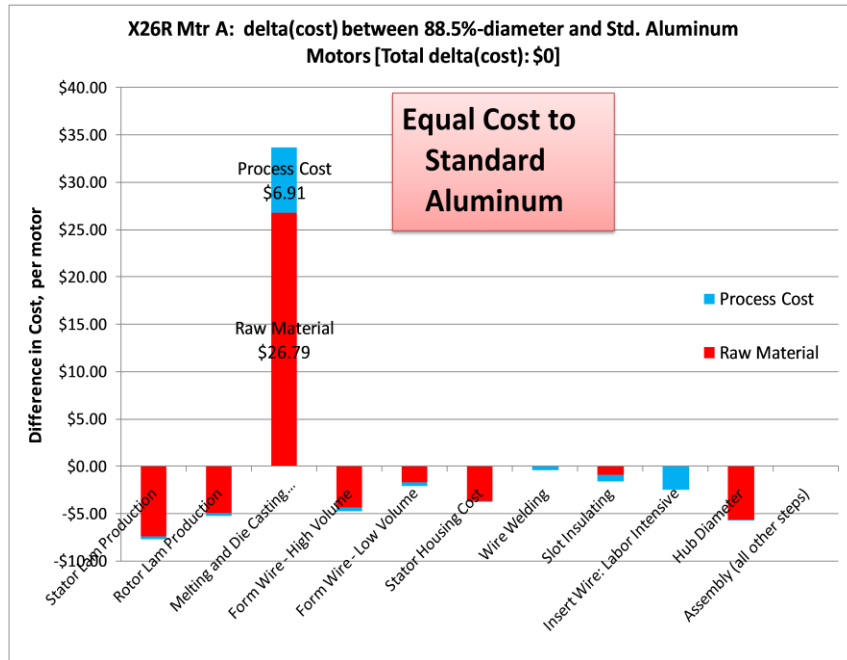
Figure 60: Difference in cost between standard aluminum baseline and 88.5% diameter copper motor for all affected steps. X26R Motor A.

7.3.2 Total Downsizing Analysis: Three Points of Interest
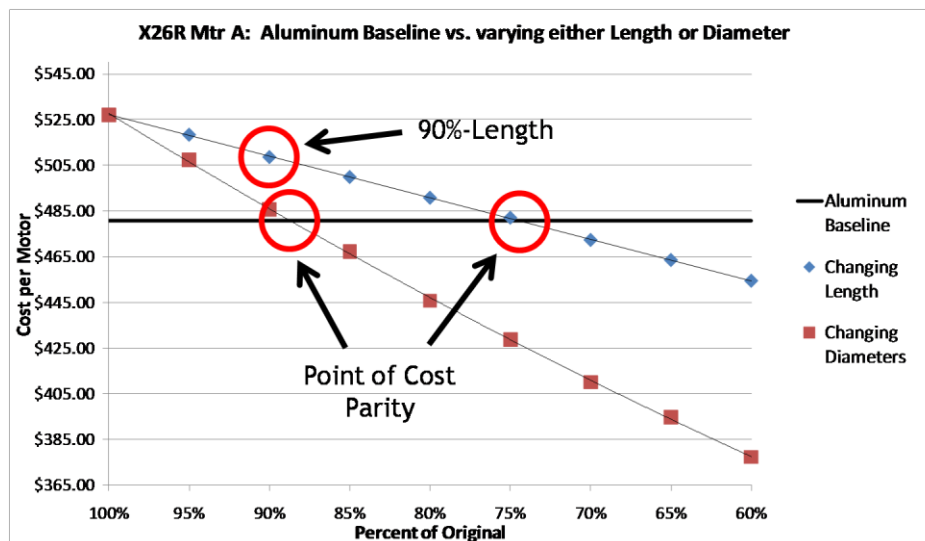
Figure 61: Motor cost vs. amount of downsizing with three points of interest highlighted.

For the X26R Motor A, there are three primary points of interest that were investigated in addition to the standard aluminum motor:

70

- Cost parity by length (~74% length copper motor)
- 90% length copper motor
- Cost parity by diameter (88.5% diameter copper motor)

Given that the Efficiency Analysis did not look at the X26R Motor A, it is impossible to make any claims as to the efficiency-size relationship of the aluminum and copper motors. Just as with the BAS+, cost parity with the aluminum baseline occurs at both 74% length and 88.5% diameter. Interestingly, the reduction of 11.5% from diameter results in a decrease of 29.9 mm, while a 74% length motor resulted in a decrease of only 14.75 mm. Additionally, the arbitrary benchmark of 90% length copper motor resulted in a motor cost significantly higher than the standard aluminum baseline, very similarly to the BAS+.

7.4   A More In-Depth Look into Die Casting

Given that die casting is the step responsible for the increase in motor cost when using copper to manufacture the squirrel cage, it is worth looking more in-depth for the individual sources of the increase in cost, specifically those dealing with the processing costs. Clearly, a reduction in motor size allows for a reduction in metal needed for die casting (by volume). However, at no point is the amount of copper used (by mass) equal to or less than the amount of aluminum used in the standard aluminum motor (Table 4 and Table 6) with either motor case. And given copper's higher price (per mass) than aluminum, material costs increase.

Figure 62 and Figure 63 show the differences in cost between the standard aluminum baseline and the 90% length copper motor for each cost type. In addition to the material costs, an increase in tooling cost also occurs. While tooling for aluminum die casting can be made from H13 tool steel and obtain a tool life of over 200,000 cycles, tooling for copper die casting must be made from more expensive nickel-based alloys, and even then a tool life of only 40,000 cycles is expected (11). GM estimates that a production volume of only 25,000 units is expected (13) and therefore the yearly cost for tooling is lower than it would be for a higher production volume (13). Additionally, the tooling for the X26R Motor A is larger than for the BAS+, which results in the difference in tooling cost between the two motor architectures (Figure 62 and Figure 63).

Additionally, given the higher melting point, thermal conductivity, and density, coupled with the lower latent heat of fusion, the cycle time for die casting equal volumes of copper vs. aluminum are vastly different[15]. Finally, the higher melting temperature and viscosity of copper, along with the requirement for a preheated die, force the need for a more sophisticated and higher-tonnage die casting machine.

---

[15] For the BAS+, the cycle time to die cast the standard aluminum squirrel cage is 62 seconds vs. 116 sec for copper of equal volume. For the X26R Motor A, the cycle time to die cast the standard aluminum squirrel cage is 77 sec vs. 146 sec for copper of equal volume.
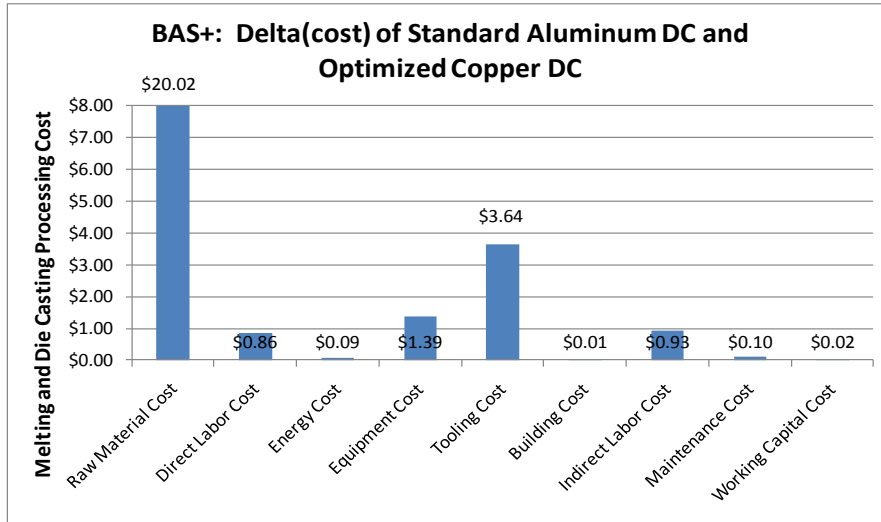
Figure 62: Difference in cost between standard aluminum baseline and 90% length copper motor for Die Casting only, broken down by cost type. BAS+.
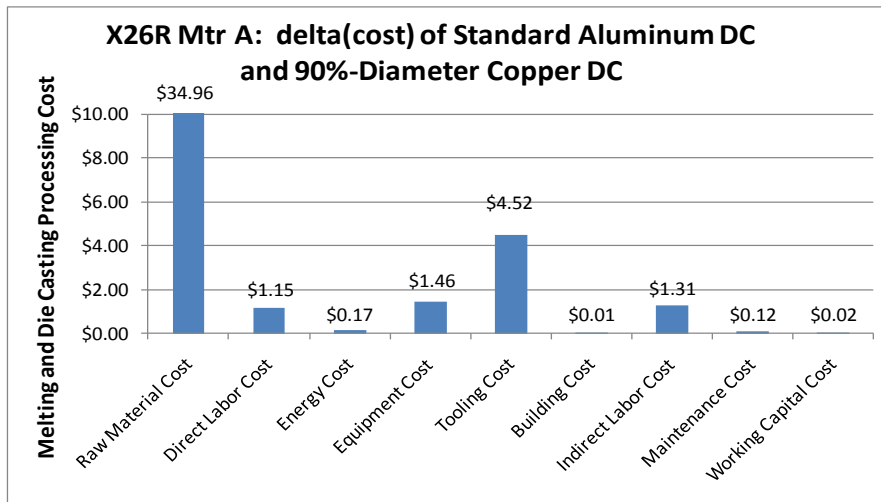
Figure 63: Difference in cost between standard aluminum baseline and 90% length copper motor for Die Casting only, broken down by cost type. X26R Motor A.

8   Discussion

8.1   Aluminum vs. Copper Die Cast Induction Motor Manufacturing Process

Given copper's higher electrical conductivity (by nearly 60%) than aluminum, the efficiency of both the BAS+ and X26R Motor A increases significantly as a result. The question surrounding this project was to assess whether or not using copper in place of aluminum die casting would ultimately increase motor cost, given that many other steps in the manufacturing process could be decreased. The Efficiency

Analysis on the BAS+ has signified that copper yields an increase in efficiency of 15% over the corresponding aluminum-based induction motor, which in turn allows for a reduction by length of 10% to the original motor(8). Nothing is known about the efficiency trends for the X26R Motor A, and as a result the 90% length was used as an arbitrary point of interest based off of the findings for the BAS+. Furthermore, no work has been done as of yet on the change in efficiency of the BAS+ as a function of motor diameter.

Downsizing to 90% length (while keeping diameter constant) still yields a 5% cost deficit over the aluminum baseline, and for both motor architectures, cost parity occurs at 74% length. Unfortunately, it is wholly probable that this much of a decrease in motor length would result in motor performance far under the required rating[16]. For both the BAS+ and X26R Motor A, downsizing to an 88.5% diameter copper motor would yield equal cost to that of the aluminum motor, but nothing is known at this point as to either the efficiency or the resulting output torque and horsepower.

As expected, the X26R Motor A is a more expensive motor to manufacture than the BAS+, due to its generally larger dimensions. However, the X26R-series motors have the advantage of allowing for the stator and rotor laminations to be blanked as a unit, thus cutting down on precious production time and raw materials. The BAS+, on the other hand, must have the laminations blanked separately due to the small air gap.

Using copper die casting in place of aluminum to manufacture the squirrel cage caused a significant increase in the overall cost of the die casting step itself. There are four main reasons for the increase in cost:

- raw copper is more expensive (per kg) than aluminum
- copper die casting requires significantly longer cycle time (by nearly a factor of 2) over that for aluminum
- copper die casting requires more sophisticated and higher-tonnage equipment
- tooling for die casting copper is more specialized (nickel-based alloys vs. H13 tool steel for aluminum) and has significantly lower tool life (~40,000 cycles vs. ~200,000 for aluminum)

The sensitivity analysis for the two motor cases involved investigating how cost changes while changing motor size. The key question was to identify if the cost parity point between the downsized copper motor and the standard aluminum baseline is the same point at which efficiency parity occurs. More specifically, for the BAS+, would cost parity occur at a 90% length copper motor? If not, where, and is this point realistically feasible? Again, given that no Efficiency Analysis could be performed on the X26R Motor A, the benchmark points for the BAS+ were used as arbitrary points of interest for the sensitivity analysis for the X26R Motor A.

Upon performing a sensitivity analysis for the two motor cases, three specific points of interest were identified and examined:

---

[16] The BAS+ is rated at 13hp (9.7 kW) and 57 ft-lbs (77 N-m). The X26R Motor A is rated at 141 hp (105 kW) and 148 ft-lbs (200 N-m).

- 90% length copper motor
- 74% length copper motor
- 88.5% diameter copper motor

The first is the efficiency equality point (i.e., the results of the Efficiency Analysis), occurring for a 90% length copper motor. The second point of interest is that for cost parity between the standard aluminum motor and the by-length downsized copper motor, resulting in a 74% length copper motor. Finally, the third point of interest is similar to point #2, but for by-diameter downsizing. As a result, the third point of interest results in an 88.5% diameter copper motor.

Unfortunately, for both the BAS+ and X26R Motor A, cost parity does not occur at 90% by length. For the BAS+, a 5.1% cost deficit still remains; for the X26R Motor A, a 4.3% cost deficit. On the other hand, nothing is currently known about the efficiency for the second point of interest, at 74% length. However, it is likely that this will result in motor performance far inferior to the standard aluminum and therefore is virtually not worth investigating. Finally, the third point of interest, at 88.5% diameter, would be worth investigating for efficiency trends given that nothing is currently known about that motor's behavior.

There is also a certain degree of sensitivity to raw material price, and how it affects overall motor cost. In using copper over aluminum and keeping the motor size constant, total motor price increases by 7.1% for the BAS+ and 9.7% for the X26R Motor A. However, a 25% decrease in material price causes a 5.3% and 6.5% reduction in 100% copper motor cost for the BAS+ and X26R Motor A, respectively. Since a 25% decrease in material price takes into account the incoming steel, copper, and aluminum universally (for the sake of this analysis), using copper over aluminum while taking into account the reduced material prices results in only a 4.9% and 6.3% cost deficit for the BAS+ and X26R Motor A, respectively. This means that a 25% reduction in material price causes the cost deficit between the standard aluminum and 100% copper motors to decrease by 2.2% for the BAS+ and 3.4% for the X26R Motor A.

The X26R Motor A experienced a greater sensitivity to material price due to its greater material use (Figure 45). Consequently, it is clear that the sensitivity to material price that a motor has is highly dependent on the individual architecture and dimensions of the motor. This is further reinforced when looking at the relative amounts of downsizing for each point of interest for the two motor cases. For example, a 74% length BAS+ copper motor results in a 17.5 mm decrease in motor length, and an 88.5% diameter BAS+ copper motor decreases diameter by 16.3 mm. For the X26R Motor A, however, the respective decreases for the two motor cases (74% length vs. 88.5% diameter) were 14.75 mm and 29.9 mm. While understanding broad cost-size trends is not possible with only two different architectures investigated, it would be useful to investigate other architectures in order to better understand these inherent trends.

8.2   Other Analyses: Friction Stir Welding and Inertia "Spin" Welding

This analysis was performed as an addendum to that for the die cast induction motor manufacturing process, and is meant as a comparison to the primary analysis outlined above.

The models developed throughout the course of this project needed to be capable of handling the manufacturing process for the initial steps of the "standard" manufacturing process for induction motors (i.e., the steps illustrated in the analysis above). However, the models also needed to incorporate additional steps for (a) other types of motor manufacturing and (b) other methods of manufacturing the squirrel cage beyond the typical die casting, notably Friction Stir Welding and Inertia "Spin" Welding.

Given the significant challenges to die casting copper, it is possible that these other methods of squirrel cage manufacturing could be cheaper. Furthermore, both FSW and Spin Welding allow the squirrel cage to be manufactured with different materials for the bars and end rings. In the induction motor architecture, the majority of the electrical conduction (and therefore magnetic field induction) occurs in the bars rather than the end rings. As a result, it is possible that using aluminum as the end ring material and copper as the bar material would result in a squirrel cage with sufficient efficiency, while simultaneously bringing both cost and weight down.

The steps relating to FSW and Spin Welding are excellent methods of estimating their respective costs, and can be used to generate approximation comparisons to die casting. However, they are not detailed enough to provide the user with a more thorough analysis unless more work was done in expanding on the intermediate calculations used within the model. This work would include, but is not limited to, a more fundamental understanding on the calculation of the cycle time and incoming material for each process, as well as the costs associated with the specialized equipment and tooling needed therein.

That said, in its current form the model is excellent at providing the user with good estimates for the production cost, to be used in comparison with the numbers generated by the die casting steps. It is worth noting that the manufacturing process for FSW- and Spin Welding-based induction motors is slightly different from the die casting-based equivalents, in that the rotor uses a slight adjustment of the steps that are turned on. Additionally, the rotor must be manufactured with no skew, due to the difficulties presented for inserting the metal bars.

In this modified manufacturing process, the Lamination and Stacking model remains much the same, with the exception of the Rotor Stacking and Interlocking step, which is now turned on. This means that the Melting and Die Casting steps of the Die Casting model are turned off in order to allow either the FSW or Spin Welding steps to be turned on. For the sake of this first-order analysis, it is assumed that the costs for end rings and extruded bars for the squirrel cage are simply the cost of the raw material itself (i.e., no actual forming or processing costs). In reality, the actual costs for the bars and end rings would be slightly more than merely the raw material but this estimation is sufficient for the high-level analysis desired from the model at this point.

The results from this preliminary analysis are in Table 8 and show a direct comparison between each of the various squirrel cage manufacturing methods, with each case number defined below. The full Preliminary Results Report is included in Appendix B, and outlines the results provided to GM. Despite the fact that many of the inputs for FSW and Spin Welding are approximated, the results provided by the models show the close similarity to ordinary die casting. In fact, the numbers are close enough to

imply that, with more research and learning, these alternate manufacturing methods might be the more cost-effective route for squirrel cage manufacturing. Additionally, if the rotor could be built with skew, it might be possible to retain minimal efficiency losses as well.

Case Number	Individual Step Cost, per motor	Total Motor Cost
1	$5.81	$403.95
2	$33.98	$432.46
3	$33.24	$420.07
4	$27.48	$403.77
5	$26.66	$413.19
6	$21.76	$408.17
7	$10.83	$396.93
8	$15.72	$401.95

Eight specific cases are investigated for the BAS+ motor:

1. Standard Aluminum motor with die casting
2. 100% size with Copper with die casting
3. 90%-by-Length Copper with die casting (Equi-efficiency to Case #1)
4. 88.5%-by-diameter Copper with die casting (Equi-cost to Case #1)
5. 90%-by-length Copper with friction stir welding
6. 90%-by-length Copper with spin welding
7. 90%-by-length Copper bars + Aluminum end rings with friction stir welding
8. 90%-by-length Copper bars + Aluminum end rings with spin welding

Table 8: Preliminary costs for die casting vs. friction stir welding vs. spin welding

9   Future Work

Clearly, the most pressing aspect of analysis in need of further development is expanding on the Efficiency Analysis. Currently, there is minimal knowledge of the sizing effects of the efficiency of the BAS+, involving only by-length analysis and 10% downsizing. It would be much more useful to apply the models used in the Efficiency Analysis for each of the points of interest for both the BAS+ and the X26R Motor A, in hopes of gaining a clearer understanding into whether the manufacturing of either of these motors with copper die casting is generally a good idea.

Given the high labor costs of many of the steps in the manufacturing process, there appears to be much room for cost savings. Additionally, some of these steps are specifically labor intensive due to the uncertainty of how to automate these steps. Currently, the labor-intensive nature of these steps results in high labor costs with low equipment costs; automating these steps would most likely dramatically increase equipment and tooling costs but would significantly decrease cycle time and the subsequent labor costs.

It would also be useful to expand on the current methods for modeling the alternative squirrel cage manufacturing steps, in order to provide the user with a more accurate representation of costs, in order to make a more informed decision into whether either Friction Stir Welding or Inertia "Spin" Welding was worth pursuing as an alternative to die casting. Furthermore, if the strength of either of these joining methods was sufficient for the motor, the use of aluminum end rings with copper bars might prove to be a smart decision. Finally, following the modification of the Friction Stir Welding step, a third alternative method of squirrel cage manufacturing could also be explored: brazing.

Since the model was designed to have the flexibility for other manufacturing methods, a deeper analysis into concentrated wound stators would be useful. Currently, the Lamination and Stacking model allows for this ability, but as of the writing of this report, no analysis has been performed. Also, the Lamination and Stacking model is broad enough in scope to allow for the investigation of other motor types, namely Permanent Magnet.

Figure 64: Example of how a stator core is manufactured using the "Slinky" method. Photo courtesy Precision Pressing Manufacturers (36).

Finally, it would be useful for the Lamination and Stacking model to be modified to allow for newer methods of motor manufacturing. One such design is commonly referred to as the "Slinky" method (Figure 64), and does not utilize cross-sectional laminations to build the stator and rotor stacks. Instead, this method cuts thin strips in the incoming steel and blanks the slots for the stator/rotor, running the length of the strip. The strip is then bent around in a spiral – similar to a slinky – in order to create the stator and rotor stack. This method of manufacturing is thought to provide the induced magnetic field with a better grain structure, which would subsequently boost the overall efficiency of the motor.

Appendix A: ReadMe file for MIT-MSL Cost Models for Induction Motors

Presented to GM to accompany the original linked Model Package.
G. Collin Mechler, MIT-MSL

There are two primary models, to be used in conjunction with those already developed by Fran Scancarello in Cost Engineering-Electric Powertrain. These models are:

- Lamination and Stacking model
- Die Casting model

The typical cost model consists of three parts: an inputs section, intermediate calculations, and an outputs section. In the case of the two MIT-MSL models, the models are all Microsoft Excel® based.

If there is any information which is not covered in this Readme specifically, each of the individual models have comments on cells where confusion may be an issue.

When using the Model Package (with five LINKED models), make sure all five models are open, otherwise the models will not function properly.

Inputs:

The inputs span over multiple tabs, broken down into input types. **The most important thing to remember while using the models is that the INPUTS ARE ALWAYS IN BLUE. Do not change any cells that are not BLUE.** All the other cells, which are in black, are equations and any changes made will affect the output(s) of the model.

Exogenous Inputs refer to inputs which help define the paradigm in which the model takes place, meaning they are not specific to the particular model. Typical exogenous inputs are employee wage, number of days worked per year, and the cost of electricity.

Other inputs are *material- or part-specific*. These inputs refer directly to the material used and the part being manufactured, respectively.

Downtime refers to the work allocation for a given step in the manufacturing process. Given that there are a number of ways a machine is not operating, the Downtime tab accounts for each of these different ways. However, there are two main types of downtime: paid downtime and unpaid downtime. Paid downtime would include scheduled worker breaks, and unpaid downtime would be when there were no shifts. Given that downtime is rarely changed, its tab is at the end.

Finally, the final main input type is *Process-Specific.* These inputs apply to the manufacturing process itself, and are specific to each of the process steps.

Intermediate Calculations:

Also referred to in the MIT-MSL models as the "---Model---" tab, this is where all of the models' calculations take place. This tab is useful if the user is interested in sub-calculations prior to the output. For example, if the user wanted to know the amount of incoming material in the Slitting operation, the "---Model---" tab would show this.

For ease of use, the ---Model--- tab is broken down into each step in the manufacturing process. Each steps subtotal is in a summary box at the top of each step. These sub-outputs are then relayed to the *Outputs* tab, where the grand total for the model is added. The ---Model--- tab displays all of the Processing Costs above each step. In the Die Casting model, the Material Cost breakdown are at the end of the ---Model--- tab but are also accounted for in the Outputs tab. For the Lamination and Stacking model, Material Costs are displayed in the Outputs tab.

Outputs:

This tab shows the grand total for each cost type after adding up each steps' intermediate subtotals. There are ten main sub-costs that contribute to the total manufacturing cost. Each of these sub-costs falls into one of two categories: *Variable Costs* and *Fixed Costs*. Variable Costs are those which scale directly with the manufacturing process. For example, energy usage increases directly with production volume. On the other hand, Fixed Costs are costs which don't necessarily scale with production volume. For example, the number of machines needed for a production volume of 500 and a PV of 50,000 may be exactly the same.

Using the Models:

If using the Model Package (i.e., all five models are linked), do not change any cells that are in GREEN, as these cells are linked. If using the models individually (i.e., not the linked Model Package), the following information is relevant:

The Lamination & Stacking and Die Casting models are unique in that they both refer to the same manufacturing process, but at different points. Consequently, it is important that the models' respective Production Volumes are correct. That is to say, if the final production volume desired is 25,000 units, the input to the Lamination model cannot be 25,000 units, given that this does not account for any kind of a reject rate. In a perfect world where reject rate is 0%, the PV for all four models (two MIT-MSL and two GM) would be identical. However, because of the imperfections in the manufacturing process, ensuring proper PV on each model is important.

The diagram on Page 3 illustrates how each model ties in with one another.

In the manufacturing process, the Die Casting model immediately follows the Lamination model. This means the Lamination model can be thought of as outputting to the Die Casting model. **As a result, the**

final PV of the Lamination model is equal to the Effective Production Volume of the FIRST STEP of the Die Casting model.

A note has been made to the END of the ---Model--- tab of the DIE CASTING model. The value in this box is the appropriate PV to input to the Lamination model if the Die Casting model will be used in conjunction with the Lamination model.

Likewise, the Effective Production Volume for the Die Casting model is simply the Effective Production Volume of the first step for the Induction Rotor Assembly model (GM).

When changing the models to investigate a new motor architecture, make sure that ALL necessary inputs have been changed, particularly those dealing with motor characteristics. The Part Data tab in the Die Casting model and the Inputs (Mat- and Part-Specific) tab in the Lamination and Stacking model are where the majority of this information can be found.

Additionally, it is a good idea to input the new motor architecture into the Area & Volume Calculations tab in the Die Casting model to calculate many of these necessary inputs.
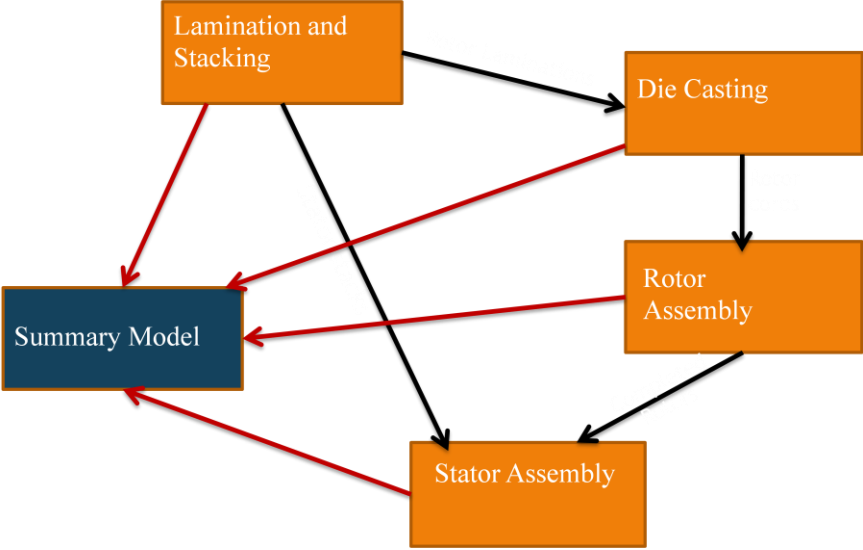

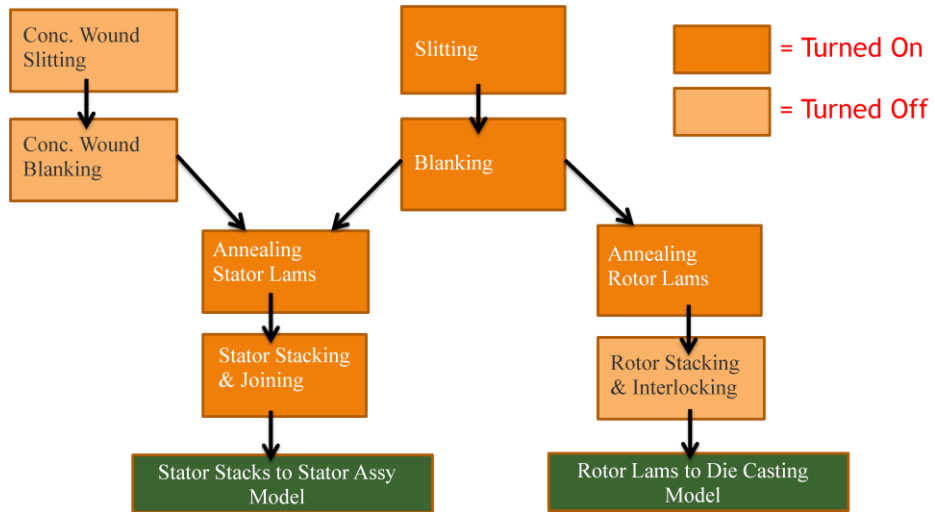**Figure 65: Process Breakdown by model showing model interaction**

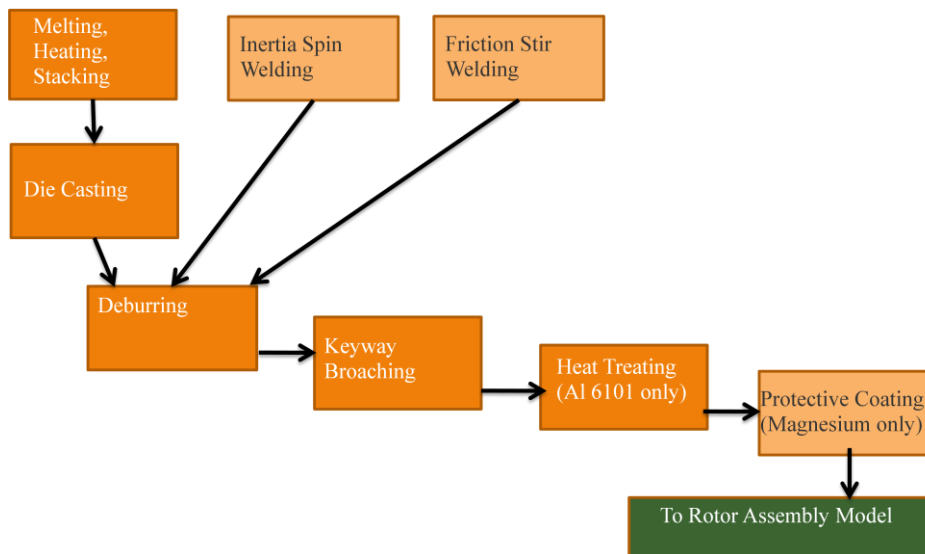**Figure 66: Process breakdown by step: Lamination and Stacking model**

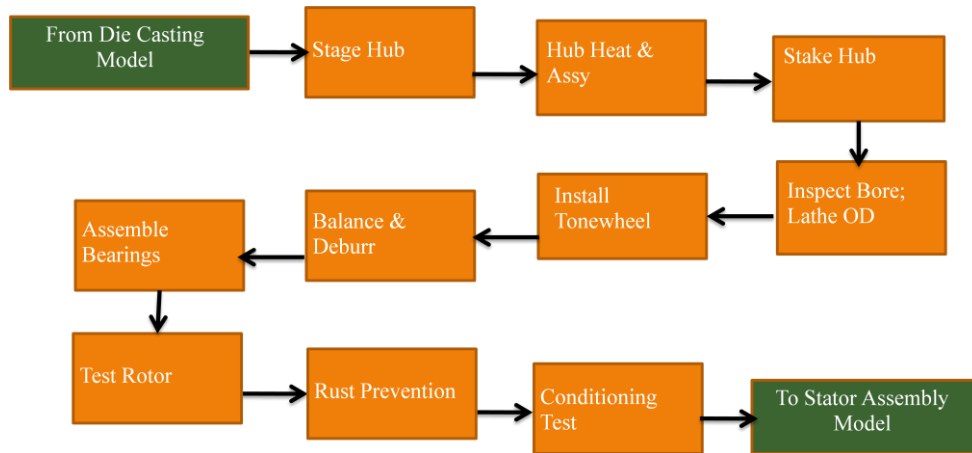**Figure 67: Process breakdown by step: Die Casting model**

Figure 68: Process breakdown by step: Induction Rotor Assy model
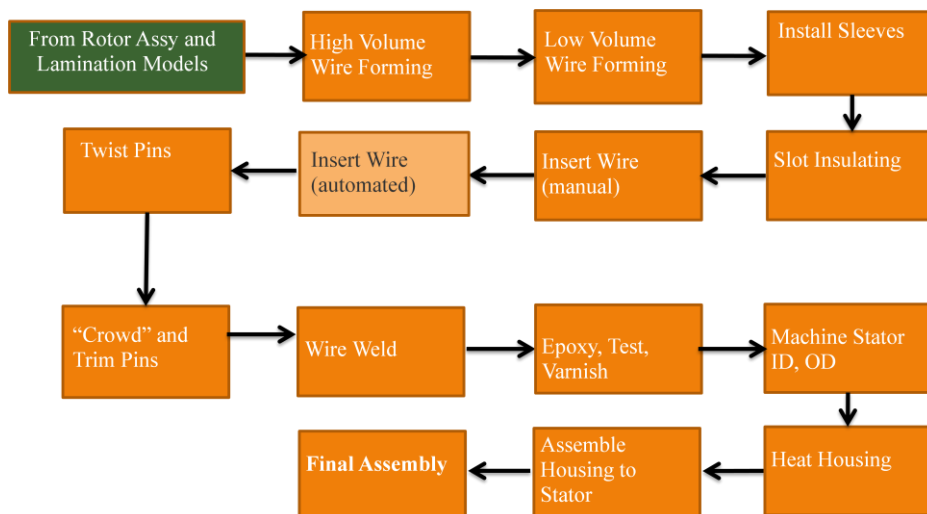

Figure 69: Process breakdown by step: Bar-Wound Stator Assy model

Appendix B: Die Casting vs. Friction Stir Welding vs. Inertia "Spin" Welding, Preliminary Report

Collin Mechler, MIT-MSL

June 28, 2010

The following explores rough ballpark figures for methods of manufacturing the squirrel cage to the rotor stack of the BAS+:

- Die Casting
- Friction Stir Welding
- Inertia "Spin" Welding

Eight specific cases are investigated for the BAS+ motor:

9. Standard Aluminum motor with die casting
10. 100% size with Copper with die casting
11. 90%-by-Length Copper with die casting (Equi-efficiency to Case #1)
12. 88.5%-by-diameter Copper with die casting (Equi-cost to Case #1)
13. 90%-by-length Copper with friction stir welding
14. 90%-by-length Copper with spin welding
15. 90%-by-length Copper bars + Aluminum end rings with friction stir welding
16. 90%-by-length Copper bars + Aluminum end rings with spin welding

Case Number	Individual Step Cost, per motor	Total Motor Cost
1	$5.81	$403.95
2	$33.98	$432.46
3	$33.24	$420.07
4	$27.48	$403.77
5	$26.66	$413.19
6	$21.76	$408.17
7	$10.83	$396.93
8	$15.72	$401.95

When using FSW or Spin Welding, the Deburring step in the Die Casting model can be turned off (in addition to the Melting and Die Casting steps. The first five cases use Die Casting, while the latter four use either of the other two methods.

The values presented in this table are to be used as a "ballpark" estimate only. For these cases, bar insertion is assumed to be automated (meaning low insertion time). However, actual bar insertion time

may be significantly longer (if manually-performed), thus increasing cost. Further work into the FSW and Spin Welding processes would be necessary to perform a detailed sensitivity analysis. However, preliminary results show that both of the alternate methods are comparable in cost to copper die casting. Additionally, costs can be significantly reduced if aluminum end rings are bonded to copper bars. It is currently unknown what this would do to motor efficiency.

Finally, die casting is the only one of these three methods that is capable of incorporating a "skew" to the rotor. For both FSW and Spin Welding, no skew is currently possible due to issues with bar insertion.

Brazing:

Currently, the Friction Stir Welding step is broad enough to easily accommodate the respective inputs for a brazing step, from a time standpoint. Implementing inputs specific to brazing is very straightforward, except for two main aspects: (a) the tooling would need to be altered, and (b) a calculation would need to be included to fully address the heating method of the brazing itself.

References

1. Tesla N, inventor; Electro-magnetic motor. patent 381969. 1888.

2. Federal Highway Administration. Licensed drivers and vehicle registrations, data sheet. 2010

3. Bureau of Transportation. Number of U.S. aircraft, vehicles, vessels, and other conveyances, data sheet. 2010

4. Outlook for hybrid and electric vehicles. International Energy Agency; 2008.

5. Press release: Without a technology breakthrough, battery costs are likely to limit widespread adoption of electric cars over the next decade, says the boston consulting group [homepage on the Internet]. The Boston Consulting Group Jan. 7, 2010. Available from: http://www.bcg.com/media/PressReleaseDetails.aspx?id=tcm:12-37343.

6. Peters DT et al. Development of the copper motor rotor -- manufacturing considerations and motor test results. Manufacturing Technology and Materials. 2004(Session 4).

7. Kirtley JL et al. Improving induction motor efficiency with die-cast copper rotor cages. IEEE Power Engineering. 2007.

8. Kirtley JL. "Efficiency Analysis," impact report.

9. General Motors R&D. Internal property.

10. Weber University. Stator Types. Available from: http://ocw.weber.edu/automotive-technology/ausv-1320-automotive-electronics.

11. Buehler Group. Presentation: Buehler Copper Rotor. 2009.

12. Fink DG, Beaty HW. *Standard Handbook for Electrical Engineers*, eleventh edition. McGraw-Hill, New York; 1978.

13. General Motors et al. Internal communications with GM. 2009-2010.

14. Kirtley J. Communications with dr. james kirtley. 2009-2010.

15. Blazek R. AM Klietka Stoc. 15 July, 2006.

16. R. Bourgeois. Pamphlet: Motor manufacturing. 2009.

17. JFE Steel Corp. JFE N-core grades and specifications [homepage on the Internet]. 2007. Available from: http://www.jfe-steel.co.jp/en/products/electrical/n_core/index.html.

18. General Electric. Series 9000 Large Synchronous Machines [homepage on the Internet]. 2010. Available from: http://www.gelighting.com/apo/products/industrial/motors_control/07.htm.

19. General Motors Powertrain. Internal property. 2009-2010.

20. Cletronics. Stator windings [homepage on the Internet]. 2010. Available from: http://www.cletronics.com/stator-windings.htm.

21. Anderson LC et al. Chapter 3: Mechanics and Manufacturing Methods. In: Axis SPA, Bank JS, Brown WC, Caine P, Cocco J, Dolan P, et al, editors. pp. 3.1-3.43.

22. Libert F et al. Manufacturing methods of stator cores with concentrated windings. Power Electronics, Machines, and Drives. 2006(The 3rd IET International Conference on Power):676-680.

23. Honda Motor Co. Stators [homepage on the Internet]. 2010. Available from: http://www.honda.com/.

24. Peters DT et al. Advances in pressure die casting of electrical grade copper. Transactions of the American Foundry Society and the One Hundred Six Annual Casting Congress. 4-7 May 2002:491-503.

25. Constantine BA. Tubular hydroforming of advanced steel and aluminum alloys: An economic evaluation using technical cost modeling [dissertation]. Cambride, MA: Massachusetts Institute of Technology.

26. Kirchain R. Process based cost modeling. In press 2009.

27. Dr.-Ing. Ernst Braun GmbH. Development of electric motors.

28. Scancarello, F., GM Cost Engineering/Electric Powertrain. GM-derived cost models. 2009-2010.

29. Ningbo Zhenyu Mould Co., Ltd. Lamination samples, progressive die, rotor casting mould. In press .

30. Infratrol. Communications with infratrol [homepage on the Internet]. 2009. Available from: http://www.infratrol.com/.

31. Somasekharan et al. Friction stir welding. In press 29 June 2004.

32. Bullis K. GM's lithium-ion hybrids. Technology Review. Mar 4, 2008.

33. Bullis K. GM's plug-in hybrid. Technology Review. Dec 5, 2006.

34. Reuters. LME copper hits record high. Reuters. 03 March, 2008.

35. US Geological Survey Copper pricing [homepage on the Internet]. 2010. Available from: www.usgs.gov.

36. Precision Pressing Manufacturers. New developments [homepage on the Internet]. 2009. Available from: http://www.ppm.co.in/aboutus.html.